CHEMICAL CONVERSION OF LIGHT ENERGY THROUGH ELECTRON TRANSFER REACTIONS

1984

HIROAKI MISAWA

CHEMICAL CONVERSION OF LIGHT ENERGY THROUGH ELECTRON TRANSFER REACTIONS

by

Hiroaki Misawa

Thesis submitted to the Graduate Faculty
in partial fulfillment of the requirements
for the degree of
Doctor of Science

The University of Tsukuba
1984

FORWARD

First of all, it should be mentioned that the investigation of this thesis has been carried out under the guidance of Professor Katsumi Tokumaru.

I express my deep gratitude to Professor Katsumi Tokumaru for his cordial guidance, advice, and encouragement. I am deeply indebted to Professor Yoshiharu Usui of Department of Chemistry, Faculty of Science, Ibaraki University, for his useful discussion and advice. I am greatly indebted to Dr. Hirochika Sakuragi for his continuous guidance and helpful advice. I am grateful to Dr. Akihide Kitamura of Department of Chemistry, College of Arts and Science, Chiba University, for his useful discussion, and also grateful to Dr. Tatsuya Kanno for his helpful discussion and advice in electrochemistry. I wish to thank Dr. Ryoichi Akaba and Dr. Tatsuo Arai for their constant discussions and suggestions.

Thanks are due to Mr. Yasuo Shimamura and Mr. Akihiro Wakisaka for their kind assistances.

I would like to acknowledge all members of Tokumaru laboratory for their friendships.

Finally, I would express my sincere thanks to my wife, my parents, and my brother.

CONTENTS

INTRODUCTION

Photo-induced charge or electron transfer reactions have been the subject of extensive investigations during the past several years. Quenching of a great variety of excited states either by electron transfer or by formation of exciplexes (hetero-excimers) has been shown to be general. It has been thought that exciplexes are very important intermidiates not only in photophysical events [1] but also in photochemical reactions,[2] since exciplex emission was observed for the first time in solution containing perylene and dimethylaniline by Leonhardt and Weller in 1963.[3] The investigations on behavior of the exciplexes are very important to understand photo-induced charge or electron transfer reactions.

Recently, light induced electron transfer reactions are of great interest in relation with construction of efficient systems for conversion and storage of solar energy into electrical or chemical energy. The investigations have been carried out both on heterogeneous systems with semiconductor electrodes or particles and on homogeneous systems with dye sensitizers. The photovoltaic effect at the semiconductor-liquid interface on light irradiation has been studied for the construction of the above heterogeneous systems since the photoelectrolysis of water at the TiO_2 electrode was done in 1971 by Fujishima and Honda.[4] More recently, the light induced water decomposition

employing platinum and ruthenium dioxide doped colloidal TiO_2 was reported,[5] and that the quantum yield of the reaction reached 0.4 ± 0.1. Although platinized TiO_2 powder has been also used to carry out the photoelectrolysis of water,[6] the band gap of TiO_2 is too large to utilize for the solar light. However, the remarkable efficiency of the separation of photogenerated electron-hole pairs in the semiconductors seems available for novel synthetic chemistry. Dye sensitized hydrogen evolution from water with visible light in homogeneous systems has been investigated with growing attention. Among the systems, ruthenium complexes (sensitizer)-methyl viologen (acceptor) is the best studied;[7] however, a few reports have appeared on utilization of organic dyes.[8] Although some organic dyes are cheaper than the metal complexes, the mechanistic studies of the organic dye-sensitized electron transfer reaction in relation with the solar energy conversion have not been carried out at all.

In these respects, in the present work, photo-induced charge and electron transfer reactions have been studied.

Eosin Y, one of xanthene dyes, was found not to be photo-bleached with triethanolamine (TEOA) on visible light irradiation in the presence of methyl viologen (MV^{2+}), and to work as an effective sensitiser to reduce MV^{2+} into $MV^{+\cdot}$ with TEOA in aqueous ethanol as described in Chapter 3. The limiting quantum yield for $MV^{+\cdot}$ production reached ca. 0.3. The value is equal or

high as compared with the value from the system employing ruthenium complexes as sensitizer. The resulting $MV^{+\cdot}$ reduced water to hydrogen in the presence of colloidal platinum in the same system.[9] The detailed kinetics and mechanism of the photo-induced reactions occurring in such a system were explored by nanosecond and microsecond laser flash photolysis techniques. The results show that the reaction is started by electron transfer from triplet excited EY^{2-} to MV^{2+} followed by electron transfer to the resulting $EY^{-\cdot}$ from TEOA.

Chapter 1 describes intrinsic reactivity of the exciplex between aromatic hydrocarbon and dibenzoyl peroxide from the viewpoint of structural factors of sensitizers.[10]

Previously, Kanno reported that irradiation of semiconductor particles (n-TiO_2 and n-CdS) suspended in organic solvents containing aromatic olefins under oxygen afforded the corresponding epoxides and carbonyl compounds.[11] Chapter 2 reports that an observation of anodic photocurrents from aromatic olefins to the excited n-TiO_2 electrode to evaluate the extent of electron transfer in the initiation process of the above reaction, and the mechanism of the reaction is discussed.[12]

References

1) For example, J. B. Birks, "Photophysics of Aromatic Molecules," Wiley-Interscience, New York (1970); M. Gordon and W. R. Ware (eds.), "The Exciplex," Academic Press, New York (1975); N. Mataga, "Kagaku Sosetsu," ed. by Chem. Soc. Jpn., Gakkai Shuppan Center Tokyo, 1982, p. 19.

2) For example, M. Ohashi, Kagaku no Ryoiki, 32, 56 (1978); F. D. Lewis, Acc. Chem. Res., 12, 152 (1979); R. A. Caldwell and D. Creed, ibid., 13, 45 (1980); R. S. Davidson, Adv. Phys. Org. Chem., 19, 1 (1983).

3) H. Leonhardt and A. Weller, Ber. Bunsenges. Phys. Chem., 67, 791 (1963).

4) A. Fujishima and K. Honda, Bull. Chem. Soc. Jpn., 44, 1148 (1971); Idem, Nature, 238, 37 (1972).

5) D. Duoughong, E. Borgarello, and M. Gratzel, J. Am. Chem. Soc., 103, 4685 (1981).

6) For example, T. Sakata and T. Kawai, Yuki Gosei Kagaku Kyokai Shi, 39, 589 (1981); A. J. Bard, J. Phys. Chem., 86, 172 (1982).

7) For example, N. Sutin, J. Photochem., 10, 19 (1979); N. Sutin and C. Creutz, Pure Appl. Chem., 52, 2717 (1980).

8) For example, J. S. Bellin, R. Alexander, and R. D. Mahoney, Photochem. Photobiol., 17, 17 (1973); K. Kalyanasundaram

and M. Gratzel, J. Chem. Soc., Chem. Commun., 1979, 1137; A. I. Krasuna, Photochem. Photobiol., 29, 267 (1979); 31, 75 (1980); K. Kalyanasundaram and D. Dung, J. Phys. Chem., 84, 2551 (1980); M. S. Chan and J. R. Bolton, Photochem. Photobiol., 34, 537 (1981).

9) H. Misawa, H. Sakuragi, Y. Usui, and K. Tokumaru, Chem. Lett., 1983, 1021.

10) H. Misawa, A. Kitamura, H. Sakuragi, and K. Tokumaru, Bull. Chem. Soc. Jpn., in press.

11) T. Kanno, T. Oguchi, H. Sakuragi, and K. Tokumaru, Tetrahedron Lett., 21, 467 (1980); T. Kanno, Thesis, University of Tsukuba, 1981.

12) H. Misawa, T. Kanno, H. Sakuragi, and K. Tokumaru, Denki Kagaku, 41, 81 (1983).

Chapter 1

REACTION EFFICIENCY OF EXCIPLEXES IN SINGLET SENSITIZED DECOMPOSITION OF DIBENZOYL PEROXIDE

Summary

Quantum yields were measured for aromatic hydrocarbon-sensitized decomposition of dibenzoyl peroxide in benzene. For the sensitizers employed, naphthalene, phenanthrene, triphenylene, and chrysene, the ratio of the rate constants for decay and radical formation from intermediate exciplexes was found to be similar (0.2 - 0.4), indicating that the reactivity of the peroxide moiety in the intermediate is independent of the structural factors of the sensitizers as far as examined.

Introduction

Exciplexes have been proposed as reactive intermediates in many photochemical reactions though they are not necessarily emissive.[1-3] In some cases the exciplexes may be too reactive to be alive in sufficiently long lifetimes to exhibit emission.[3,4] However, few works have been carried out to actually examine intrinsic reactivity of the exciplexes from the viewpoint of structural factors of sensitizers.[2,5,6]

Previously, singlet excited aromatic hydrocarbons have been revealed to sensitize decomposition of dibenzoyl peroxide (BPO) in solution.[7-9] The reaction was proposed to proceed through short lived reactive exciplexes which either bring about homolytic decomposition of the peroxide moiety into free radicals or deactivate into the original components in the ground state as shown in the following scheme, where Sens and P denote a sensitizer and the peroxide, respectively,

Scheme 1

$$^1\text{Sens}^* + \text{P} \xrightarrow{k_q} {}^1(\text{Sens}\cdot\text{P})^* \qquad (1)$$

$$^1(\text{Sens}\cdot\text{P})^* \xrightarrow{k_r} \text{Free radicals} + \text{Sens} \qquad (2)$$

$$^1(\text{Sens}\cdot\text{P})^* \xrightarrow{k_d} \text{Sens} + \text{P} \qquad (3)$$

and k_q, k_r, and k_d mean the rate constants of the processes concerned.

This Chapter describes an attempt to determine the relative reactivity of the exciplexes in singlet sensitized decomposition of BPO in relation to structural factors of the hydrocarbon sensitizers.

Results and Discussion

Benzene solutions of a sensitizer (3.0×10^{-3} - 3.0×10^{-2} mol/dm^3) and varying concentrations of BPO (1.2×10^{-3} - 3.1×10^{-2} mol/dm^3) were irradiated under argon atmosphere with 366 nm light (for chrysene as sensitizer) or 313 nm light (for triphenylene, phenanthrene, and naphthalene) isolated from a 400 W high pressure mercury lamp, and the quantum yields for decomposition of BPO were dertermined at low conversion of BPO (less than 20 %) using potassium tris(oxalato)ferrate(III) actinometry.[10)]

According to Scheme 1, the quantum yield for disappearance of BPO is expressed by Eq. 4, where τ_S^0 means the lifetime of the singlet excited sensitizer in the absence of the peroxide.

$$\Phi^{-1} = (1 + 1/k_q \tau_S^0 [P])(1 + k_d/k_r) \qquad (4)$$

For each sensitizer employed, the reciprocal of the quantum yield is linearly correlated with the reciprocal of the peroxide concentration, and the intercept, $(k_r + k_d)/k_r$, exceeds unity (Figure 1). This means clearly that the reaction proceeds through formation of some reactive intermediates like exciplexes. The results analyzed according to Eq. 4 are summarized in Table 1.

In Table 1 are also listed the $k_q \tau_S^0$ values determined by fluorescence quenching in benzene using the single photon

counting technique,[11] the singlet excitation energies[10] and oxidation potentials[12] of the sensitizers. The $k_q\tau_S^0$ value obtained from the quantum yield measurements for each sensitizer satisfactorily agrees well with that from the fluorescence quenching.

As Table 1 indicates, the observed ratios of the rate constants for decay and radical formation from the exciplexes, k_d/k_r, are not significantly varied (0.21 - 0.41) among the unsubstituted polycyclic aromatic hydrocarbons employed, naphthalene, phenanthrene, triphenylene, and chrysene. This fact indicates that the reactivity of the peroxide moiety in the intermediate does not depend upon such structural factors of the sensitizers as the singlet excitation energies of the sensitizers, E_S, and the extent of charge transfer from the excited sensitizer to BPO in the exciplex, $E_{ox} - E_S$. This observation might be accounted for by the facts that the low energy (ca. 31 kcal/mol)[13] is required for the cleavage of the peroxide linkage compared to the singlet excitation energies of the sensitizers (Table 1) and that the overall process of the sensitization gives free radical products arising benzoyloxyl and phenyl radicals, but not any ionic products at all.[7-9]

Attempts to determine the quantum yields by employing other sensitizers like anthracene, 9,10-diphenylanthracene, pyrene, and perylene were abandoned, since these sensitizers were found to be fairly consumed during the reaction in contrast to the above

sensitizers which were recovered more than 80% after the reaction.

Conclusion

The results reported in this Chapter shows that the singlet sensitized decomposition of dibenzoyl peroxide proceeds through the formation of some reactive intermediates such as exciplexes. The reactivity of the exciplexes does not depend upon structural factor of the sensitizers. This result reflects that the low energy is required for the degradation of the peroxide linkage compared to the singlet excitation energies of the sensitizers and that the overall process of the sensitization gives free radical products, but not any ionic products at all.

Experimental

materials. Dibenzoyl peroxide was purified by reprecipitation from dichloromethane-methanol. Triphenylene was prepared according to literature.[14] The other aromatic hydrocarbons, naphthalene, phenanthrene, chrysene, anthracene, 9,10-diphenylanthracene, pyrene, and perylene, were commercially available. The aromatic hydrocarbons were purified by column chromatography on silica gel with petroleum ether as eluent and recrystallized from hexane. Benzene (special grade) was distilled before use.

Measurement of quantum yields. The quantum yields for disappearance of BPO were determined in benzene under argon atmosphere employing potassium tris(oxalato)ferrate(III) as actinometer. Irradiation was carried out with 366 nm light for chrysene, anthracene, 9,10-diphenylanthracene, pyrene, and perylene and with 313 nm light for naphthalene, phenanthrene, and triphenylene. From a 400 W high pressure mercury lamp 366 nm light was isolated through a Toshiba UV-D36B glass filter and 313 nm light through a Toshiba UV-D33S and a K_2CrO_4/Na_2CO_3 solution filter.[11] The amounts of the remaining BPO were determined by HPLC (column: Zorbax ODS, solvent: CH_3OH-H_2O=85:15). Although BPO was decomposed on direct irradiation with 313 nm light, its quantum yield was less than 1% compared with the sensitized decompositions and can be satisfactorily neglected in the present investigation.

References

1) P. S. Engel and B. M. Monroe, Adv. Photochem., 8, 245 (1970); M. Koizumi, S. Kato, N. Mataga, T. Matsuura, and Y. Usui, "Photosensitized Reactions," Kagaku Dojin, Kyoto, 1978, p. 271; H. Sakurai and C. Pac, "Kagaku Sosetsu," ed. by Chem. Soc. Jpn., Gakkai Shuppan Center, Tokyo, 1982, p. 37, 75.

2) R. A. Caldwell and D. Creed, Acc. Chem. Res., 13, 45 (1980).

3) R. S. Davidson, Adv. Phys. Org. Chem., 19, 1 (1983).

4) H. Sakuragi, K. Tokumaru, H. Itoh, K. Terakawa, K. Kikuchi, R. A. Caldwell, and C.-C. Hsu, J. Am. Chem. Soc., 104, 6796 (1982).

5) H. D. Becker, Pure Appl. Chem., 54, 1589 (1982).

6) A. M. Swinnen, M. van der Auweraer, F. C. de Schryver, C. Windels, R. Goedeweeck, A. Vannerem, and F. Meeus, Chem. Phys. Lett., 95, 467 (1983); F. C. de Schryver, N. Boens, and J. Put, Adv. Photochem., 10, 359 (1977).

7) T. Nakata, K. Tokumaru, and O. Simamura, Tetrahedron Lett., 1967, 3303; T. Nakata and K. Tokumaru, Bull Chem. Soc. Jpn., 43, 3315 (1970).

8) K. Tokumaru, A. Oshima, T. Nakata, H. Sakuragi, and T. Mishima, Chem. Lett., 1974, 571.

9) A. Kitamura, H. Sakuragi, M. Yoshida, and K. Tokumaru, Bull.

Chem. Soc. Jpn., 53, 1393, 2413 (1980).

10) S. L. Murov, "Handbook of Photochemistry", Marcel Dekker, New York, 1973.

11) A. Kitamura, Thesis, University of Tsukuba, 1980.

12) The oxidation potentials were determined vs. SCE in acetonitrile using tetraethylammoniumperchlorate (0.1 mol/dm^3) as a supporting electrolyte.

13) I. Jaffe, E. J. Prosen, and M. Szwarc, J. Chem. Phys., 27, 416 (1957).

14) T. Sato, Yuki Gosei Kagaku Kyokai Shi, 30, 293 (1972).

Table 1. Relative Reactivity of the Exciplexes in Singlet Sensitized Decomposition of Dibenzoyl Peroxide and Structural Factors of the Sensitizers

Sensitizer	k_d/k_r	$k_q\tau_S^o$ a) /$dm^3 mol^{-1}$	$k_q\tau_S^o$ b) /$dm^3 mol^{-1}$	E_S c) /kcal mol^{-1}	/eV	E_{ox} d) /V	$E_{ox}-E_S$ /eV
Naphthalene	0.41	930	810	92	3.99	1.87	-2.12
Triphenylene	0.29	200	170	83.4	3.62	1.80	-1.82
Phenanthrene	0.38	400	310	82.8	3.59	1.71	-1.88
Chrysene	0.21	230	240	79.2	3.43	1.56	-1.87

a) From quantum yield measurements. b) From fluorescence quenching. c) Singlet excitation energy from ref. 11. d) Oxidation potential vs. SCE in CH_3CN with Et_4NClO_4.

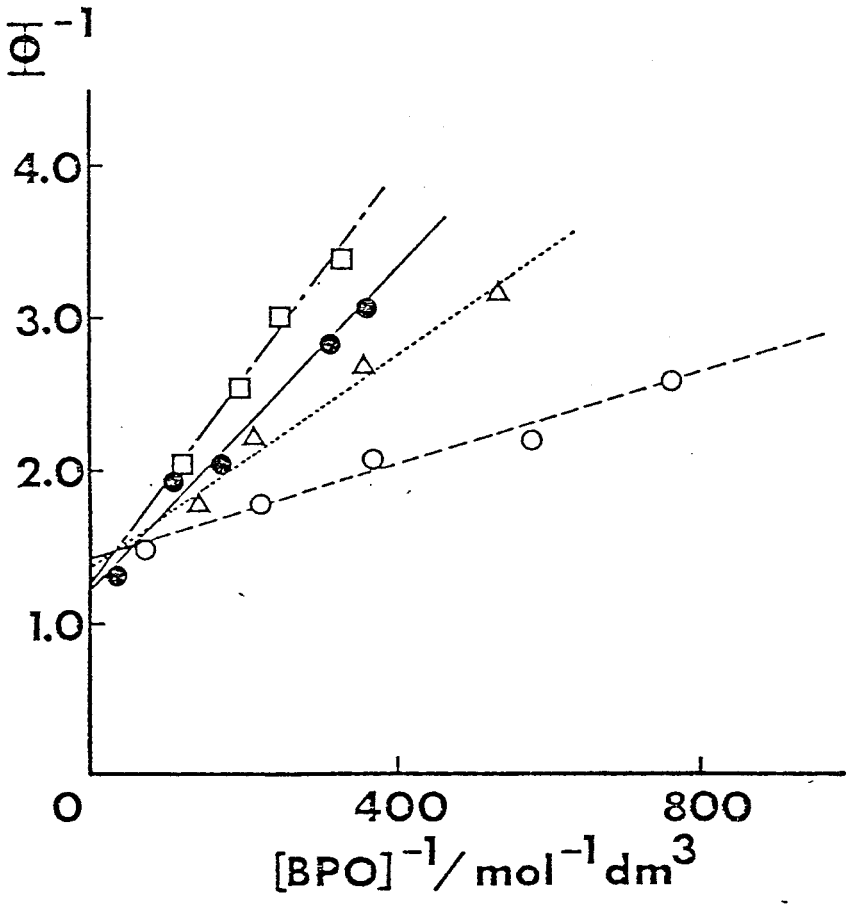

Fig. 1 Stern-Volmer Plots of Reciprocal Quantum Yields vs. Reciprocal Concentrations of BPO in Aromatic Hydrocarbon Sensitized Decomposition of BPO; Sensitizers: Naphthalene (O), Triphenylene (□), Phenanthrene (△), and Chrysene (●).

Chapter 2

PHOTOELECTROCHEMICAL INVESTIGATION ON THE MECHANISM OF TITANIUM DIOXIDE PHOTOCATALYZED OXYGENATION OF AROMATIC OLEFINS

Summary

Anodic photocurrents were measured between various aromatic olefins and the excited titanium dioxide electrode in order to reveal the primary process of titanium dioxide photocatalyzed-oxygenation of these olefins. The photocurrents increased with increasing oxidation potentials of the olefins; however the reactivity of the olefins in the semiconductor photocatalyzed oxygenation did not necessarily correspond with the magnitude of the photocurrents. The initiation process of the photocatalyzed oxygenation is suggested to be electron transfer from the olefin to the positive holes of the excited n-TiO_2; however the efficiency of the reaction is controlled not only by the electron transfer process but by radical chain processes.

Introduction

The photocatalytic effects of semiconductor have been recently concerned with the construction of efficient systems for conversion of solar energy into chemical and electrical energy since the photoelectrolysis of water at the semiconductor electrode was done in 1971 by Fujishima and Honda.[1] The charge separation in the semiconductors is carried out by the electric field formed at the interface between the semiconductor and an electrolyte solution. The separation of photogenerated electron-hole pairs into the components before recombination is one of the most important subjects in relation to the useful storage and conversion of solar energy. A number of photocatalytic reactions employing semiconductors in solution have been extensively investigated.[2-4] Especially, these studies have focused on the production of hydrogen from water.[5,6]

More recently the dispersed semiconductors have been used to induce novel synthetic chemistry.[7,8] Bard and coworkers reported that platinized n-TiO_2 was more effective than n-TiO_2 in the photodecarboxylation of acetate.[9]

Previously, Kanno reported that irradiation of semiconductor particles (n-TiO_2 and n-CdS) suspended in organic solvents containing aromatic olefins under oxygen afforded the corresponding epoxides and carbonyl compounds.[10] (Scheme 1)

Scheme 1

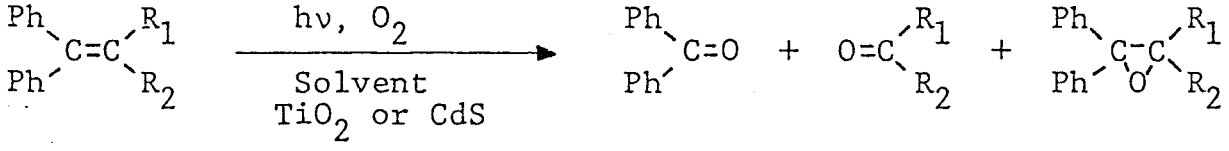

The photocatalyzed oxygenation proceeded efficiently with the olefins such as 2-methoxy-1,1-diphenylethylene, 2-methyl-1,1-diphenylpropene, 1,1-diphenylethylene, and 2-phenylpropene, which have the oxidation potentials more cathodic than 1.6 V vs. Ag/0.1 mol dm^{-3} $AgNO_3$.[11] On the other hand, among the olefins investigated, 2-cyano-1-phenylethylene, ethyl 3-phenyl propenoate, 4-phenyl-3-buten-2-one, and cyclooctene, of which the oxidation potentials were more anodic than 2.0 V, were practically not oxidized.[11] These results strongly suggest that the primary process of the reaction is electron transfer from the olefins to the positive holes generated in the valence band of the semiconductors under illumination.[10]

Recently, Fox and coworkers carried out semiconductor photocatalyzed oxygenation of aromatic and non-aromatic olefins[12] and observed analogous results to those by Kanno.[10]

Kagiya and coworkers showed that secondary amines could be synthesized from primary amines in an aqueous solution by using platinized n-TiO_2 powder.[13]

Shimamura reported that irradiation of powdered titanium

dioxide suspended in solution containing aromatic compounds and water under oxygen induced hydroxylation of aromatic nuclei giving phenolic compounds and oxidation of side chains of the aromatic compounds, and showed that the presence of oxygen is essential for the reaction and that under oxygen oxidation of water contributes to aromatic hydroxylation and oxidation of toluene as a substrate leads to oxidation of its side chain.[14)]

This chapter describes an attempt to elucidate the mechanism of TiO_2-photocatalyzed oxygenation of the aromatic olefins by determining anodic photocurrents from the olefins to the excited n-TiO_2 electrode and by estimating the extent of electron transfer in the initiation process of the above reaction in relation to the oxidation potentials of olefins.[15)]

Results and Discussion

Cyclic voltammograms of trans-stilbene at an n-TiO_2 electrode are shown in Figure 1. As shown in curve a and c, negligibly small background currents were observed in the dark with and without trans-stilbene in acetonitrile solutions containing 0.1 mol/dm^3 tetraethylammonium perchlorate (TEAP) as a supporting electrolyte. Neither reduction wave nor oxidation wave was observed in the dark in the potential range of -0.5 - 0.8 V vs. $Ag/AgNO_3$. In an acetonitrile solution containing 0.1 mol/dm^3 TEAP without trans-stilbene, irradiation of the n-TiO_2 electrode with 366 nm light caused an anodic photocurrent at more positive potentials than 0.05 V (curve b). This photocurrent can probably be attributed to oxidation of TEAP or acetonitrile. In the presence of 2.0×10^{-2} mol/dm^3 trans-stilbene, the onset photopotential, V_{on}, was slightly shifted to a more negative potential, -0.1 V, and a large increase in the anodic photocurrent was observed at 0.5 V (curve d). This photocurrent can clearly be due to the oxidation of trans-stilbene, which has a cathodic oxidation potential. On the other hand, in the presence of the olefins which had more anodic oxidation potentials than 1.9 V, for example, cyclooctene and 4-phenyl-3-buten-2-one, the photocurrents were scarcely observed.

The net photocurrent, i_p, was defined as difference in the photocurrents with and without an olefin. The behavior of the

i_p values with the sweeping potential is shown in Figure 2.

Correlation of the i_p values at 0.5 V with the oxidation potentials of the olefins employed is illustrated in Figure 3. The i_p value increases with increasing oxidation potential of the olefins. On the other hand, for cyclooctene and 4-phenyl-3-buten-2-one which have more anodic oxidation potentials, the i_p values can be hardly detected at this potential. These results suggest that the net photocurrent, i_p, is afforded by the electron transfer from the olefin to the positive holes in the valence band of the n-TiO_2 electrode under illumination and the extent of the electron transfer is controlled by the oxidation potential of olefins.

The i_p value of each olefin should be compared with the reaction efficiency of the olefin in the semiconductor-photocatalyzed oxygenation. The more cathodic the oxidation potentials of the olefins, the larger photocurrents and the higher reactivity tend to be exhibited in the n-TiO_2 photocatalyzed oxygenation On the other hand, the olefins of low reactivity in the photocatalyzed oxidation, the photocurrents were scarcely observed, suggesting that the electron transfer from these olefins to the positive holes of excited n-TiO_2 electrode under illumination did not occur. Consequently it is indicated that the electron transfer is the primary process in the semiconductor photocatalyzed oxygenation. trans-Stilbene had a more cathodic oxidation potential and showed a larger photocurrent than 1,1-diphenyl-

ethylene but the reactivity of the former in semiconductor photocatalyzed oxygenation was lower than that of the latter which showed a small photocurrent. Kanno described that the semiconductor photocatalyzed oxygenation proceeded through electron transfer from the olefin to the positive holes of the excited n-TiO_2 generating olefin cation radicals followed by free radical chain reactions including oxygen (Figure 4).[11] Moreover, stilbene has a lower reactivity in radical addition than 1,1-diphenylethylene and styrene.[16] These facts indicate that the reaction efficiency of the n-TiO_2 photocatalyzed oxygenation depends not only on the electron transfer efficiency from the olefin to the positive holes in the excited semiconductor but on the reactivity of the resulting radical species in the dark reactions (Table 1).

Conclusion

This work shows that the extent of the anodic photocurrents from several aromatic olefins to the excited n-TiO_2 electrode depends upon the oxidation potentials of the olefins. It is reasonable to suppose that the initiation process of the semiconductor photocatalyzed oxygenation is electron transfer from the olefin to the positive holes of excited n-TiO_2. However, the reaction efficiency of TiO_2-photocatalyzed oxygenation is not correlated with the magnitude of the anodic photocurrent. The results show that the efficiency of the reaction is controlled not only by the electron transfer process but also by the subsequent radical chain processes.

Experimental

Materials. 2-Methyl-1,1-diphenylpropene (1), 1,1-diphenylethylene (2), 2-phenylpropene (3), cyclooctene (4), and 4-phenyl-3-buten-2-one (5) were purified by distillation (bp: 1, 115-116°C/4mmHg; 2, 102-104°C/3mmHg; 3, 53-54°C/ 30mmHg; 4, 81-82°C/133mmHg; 5, 60-61°C/4mmHg). trans-Stilbene was recrystallized three times from ethanol. Tetraethylammonium perchlorate (TEAP) (Nakarai, polarographic grade) as supporting electrolyte and acetonitrile (Nakarai, HPLC grade) were commercially available and were used without further purification.

Measurement of photocurrents. Figure 5 shows an apparatus for the measurement of photocurrents. The working electrode was a polycrystalline n-TiO_2 plate prepared by the following procedures.[17] A thin titanium plate (0.1-0.2 mm in thickness) was heated strongly in an oxidation flame of a town gas burner for 30 min. The coating of the oxidized titanium was formed on the metal titanium. The plate was cooled to room temperature and was cut into a square, the area being 0.342 cm^2. The working electrode was contacted to a copper wire with conductive silver paste which was covered with rapid-drying epoxy cement. The electrode, copper wire, and all sides of the plate, except for the newly formed titanium dioxide surface, were covered with slow-drying epoxy cement. Before use, the surface of the electrode was etched with dilute hydrochloric acid for 30-

40 s and washed with distilled water and special grade acetonitrile. A platinum plate was used as a counter electrode. The working electrode potential with respect to Ag/0.1 mol dm^{-3} $AgNO_3$ and the currents between the n-TiO_2 electrode and the platinum electrode were measured by sweeping the potential from -0.5 V to 0.8 V at 70 mV/s on a Hokuto HA-201 potentiostat equipped with a Hokuto HB-104 function generator. The voltammetric curves were put out on Rikadenki RW-11 recorder. Argon gas was bubbled into a solution for at least 30 min before each measurement and kept bubbling during the measurements. A 500 W xenon lamp (Ushio UI-501C) was employed as a light source. Light with wavelength of about 366 nm was isolated through two glass filters (Toshiba UV-D36B and UV-35). An acetonitrile solution contained 2.0×10^{-2} mol dm^{-3} olefin and 0.1 mol dm^{-3} TEAP as supporting electrolyte.

References

1) A. Fujishima and K. Honda, Bull. Chem. Soc. Jpn., 44, 1148 (1971); Idem, Nature, 238, 37 (1972).

2) T. Watanabe, T. Takizawa, and K. Honda, Syokubai, 20, 370 (1978).

3) T. Freund and W. P. Gommes, Catal. Rev., 3, 1 (1969).

4) A. Heller, Acc. Chem. Res., 14, 154 (1981).

5) A. J. Bard, J. Photochem., 10, 59 (1979); Idem, J. Phys. Chem., 86, 172 (1982).

6) M. S. Wrighton, Acc. Chem. Res., 12, 303 (1979).

7) I. Izumi, F.-R. F. Fan, and A. J. Bard, J. Phys. Chem., 85, 218 (1981).

8) M. Fujihira, Y. Satoh, and T. Osa, Nature, 293, 206 (1981); Idem, Chem. Lett., 1981, 1053; Idem, J. Electroanal. Chem., 126, 277 (1981); Idem, Bull. Chem. Soc. Jpn., 55, 666 (1982).

9) B. Kraeutler and A. J. Bard, J. Am. Chem. Soc., 100, 2239, 5895 (1978).

10) T. Kanno, T. Oguchi,88 H. Sakuragi, and K. Tokumaru, Tetrahedron Lett., 21, 467 (1980).

11) T. Kanno, Thesis, University of Tsukuba, 1981.

12) M. A. Fox and C.-C. Chen, J. Am. Chem. Soc., 103, 6757 (1981); M. A. Fox, B. Lindig, and C.-C. Chen, ibid., 104, 5828 (1982).

13) S. Nishimoto, B. Ohtani, T. Yoshikawa, and T. Kagiya, J. Am. Chem. Soc., 105, 7180 (1983).

14) Y. Shimamura, H. Misawa, T. Oguchi, T. Kanno, H. Sakuragi, and K. Tokumaru, Chem. Lett., 1983, 1691.

15) H. Misawa, T. Kanno, H. Sakuragi, and K. Tokumaru, Denki Kagaku, 41, 81 (1983).

16) O. Simamura, T. Migita, N. Inamoto, and K. Tokumaru, "Yuriki Hanno," Tokyo Kagaku Dojin (1969), Chapter 9.

17) A. Fujishima, K. Kohayakawa, K. Honda, J. Electrochem. Soc., 122, 1487 (1975).

Table 1. Summary of the reaction efficiency for semiconductor phtocatalyzed oxygenation of various olefins.

Olefin	Photocurrent /mA cm^2	Reactivity of chain processes	Total Reactivity
trans-Stilbene	190	–	–
2-Methyl-1,1-diphenyl-propene	111	+	++
1,1-Diphenylethylene	24	++	+++
2-Phenylpropene	15	+	+
Cyclooctene	5	–	+
4-Phenyl-3-buten-2-one	13	–	–

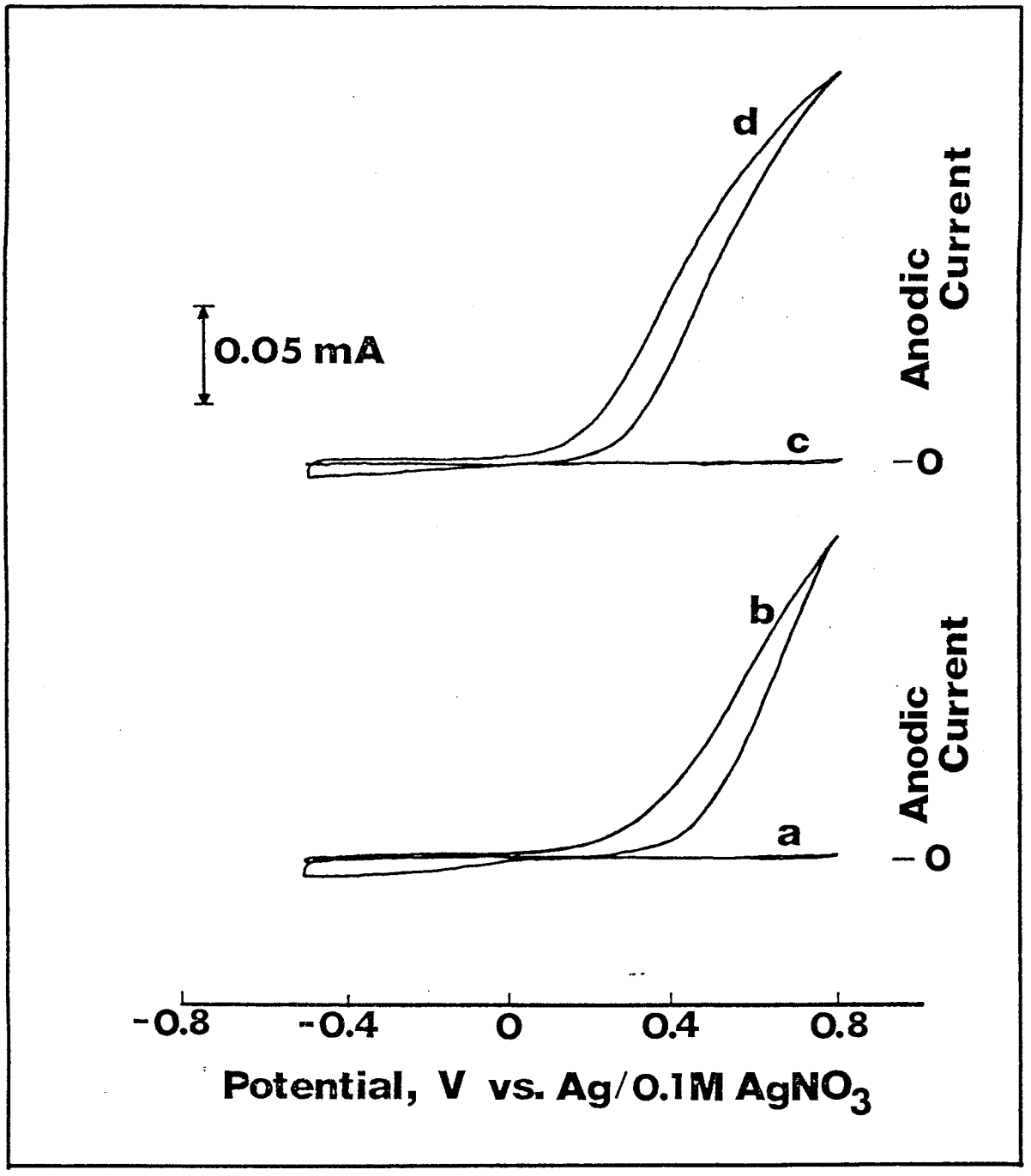

Figure 1. Voltammetric curves on irradiation of n-TiO_2 in MeCN containing 0.1 mol/dm^3 Et_4NClO_4; scan rate 70 mV/s. (a) Dark cyclic voltammogram on TiO_2 without stilbene. (b) Current-potential curve under illumination with 366 nm light on TiO_2 without stilbene. (c) Dark cyclic voltammogram on TiO_2 with 0.2 mol/dm^3 stilbene. (d) Current-potential curve under illumination with 366 nm light on TiO_2 with 0.2 mol/dm^3 stilbene.

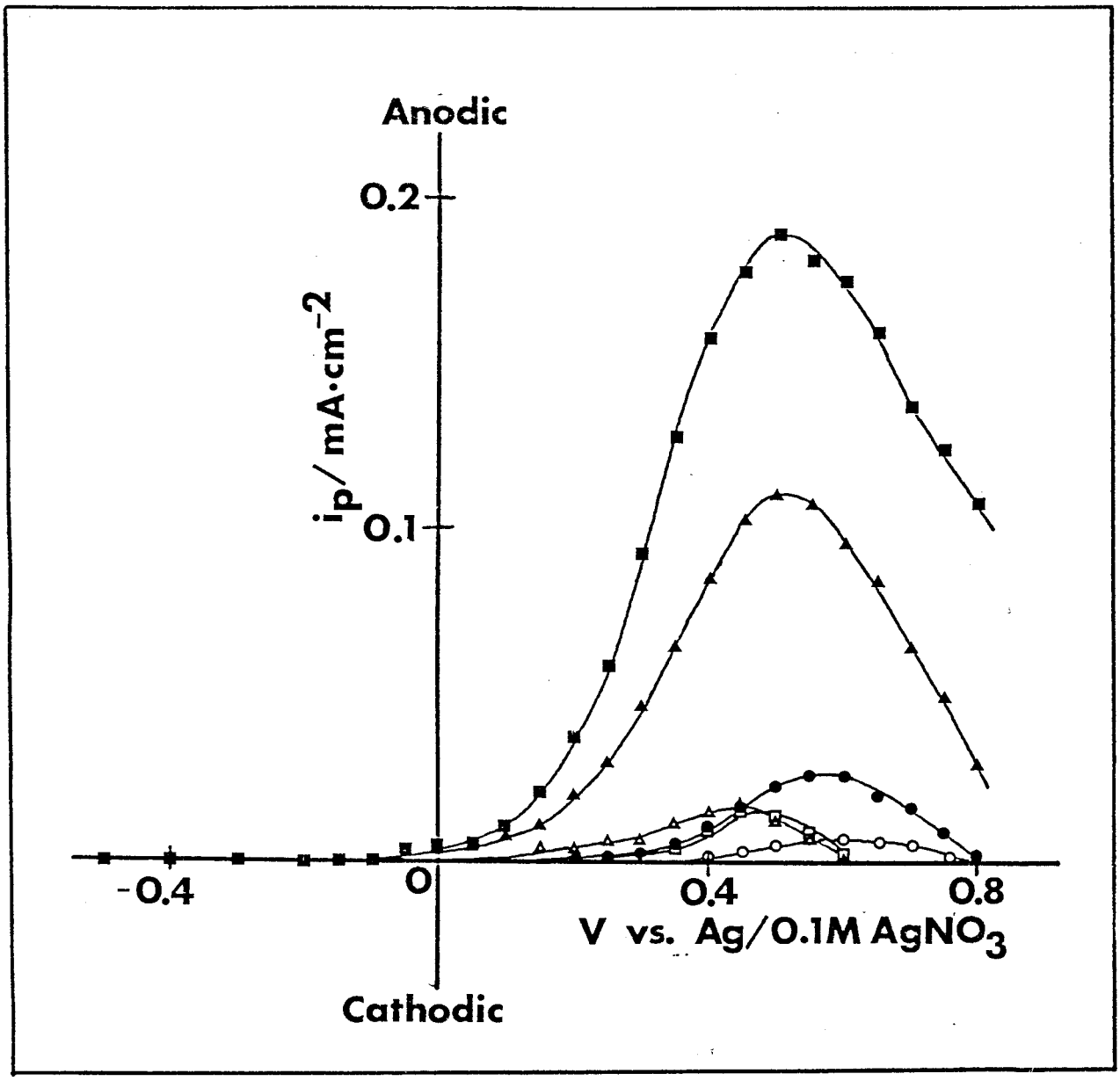

Figure 2. Current-potential curves on irradiation of n-TiO_2 in MeCN solution containing 0.1 mol/dm^3 Et_4NClO_4 with various aromatic olefins. (▣) trans-Stilbene, (▲) 2-methyl-1,1-diphenylpropene, (●) 1,1-diphenylethylene, (△) 2- phenylpropene, (○) cyclooctene, and (□) 4-phenyl-3-buten-2-one.

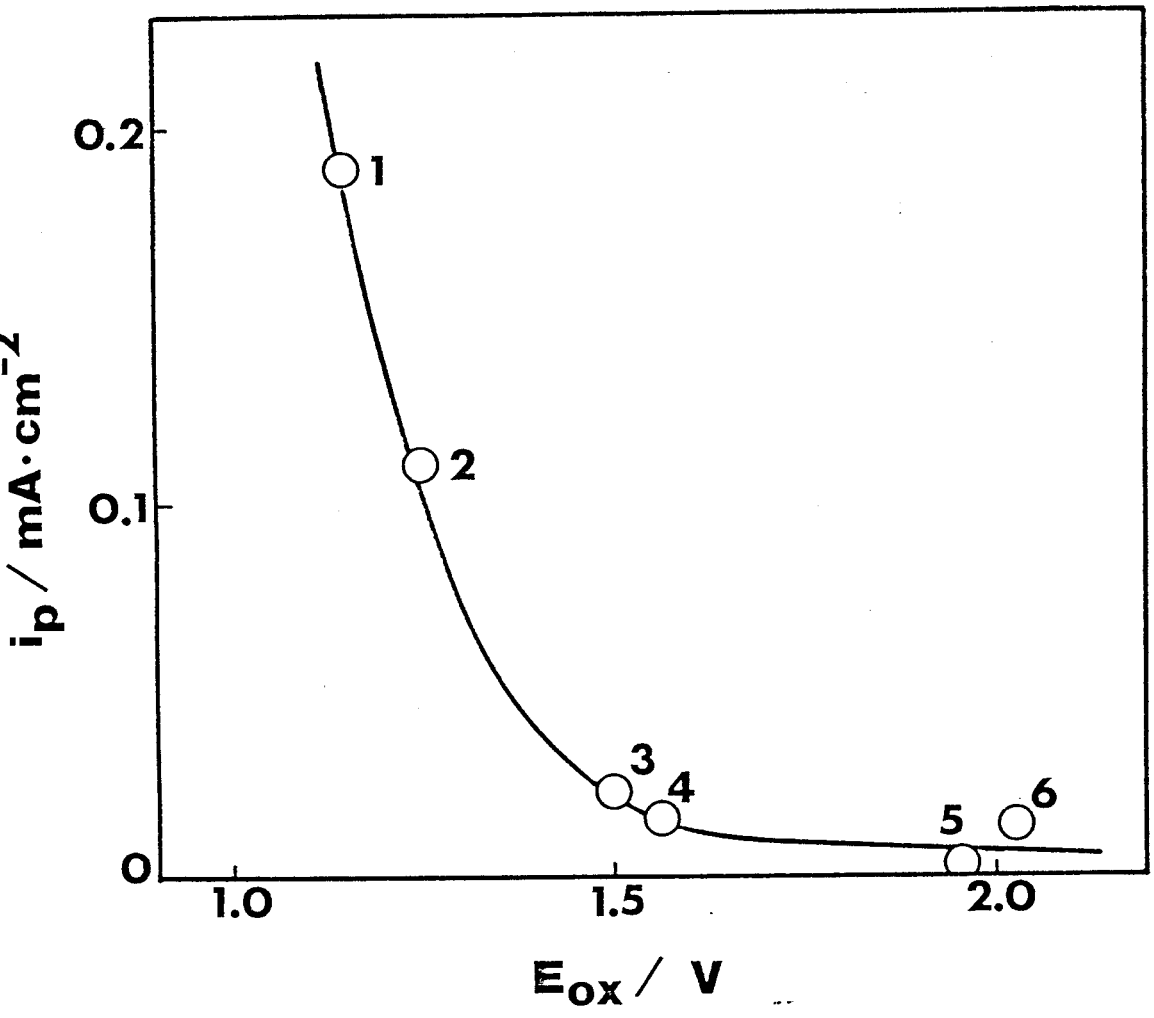

Figure 3. Correlation of photocurrent (i_p/mA cm^{-2}) with oxidation potentials (E_{ox}/V vs. Ag/$AgNO_3$) in MeCN soltion with 0.1 mol/dm^3 Et_4NClO_4. (1) trans-Stilbene, (2) 2-methyl-1,1-diphenylpropene, (3) 1,1-diphenylethylene, (4) 2-phenylpropene, (5) cyclooctene, and (6) 4-phenyl-3-buten-2-one.

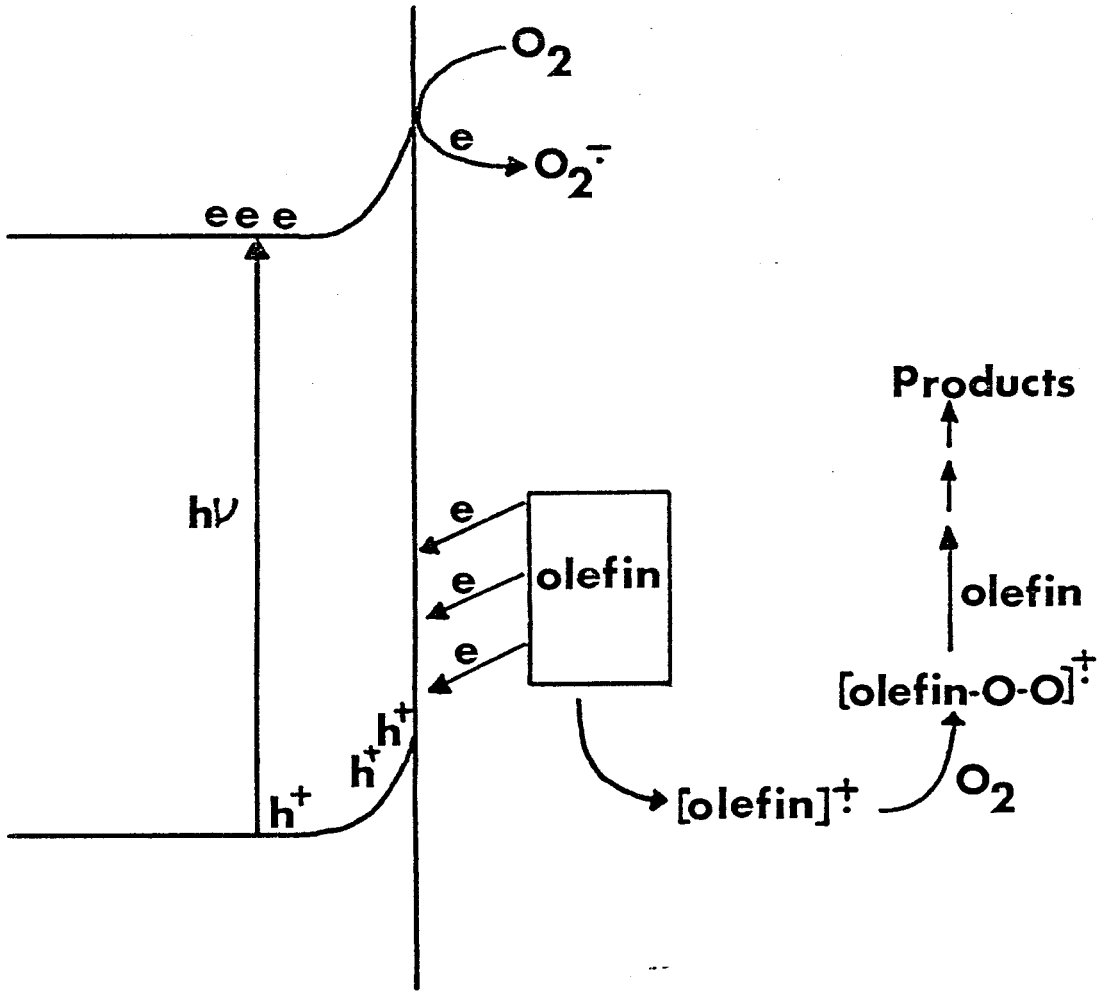

Figure 4. Schematic representation of semiconductor photocatalyzed oxygenation of olefins.

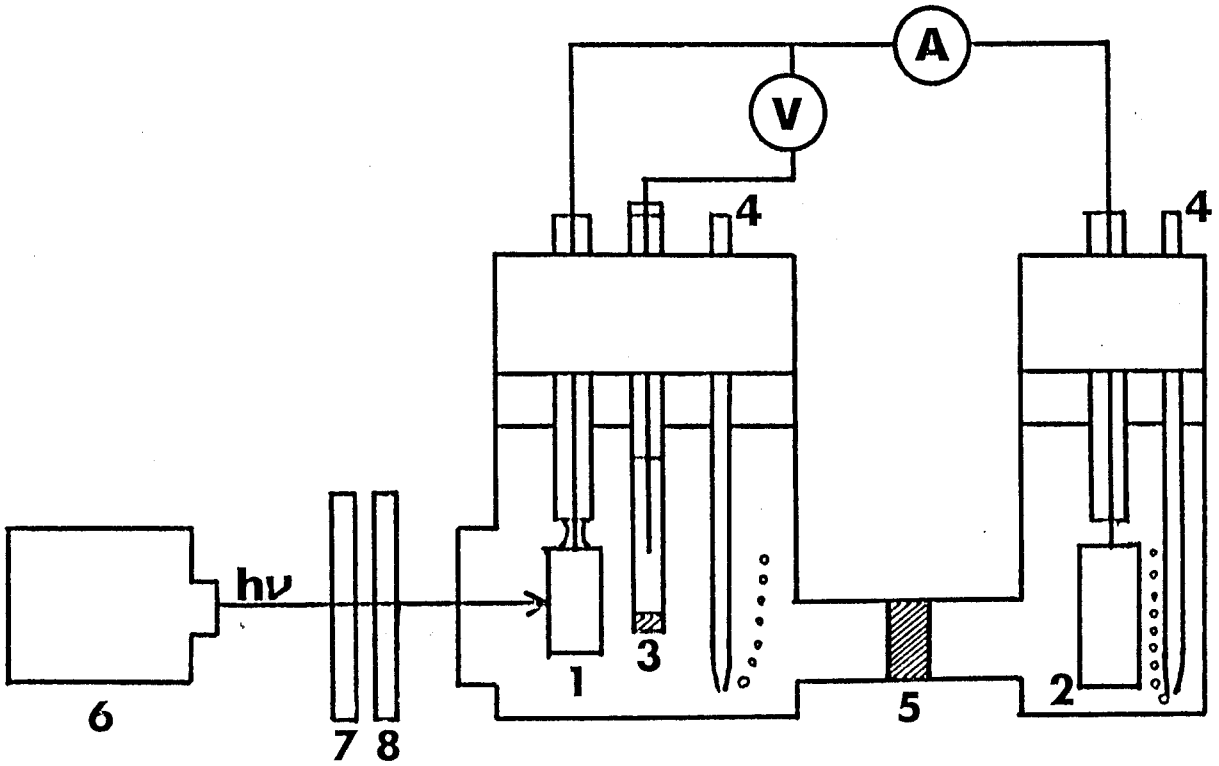

Figure 5. Apparatus for the measurement of voltammetric curves on TiO_2. (1) n-TiO_2 electrode, (2) Pt electrode, (3) Ag/0.1 mol /dm^3 $AgNO_3$ reference electrode, (4) Ar gas, (5) glass frit, (6) 500 W Xe lamp, (7) Toshiba UV-D36B glass filter, (8) Toshiba UV-35 glass filter.

Chapter 3

PHOTOSENSITIZING ACTION OF EOSIN Y FOR VISIBLE LIGHT INDUCED HYDROGEN EVOLUTION FROM WATER

Summary

Eosin Y was not photobleached with triethanolamine (TEOA) on visible light irradiation in the presence of methyl viologen (MV^{2+}), and worked as an effective sensitizer to reduce MV^{2+} into $MV^{+\cdot}$ with TEOA in aqueous ethanol. The resulting $MV^{+\cdot}$ reduced water to hydrogen in the presence of collidal platinum in the same solvent. The quantum yield for $MV^{+\cdot}$ formation was determined to be ca. 0.3. Nanosecond and microsecond laser flash photolysis techniques enabled to elucidate the detailed mechanism. The photo-induced MV^{2+} reduction are revealed to be initiated by electron transfer from triplet excited Eosin Y to MV^{2+} followed by electron transfer to the resulting $EY^{-\cdot}$ from TEOA.

Introduction

Currently considerable efforts have been devoted to achievement of hydrogen evolution from water through visible light-induced redox reactions in relation to solar energy conversion and storage.[1] The general scheme of a suitable electron transfer system is shown below:

$$S \xrightarrow{h\nu(\text{visible light})} S^* \quad (1)$$

$$S^* + A \longrightarrow S^{+\cdot} + A^{-\cdot} \quad (2)$$

$$2A^{-\cdot} + 2H_2O \xrightarrow{\text{Catalyst}} H_2 + 2OH^- + 2A \quad (3)$$

$$S^{+\cdot} + D \longrightarrow S + D^{+\cdot} \quad (4)$$

$$D^{+\cdot} \longrightarrow \text{Products} \quad (5)$$

where S stands for a photosensitizer, A and D are an electron acceptor and an electron donor, respectively, and water reduction to hydrogen achieves with a redox catalyst. In most investigations methyl viologen (MV^{2+}) has been employed as the electron acceptor (A) and triethanolamine (TEOA) or ethylenediaminetetraacetic acid (EDTA) as the irreversible electron donor (D), and colloidal platinum or hydrogenase is required as the redox catalyst. Among sensitizers, ruthenium complexes,[2] porphyrins,[3-12] and phthalocyanines[13] have almost exclusively been employed in these studies; however, only a few

reports have appeared on utilization of organic dyes.[14-18] For the purpose of solar energy conversion, it is important that the chromophore absorbs a large part of the solar spectrum, has an appropriate redox potential, and is inexpensive and readily available. Some organic dyes are cheaper than the above metal complexes and fill moderately the other terms.

Previously, Bellin and coworkers[14] have found that proflavin, one of acridine dyes, worked as an effective sensitizer to reduce MV^{2+} into $MV^{+\cdot}$ with EDTA, and the quantum yield for $MV^{+\cdot}$ production achieved 0.72 under optimal conditions.[14] They suggested that the reaction proceeded through the electron transfer from EDTA to singlet excited proflavin and subsequent reaction between the resulting one electron reduced proflavin and MV^{2+} (reduction cycles); however, the detailed investigation for the dynamics of each reaction process was not carried out at all. On the other hand, Kalyanasundaram and coworkers[16] performed a laser flash photolysis of the proflavin-MV^{2+}-EDTA system, and showed that the reaction at low MV^{2+} concentrations ($<5 \times 10^{-5}$ mol/dm^3) was initiated by the electron transfer from EDTA to triplet excited proflavin (reduction cycles), and that at much higher concentration of MV^{2+} the $MV^{+\cdot}$ formation occurred both by the reduction cycles and by the electron transfer from singlet excited proflavin to MV^{2+} and subsequent reaction between the resulting one electron oxidized proflavin and EDTA (oxidation cycles).[16] However, the

detailed evaluation of the rate constants of the system was not attempted because of overlapping of the spectra of the various transient species. Bolton and coworkers[17] reported a comprehensive study, using continuous light irradiation and microsecond flash photolysis techniques, of the mechanism of the electron transfer reaction from EDTA to MV^{2+} sensitized by acridine orange.[17] They showed that the $MV^{+\cdot}$ formation occurred not only by oxidation cycles via triplet excited acridine orange but also by reduction cycles via singlet excited acridine orange. However, they did not determine the exact rate constant of the fast stage of the reactions in the nanosecond domain. In spite of the importance of the electron transfer reactios sensitized by organic dyes in solar energy conversion and storage, little is known about the mechanism of these reactions.

We selected Eosin Y (2′,4′,5′,7′-tetrabromofluorescein disodium salt) which is one of xanthene dyes as a sensitizer. Xanthene dyes are known to be irreversibly photobleached in alcoholic solutions under nitrogen into their leuco-forms;[19,20] the resulting matters cannot be reconverted to the starting dyes on contact with air. This behavior is in remarkable contrast with thiazine dyes which are reversibly photoreduced under nitrogen in alcoholic solutions into the leuco-forms;[19,21] the starting dyes can be recovered on contact with air. However, we have recently found that Eosin Y (EY^{2-}) is not photobleached in the presence of MV^{2+} and TEOA, and works as an effective

sensitizer for reduction of MV^{2+} into $MV^{+\cdot}$, which subsequently reduces water to hydrogen in the presence of colloidal platinum.[22] Moreover, we have carried out a detailed mechanistic study of the electron transfer processes in the EY^{2-}-MV^{2+}-TEOA system using nanosecond and microsecond laser flash photolysis techniques.

Recently, several workers[3,9-12] have found that positively charged water-soluble zinc porphyrins photosensitize the reduction of MV^{2+} to $MV^{+\cdot}$ with high efficiency despite very slow forward electron transfer. However, negatively charged substituents on porphyrins prevent to yield $MV^{+\cdot}$ despite the high probability of forward electron transfer. It can be explained that with the use of a positively charged porphyrin the electrostatic repulsion in the ion pair formed by the forward electron transfer effectively leads to separated ion products before the recombination between the radical ion pairs can accomplish.[3,9-12] In contrast with these reports, Eosin Y, which has two negative charges, is found to be an efficient photosensitizer of MV^{2+} reduction. This chapter deals with the mechanistic study of photoinduced electron transfer reactions of EY^{2-} employing steady-state irradiation and nanosecond laser flash photolysis techniques.

Results

1. Continuous Irradiation

1.1 Absorption Spectrum Change on Steady Light Irradiation

Irradiation of methylene blue (MB^+) (1.5×10^{-5} mol/dm^3) and TEOA (1.0×10^{-2} mol/dm^3) in a 1:1 ethanol-water (pH 5) mixture with visible light of λ>550 nm from a tungsten-bromine lamp under nitrogen atmosphere led to monotonous decrease of the absorption of the starting dye. On introduction of air to the irradiation mixture, the absorption band of MB^+ was recovered unchanged as before the irradiation (Figure 1). However, irradiation of EY^{2-} (1.7×10^{-5} mol/dm^3) in a 1:1 ethanol-water (pH 5) solution containing TEOA (5.1×10^{-2} mol/dm^3) with visible light of λ>450 nm resulted in rapid bleaching of EY^{2-} in 60 s, and the original color of the dye was not recovered at all on introduction of air into the solution after the irradiation (Figure 2). This behavior of EY^{2-} is in remarkable contrast with MB^+ which are reversibly photoreduced into the leuco-form under nitrogen atmosphere in alcoholic solutions.

Addition of MV^{2+} (5.1×10^{-2} mol/dm^3) to a solution of MB^+ (1.5×10^{-5} mol/dm^3) and TEOA (1.0×10^{-2} mol/ dm^3) in a 1:1 ethanol-water (pH 5) mixture on irradiation with visible light of λ>550 nm under nitrogen atmosphere led to decrease of the absorption band of the starting dye during the initial illumination

(Figure 3). On prolonged illumination, small absorption bands appeared around 395 and 602 nm due to the formation of $MV^{+\cdot}$ by one electron reduction of MV^{2+}. Introduction of air to the irradiation mixture caused quick disappearance of the $MV^{+\cdot}$, and the absorption of the starting MB^{+} was recovered completely. These results show that the $MV^{+\cdot}$ is produced by electron transfer from TEOA to MV^{2+} by sensitization with MB^{+}, though with a very low efficiency.

Irradiation of an aqueous ethanol solution of EY^{2-} (1.7×10^{-5} mol/dm^3) in the presence of TEOA (4.7×10^{-2} mol/dm^3) and MV^{2+} (5.2×10^{-3} mol/dm^3) with visible light (λ>450 nm) under nitrogen atmosphere caused rapid growth of the absorption bands around 602 and 395 nm due to the production of $MV^{+\cdot}$ in an amount of 1.6×10^{-4} mol/dm^3 in 90 s. This result clearly indicates that EY^{2-} acts as an effective sensitizer to induce reduction of MV^{2+} by TEOA. The amount of the resulting $MV^{+\cdot}$ during the irradiation means that the electron transfer through EY^{2-} was cycled 9 times in the irradiation period. On introduction of air into the irradiated solution, the resulting absorption due to $MV^{+\cdot}$ disappeared completely and the absorption band of EY^{2-} was recovered quantitatively (Figure 4). It is noticeable that EY^{2-} sensitizes more efficiently the reduction of MV^{2+} by TEOA than MB^{+}, although EY^{2-} is irreversibly and MB^{+} is reversibly photobleached on irradiation with TEOA.

On the other hand, when EY^{2-} (1.7×10^{-5} mol/dm^3) was

irradiated in the precence of only MV^{2+} (5.1×10^{-3} mol/dm^3) in 1:1 ethanol-water (pH 5) without TEOA with light of λ>450 nm under nitrogen atmosphere, the absorption spectrum was not changed at all.

1.2 Complex Formation Between EY^{2-} and MV^{2+} in the Ground State

The absorption band of EY^{2-} was shifted on addition of MV^{2+} in a 1:1 ethanol-water (pH 5) mixture as depicted in Figure 5. This indicates the formation of a complex between EY^{2-} and MV^{2+}. Also, MV^{2+} effectively quenched fluorescence of EY^{2-} in a 1:1 ethanol-water (pH 5) mixture in intensity but did not affect the fluorescence lifetime at all (Figure 6). These facts mean that EY^{2-} forms a non-fluoresent complex with MV^{2+} in the ground state as shown in Eq. 1, but singlet excited EY^{2-} is not quenched with MV^{2+}.

$$EY^{2-} + MV^{2+} \overset{K}{\rightleftharpoons} (EY^{2-} \cdots MV^{2+}) \quad (1)$$

Figure 6 shows the plot of the ratios of luminesence intensities, (I_0/I), in the absence of and in the presence of MV^{2+} against the MV^{2+} concentrations in a 1:1 ethanol-water (pH 5) mixture affording a linear relationship. This relationship can be expressed by Eq. 2:

$$I_0/I = 1 + K[MV^{2+}] \qquad (2),$$

where K denotes the equilibrium constant, which corresponds to the apparent Stern-Volmer constant. The equilibrium constant is obtained from the slope in Figure 6 as nearly 600 mol^{-1} dm^3 in a 1:1 ethanol-water (pH 5) mixture. The equilibrium constant was strongly dependent upon the ionic strength of the medium, and decreased with the increase of the ionic strength[23]. This fact shows that the complex in the ground state is produced by electrostatic attraction between EY^{2-} and MV^{2+} and not by their hydrophobic interaction.

1.3 Quantum Yields

Quantum yields were determined on irradiation of sample solutions in a mixture (1:1 by volume, 4 ml) of ethanol and water which was adjusted to pH 5 with phthalate buffer with 490 nm light obtained through a monochromator (slit width: 20 nm) from a 500 W xenon lamp employing potassium tris(oxalato)ferrate(III) actinometry.

The quantum yield for disappearance of EY^{2-} (8.6×10^{-5} mol/dm^3) in the presence of TEOA [$(3.0\text{-}12.0) \times 10^{-3}$ mol/dm^3] alone was determined by following the decrease of absorption of EY^{2-} at 480 nm (molar absorption coefficient: 2.03×10^4 dm^3 mol^{-1} cm^{-1}). As indicated in Figure 7, the reciprocal of the quantum yield shows a linear Stern-Volmer relationship against

the reciprocal of the concentration of TEOA. The limiting quantum yield, the quantum yield extrapolated to infinite concentration of TEOA, was 0.11.

The quantum yield of $MV^{+\cdot}$ production in the three-component system (EY^{2-}-MV^{2+}-TEOA) was determined by the absorption of the resulting $MV^{+\cdot}$ on irradiation of EY^{2-} (8.6×10^{-5} mol/dm^3) with 490 nm light as above in the presence of a fixed concentration of MV^{2+} (1.0×10^{-3} mol/dm^3) and varying concentrations of TEOA [$(3.0\text{-}12.0) \times 10^{-3}$ mol/dm^3]. The results fit the Stern-Volmer relationship as depicted in Figure 8 with the limiting quantum yield of 0.29.

On the other hand, on irradiation of EY^{2-} (8.6×10^{-5} mol/dm^3) with a fixed concentration of TEOA (1.0×10^{-2} mol/dm^3) and varied concentrations of MV^{2+} (1.0×10^{-5}-1.0×10^{-3} mol/dm^3) the quantum yield for $MV^{+\cdot}$ production increased from 0.15 to 0.20 with increasing concentration of MV^{2+} from 1.0×10^{-5} to 1.0×10^{-4} mol/dm^3, and then remained nearly 0.20 despite the increase in MV^{2+} concentration up to nearly 1.0×10^{-3} mol/dm^3 as shown in Figure 9. The observed insensitivity of the quantum yield to the MV^{2+} concentration in more than 1.0×10^{-4} mol/dm^3 must be related with the formation of the complex between EY^{2-} and MV^{2+}.

1.4 Hydrogen Evolution

To examine the formation of hydrogen from the present sensitizing system, the irradiation was carried out with added

colloidal platinum catalyst carried by poly vinyl alcohol (PVA) and the resulting hydrogen was determined. In a typical run, 10 ml of a 1:1 ethanol-water (pH 5) mixture containing 5.0×10^{-4} mol/dm^3 EY^{2-}, 1.0×10^{-4} mol/dm^3 MV^{2+}, 1.0×10^{-2} mol/dm^3 TEOA, and 6.6×10^{-5} mol/dm^3 colloidal platinum-PVA catalyst was irradiated under stirring through a 450 nm cut-off filter with a 500 W xenon lamp. After the irradiation for 5 h, 1.9 ml of hydrogen was generated.

The yield of hydrogen was found to depend strongly on the concentration of MV^{2+}. The effect of the MV^{2+} concentration on hydrogen evolution is illustrated in Figure 10. The high concentration of MV^{2+} tended to suppress the production of hydrogen.

The hydrogen evolution was influenced by temperature, solvent, and inorganic additives as shown in Tables 1, 2, and 3, respectively.

2. Laser Pulse Excitation

To determine the kinetics of the transient species in the photoinduced electron transfer, nanosecond laser flash photolysis was carried out for EY^{2-}-MV^{2+}, EY^{2-}-TEOA, and EY^{2-}-MV^{2+}-TEOA systems.

On excitation of EY^{2-} (1.0×10^{-3} mol/dm^3) in a 1:1 ethanol-water (pH 5) mixture with a 337.1 nm laser pulse transient absorptions appeared, which are assigned to the triplet excited state of EY^{2-} [$^3(EY^{2-})^*$], its one electron reduced form ($EY^{3-\cdot}$),

and the one electron oxidized form ($EY^{-\cdot}$)of the dye.[24] Figures 11 and 12 illustrate the transient absorption spectra obtained under argon and oxygen atmosphere, respectively. The broad transient absorption band around 600 nm is assigned to the T-T absorption of EY^{2-}.[24] As comparison between Figures 11 and 12 indicates, the absorption band around 415 nm was quenched effectively by oxygen but that around 440 nm was not quenched by oxygen, and accordingly, these bands are safely assigned to $EY^{3-\cdot}$ and $EY^{-\cdot}$, respectively.

Moreover, it is worth mentioning that the absorptions of both $EY^{3-\cdot}$ and $EY^{-\cdot}$ appeared simultaneously within 25 ns after the laser pulse. These results will be discussed later.

The two-component system of EY^{2-} and MV^{2+} was examined in aqueous ethanol by nanosecond and microsecond laser flash photolyses. The kinetic analysis of this system was carried out by monitoring the characteristic absorption of $MV^{+\cdot}$ at 395 nm, the T-T absorption of $^{3}(EY^{2-})^{*}$ at 650 nm, the absorption of $EY^{3-\cdot}$ at 415 nm, and that of $EY^{-\cdot}$ at 462 nm, respectively.

After laser excitation, decay of the T-T absorption of $^{3}(EY^{2-})^{*}$ was accompanied by synchronized buildup of the $MV^{+\cdot}$ absorption. The increase of MV^{2+} concentration tended to reduce the intensity of the T-T absorption observed immediately after laser excitation (25 ns). The increase of MV^{2+} concentration to 1.5×10^{-2} mol/dm^3 did not result in the appearance of the T-T absorption, and the buildup of only a small absorption band due

to $MV^{+\cdot}$ was observed. This fact indicates that excitation of the complex formed in the ground state does not efficiently result in the electron transfer and that excitation of uncomplexed EY^{2-} is efficient to reduce MV^{2+}.

Figures 13 and 14 illustrate oscilloscope traces of these events. As indicated in Figure 14-a, the absorption of $MV^{+\cdot}$ gradually built up in overlapping with the $EY^{3-\cdot}$ absorption which had arisen immediately after the laser pulse and attained at the plateau. However, the absorption of $EY^{3-\cdot}$ around 415 nm did not decay during the time domain of $MV^{+\cdot}$ buildup. The pseudo-first order rate constant for the buildup of $MV^{+\cdot}$, $^{1}k_{MV^{+\cdot}}$, can be estimated by Eq. 3:

$$^{1}k_{MV^{+\cdot}} = \{\ln(A_p - A_0) - \ln(A_p - A_t)\}/t \qquad (3),$$

where A_p, A_t, and A_0 represent the absorbances respectively in the plateau region (see Figure 14), at the time t, and due to $EY^{3-\cdot}$ which quickly built up after laser excitation.

Experiments performed with a series of MV^{2+} concentrations showed that the kinetics of the quenching of the T-T absorption and the buildup of $MV^{+\cdot}$ are of the pseudo-first order with respect to MV^{2+} as shown in Figure 15. The slope of the plot in Figure 15 indicates second order rate constants to be $k_{MV^{+\cdot}}=4.0 \times 10^9$ dm^3 mol^{-1} s^{-1} for the $MV^{+\cdot}$ buildup and $k_{T-T}=2.0 \times 10^9$ dm^3 mol^{-1} s^{-1} for the quenching of T-T absorption, respectively.

These values conform with each other . Accordingly, it is clear that $MV^{+\cdot}$ is produced by electron transfer from the triplet excited state of EY^{2-} to MV^{2+} as shown in Eq. 4;

$$^3(EY^{2-})^* + MV^{2+} \xrightarrow{k(MV^{2+})} EY^{-\cdot} + MV^{+\cdot} \qquad (4)$$

The quenching rate constant is obtained as $k(MV^{2+})=3.0 \times 10^9$ dm^3 mol^{-1} s^{-1} as the average of the above values.

Oscilloscope traces in Figure 16 shows the long-time behavior of the $MV^{+\cdot}$ absorption at 395 nm and the $EY^{-\cdot}$ absorption at 462 nm.[25] The signal at 395 nm decays concomitantly with the 462 nm absorption decay, indicating that the back electron transfer from $MV^{+\cdot}$ to $EY^{-\cdot}$ occurred in this time domain as described by Eq. 5;

$$EY^{-\cdot} + MV^{+\cdot} \xrightarrow{k(back)} EY^{2-} + MV^{2+} \qquad (5),$$

where k(back) denotes the rate constant of this process. The rate constant exhibits second order characteristics and the kinetic evaluation yields $k(back)=6.0 \times 10^9$ dm^3 mol^{-1} s^{-1}.

In laser flash photolysis experiments in 1:1 ethanol-water (pH 5) solutions containing only TEOA and EY^{2-} (1.0×10^{-3} mol/dm^3), even at a relatively high TEOA concentration (1.3×10^{-2} mol/dm^3), the lifetime of T-T absorption of EY^{2-} remained unchanged and the characteristic absorption of $EY^{3-\cdot}$ at 415 nm

did not increase after the very rapid formation immediately after a laser pulse.

The three component system, EY^{2-} (1.0×10^{-3} mol/dm^3)-MV^{2+} (7.0×10^{-4} mol/dm^3)-TEOA was investigated with varying concentrations of TEOA. Figure 17 depicts buildup curves of $MV^{+\cdot}$ (395 nm) and shows that the rate was not affected by the presence of and increase of the concentration of TEOA. The rate constants for the $MV^{+\cdot}$ formation are estimated as in the EY^{2-}-MV^{2+} system and are plotted against TEOA concentrations in Figure 18, which again shows that the rate constants are almost unchanged with the TEOA concentration.

Figure 19 illustrates the decay curves of the 395 nm absorption 1.5 μs after the excitation examined with varying concentrations of TEOA. The decay of $MV^{+\cdot}$ became slow with increasing concentration of TEOA and, at [TEOA]=2.0×10^{-3} mol/dm^3, the absorption did not decay at all.

These results indicate that the primary electron transfer in the three-component system occurs exclusively via a reaction between the triplet excited state of EY^{2-} and MV^{2+}. The resulting $MV^{+\cdot}$ can be sufficiently long lived in the presence of a sufficient concentration of TEOA which will efficiently reduce $EY^{-\cdot}$ into EY^{2-} to intercept the back electron transfer between $EY^{-\cdot}$ and $MV^{+\cdot}$. Therefore, the overall electron transfer process may be written as follows:

$$^3(EY^{2-})^* + MV^{2+} \longrightarrow EY^{-\cdot} + MV^{+\cdot} \qquad (6)$$

$$EY^{-\cdot} + TEOA \longrightarrow EY^{2-} + TEOA^{+\cdot} \qquad (7),$$

Discussion

1. EY^{2-}-TEOA System

As mentioned earlier, EY^{2-} is photobleached with TEOA; however, the transient spectroscopy showed that the triplet state of EY^{2-} is not quenched by TEOA in the time domain of the order of 20 μs, which suggests that the quenching will take place in late time domain after the excitation. If the photoreduction of EY^{2-} by TEOA proceeds via the triplet excited state as shown in Figure 20,[24] the Stern-Volmer equation of EY^{2-} disappearance can be written as follows:

$$\Phi^{-1} = \Phi_{ST}^{-1}(1 + 1/k_q\tau_T[TEOA])(1 + k_d"/k_r) \quad (8)$$

where Φ_{ST} denotes the triplet yield, k_i (i=q, r, and d") represent the corresponding rate constants shown in Figure 20. The ratio of the intercept to the slope in the plot in Figure 7, gives 112 $dm^3\ mol^{-1}$ as the value of $k_q\tau_T$. The fluorescence of EY^{2-} was quenched by addition of TEOA and the Stern-Volmer plot was found to be linear (Figure 21). The Stern-Volmer constants, which are estimated by both fluorescence intensity and lifetime, are $k_q\tau_S$=1.0 and 1.9 $dm^3\ mol^{-1}$, respectively. These results clearly indicate that the photoreduction of EY^{2-} by TEOA proceeds via the triplet excited state of EY^{2-} as shown in Figure 20. The quenching rate constant (k_q) of this process can be estimated

from the Stern-Volmer constant ($k_q\tau_T$) and the lifetime of $^3(EY^{2-})^*$ (5.28 μ s) to be nearly $k_q=2 \times 10^7$ dm^3 mol^{-1} s^{-1}. The above result means that the transient absorption of $^3(EY^{2-})^*$ is scarcely quenched by TEOA of which the concentration is less than 1×10^{-2} mol/dm^3. The laser excitation of EY^{2-} in aqueous alcohol in the absence of TEOA led to the rapid formation of $EY^{3-}\cdot$ and $EY^{-}\cdot$ within 25 ns after the pulse excitation, which corresponds to the time constant of the apparatus employed. One could suppose that irradiation of EY^{2-} with added TEOA, the resulting $EY^{-}\cdot$ will react with TEOA.[24] However, the Stern-Volmer equation for the D-D mechanism [interaction of $^1(EY^{2-})^*$ or $^3(EY^{2-})^*$ with EY^{2-}] does not satisfy the results of the Stern-Volmer plot in Figure 7, so that the photoreduction of EY^{2-} under the condition of the continuous light irradiation proceeds via the triplet excited state of EY^{2-}.

Previously, it was reported that excitation of EY^{2-} in the absence of donors such as TEOA gave $EY^{3-}\cdot$ and $EY^{-}\cdot$ by disproportionation between the triplet state EY^{2-} and the ground state EY^{2-} (D-D mechanism) with a rate constant $k_{D-D}=8 \times 10^8$ dm^3 mol^{-1} s^{-1} on the basis of the microsecond flash photolysis work.[24] However, the present results show that the rate constant for the formation of $EY^{3-}\cdot$ and $EY^{-}\cdot$ must be larger than 10^{10} dm^3 mol^{-1} s^{-1}. Therefore, it is reasonable to suppose that these radical ions are directly produced from the singlet excited state of EY^{2-} ($^1D^*$-D) but not from the triplet excited state of EY^{2-} ($^3D^*$-D).

2. EY^{2-}-MV^{2+} System

Although the continuous light irradiation of EY^{2-} in the presence of MV^{2+} does not result in the formation of $MV^{+\cdot}$, the laser pulse excitation was found to give $MV^{+\cdot}$ and $EY^{-\cdot}$, which subsequently recombined to result in EY^{2-} and MV^{2+}. A finding in the effect of a high concentration of MV^{2+} to reduce the formation of $MV^{+\cdot}$ and to suppress the formation of any detectable amount of $^{3}(EY^{2-})^{*}$ indicates that the excitation of the ground state complex between EY^{2-} and MV^{2+} is not effective to reduce MV^{2+} into $MV^{+\cdot}$ or the resulting pair between $EY^{-\cdot}$ and $MV^{+\cdot}$ would quickly undergo back electron transfer.

3. EY^{2-}-MV^{2+}TEOA System

The continuous light irradiation of the EY^{2-}-MV^{2+}-TEOA system led to the reduction of MV^{2+} into $MV^{+\cdot}$. However, it is important to differentiate whether the reaction is started by electron transfer from excited EY^{2-} to MV^{2+} followed by electron transfer to the resulting $EY^{-\cdot}$ from TEOA or by the reaction between excited EY^{2-} and TEOA followed by the reaction between the resulting $EY^{3-\cdot}$ and MV^{2+}; both processes are thermodynamically possible. The results of the laser spectroscopy clearly indicates that the reaction is initiated by the electron transfer from the triplet EY^{2-} to MV^{2+}. This process is not observable under the continuous light irradiation. This result is very

significant since the mechanism for the dye-sensitized reduction of MV^{2+} has not been very clear. If the back electron transfer from $MV^{+\cdot}$ to $EY^{-\cdot}$ does not occur in the presence of TEOA (2.0×10^{-2} mol/dm^3) (Figure 19), the rate constant for reaction (7) is evaluated to be nearly 6×10^8 dm^3 mol^{-1} s^{-1} from the data summarized in Figure 22 .

4. Free Energy Change of the Dye-sensitized Electron Transfer Process

The overall standard free-energy change of the photo-induced electron transfer processes (ΔG) can be estimated from the relevant redox potentials. The redox potentials of the triplet excited state of sensitizers [$E_0(S^{+\cdot}/{}^3S^*)$ and $E_0({}^3S^*/S^{-\cdot})$] can be estimated by combining the triplet excitation energies and the ground state redox potentials as shown in Eq. (9) and (10), respectively;

$$E_0(S^{+\cdot}/{}^3S^*)=E_0(S^{+\cdot}/S) - E_T \qquad (9),$$

$$E_0({}^3S^*/S^{-\cdot})=E_0(S/S^{-\cdot}) + E_T \qquad (10),$$

where S denotes a sensitizer. The estimated values for EY^{2-} and MB^+ are listed in Table 4. The free energy changes (ΔG) for the following processes (Eq. 11, 12, and 13) are given by Eqs. 14, 15, and 16, respectively.

$$^3S^* + MV^{2+} \longrightarrow S^{+\cdot} + MV^{+\cdot} \quad (11)$$

$$^3S^* + TEOA \longrightarrow S^{-\cdot} + TEOA^{+\cdot} \quad (12)$$

$$S^{-\cdot} + MV^{2+} \longrightarrow S + MV^{+\cdot} \quad (13)$$

$$\Delta G(kcal/mol)=23.06[E_0(S^{+\cdot}/^3S^*)-E_0(MV^{2+}/MV^{+\cdot})] \quad (14)$$

$$\Delta G(kcal/mol)=23.06[E_0(^3S^*/S^{-\cdot})-E_0(TEOA^{+\cdot}/TEOA)] \quad (15)$$

$$\Delta G(kcal/mol)=23.06[E_0(S/S^{-\cdot})-(E_0(MV^{2+}/MV^{+\cdot})] \quad (16)$$

The estimated values listed in Table 5 show that among the sensitizers examined the overall standerd free-energy changes with EY^{2-} are much more negative than those with MB^+ (Figure 23). In contrast, with MB^+ the overall ΔG for MV^{2+} reduction process is positive (Figure 23), so that the electron transfer process 11 and 13 should be prohibited on the thermodynamic ground.

5. Catalytic Production of Hydrogen

The addition of platinum catalyst to the EY^{2-}-MV^{2+}-TEOA system led to the production of hydrogen. As Figure 10 indicates, high concentrations of MV^{2+} tended to suppress the production of hydrogen. This result does not agree with the

effect of the MV^{2+} concentration on the quantum yield; the quantum yield of the $MV^{+\cdot}$ production remained nearly 0.20 despite increase in the MV^{2+} concentration from 1.0×10^{-4} to 1.0×10^{-3} mol/dm^3. This means that the electron transfer process from $MV^{+\cdot}$ to the colloidal platinum-PVA was inhibited when the irradiation was carried out in the presence of a high concentration of MV^{2+}.

Previously, it has been reported that $MV^{+\cdot}$ tends to dimerize in aqueous solutions;[26]

$$2MV^{+\cdot} \underset{K=714\ dm^3\ mol^{-1}}{\rightleftharpoons} (MV^{+\cdot})_2 \qquad (17).$$

The standard free-energy change in the dimerization of $MV^{+\cdot}$ is estimated as -3.9 kcal mol^{-1}, and the dimer, which is much more stable than the monomer, has a redox potential E_0= -0.29 V vs. NHE.[27] Consequently, for the cation radical dimer to reduce water and to produce hydrogen it is neccessary that the solution has pH<5, since the reduction potential of water, $E(H^+/H_2)$, is larger than -0.295 V vs. NHE at pH<5. Accordingly, it is likely that at high concentrations of MV^{2+}, the resulting $MV^{+\cdot}$ tends to dimerize, and the resulting dimer is not sufficiently capable of reducing water by the assistance of the colloidal platinum.

6. Estimation of the Rate Constants in the Electron Transfer and its Efficiency

Several attempts have been done to estimate the rate constants involved in and the efficiency of the photo-induced intermolecular electron transfer from the triplet excited state sensitizers to MV^{2+}.[9,10] Scheme 1 shows the mechanism for the electron transfer in the EY^{2-}-MV^{2+} system.

Scheme 1

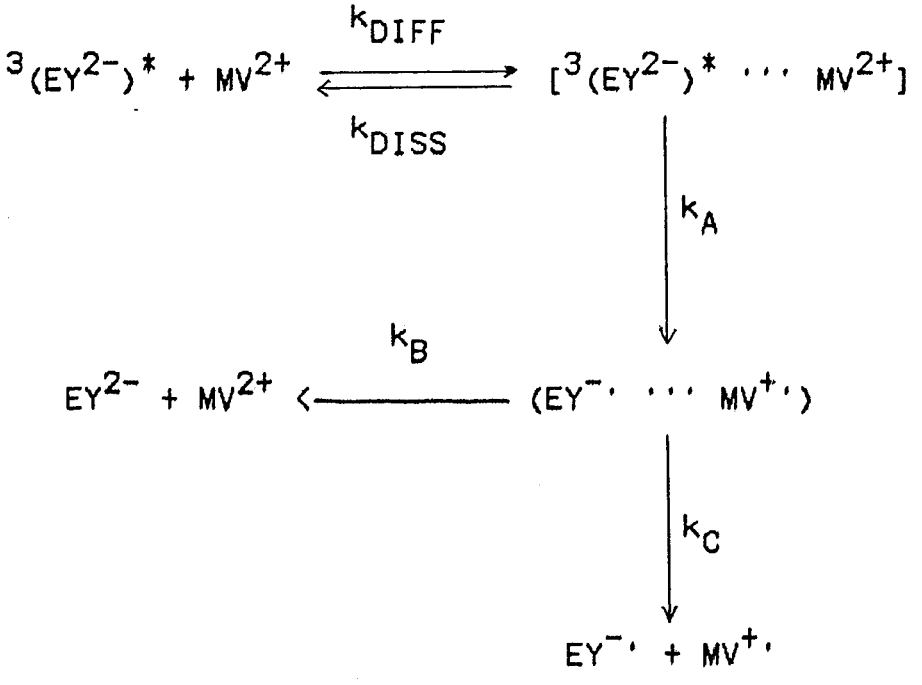

Thus, interaction between $^3(EY^{2-})^*$ and MV^{2+} gives an encounter complex within which there is virtually no binding energy between the reactants. The formation of such an encounter complex may be

a diffusion-controlled process (k_{DIFF}) and, since the complex may be a very weak one, it may be reverible (k_{DISS}). Once formed, the complex may undergo electron transfer to form a geminate ion pair (k_A) wherein the redox products are caged by the solvent. The geminate ion pair may collapse either to reform the ground state reactants (k_B) or to give separated ion products (k_C).

The rate of formation of the encounter complex (k_{DIFF}) can be calculated from the Debye expression for diffusional encounter between two ions (A and B) of charges Z_A and Z_B as written in Eq. 18;

$$k_{DIFF} = 4\pi r_{AB} D_{AB} N_A \delta / (\exp \delta - 1) \qquad (18)$$

where

$$\delta = Z_A Z_B e^2 / \epsilon k T r_{AB} \qquad (19)$$

and a distance between A and B, r_{AB}=10 Å, the diffusion constant $D_{AB}=10^{-5}$ cm^2 s^{-1}; N_A, k and ϵ are the Avogadro's constant, the Boltzmann's constant, and the dielectric constant of the solvent, respectively.[10)]

The standard free energy change(ΔG^0) associated with the formation of a very weakly bound complex between charged ions can be calculated from Eq. 20;[28)]

$$\Delta G^0 = Z_A Z_B e^2 / r_{AB} \qquad (20).$$

The free energy change can be employed to estimate the equilibrium constant for the formation of the encounter complex (K) as in Eq. 21:

$$\Delta G^{\emptyset} = -RT\ln K \qquad (21),$$

and

$$K = k_{DIFF}/k_{DISS} \qquad (22),$$

so that the value of k_{DISS} can be obtained (Table 6).

Now, the bimolecular triplet quenching rate constant $k(MV^{2+})$ can be expressed as in Eq. 23:

$$k(MV^{2+}) = k_{DIFF}\, k_A/(k_A + k_{DISS}) \qquad (23),$$

so that k_A can be evaluated. However, the measured $k(MV^{2+})$ value is strongly dependent upon the ionic strength (μ) of the medium, and the calculated k_{DIFF} and k_{DISS} values refer to zero ionic strength. Thus, the measured $k(MV^{2+})$ value has been corrected to zero ionic strength using the relationship as in Eq. 24:

$$\log k(MV^{2+}) = \log k(MV^{2+})^{\emptyset} + 1.02\, Z_A\, Z_B\, \mu^{1/2} \qquad (24),$$

and the calculated value $k(MV^{2+})^{\emptyset}$ is given in Table 6 ($\mu^{1/2}$ = 0.19 under the experimental condition). Employing these values,

together with the calculated k_{DIFF} and k_{DISS} values, allows caluclation of k_A (Table 6) which applies the rate constant of electron transfer from $^3(EY^{2-})^*$ to MV^{2+}. The probability of electron transfer (P) can be expressed in the form,

$$P = k_A/(k_A + k_{DISS}) = k(MV^{2+})^0/k_{DIFF} \qquad (25),$$

so that P can be obtained (Table 6). It can be seen from Table 6 that the EY^{2-}-MV^{2+} system has a large probability of the electron transfer. This shows that the electrostatic attraction between the reactants favors the forward electron transfer process.

The geminate ion pair formed in the electron transfer process (k_A) can dissociate to ground state reactants (k_B), which must proceed through spin inversion from the resulting triplet in radical pair to singlet pair, or to separated ion products (k_C), and the partition between these two decay process controls the yield of redox products. Once formed, the redox products will recombine via a diffusion controlled back electron transfer step k_{-C} as shown in Eq. 26:

$$EY^{-\cdot} + MV^{+\cdot} \underset{k_C}{\overset{k_{-C}}{\rightleftharpoons}} (EY^{-\cdot} \cdots MV^{+\cdot}) \xrightarrow{k_B} (EY^{2-}, MV^{2+}) \qquad (26).$$

The procedure outlined above for calculation of k_{DIFF}, k_{DISS}, and k_A can be employed to estimate k_{-C}, k_C, and k_B. The equilibrium constant (K′) for formation of an ion pair from the separated ion products can be expressed as shown in Eq. 27;

$$K' = k_{-C}/k_C \qquad (27).$$

The rate constant $k(back)^{\emptyset}$ corrected to zero ionic strength can be written as in Eq. 28:

$$k(back)^{\emptyset} = k_{-C}\, k_A/(k_B + k_C) \qquad (28).$$

These derived values are collected in Table 7. The rate constants of both forward and back electron transfer processes are summarized in Figure 22. Now, the yield of redox products depends upon the partition fraction of the ion pair

$$\Phi_S = k_C/(k_B + k_C) \qquad (29)$$

and Φ_S is related to the quantum yield for formation of separated products, Φ_{ions}.[10,29]

$$\Phi_{ions} = \Phi_{ST} \times \Phi_Q \times \Phi_S \qquad (30).$$

The symbols Φ_{ST} and Φ_Q refer to the quantum yield for the formation of the triplet excited state of EY^{2-} (Φ_{ST} = 0.64)[30] and the probability of quenching the triplet excited state of EY^{2-} a given concentration of quencher as shown in Eq. 31:

$$\Phi_Q = k(MV^{2+})[MV^{2+}]/\{k(MV^{2+})[MV^{2+}] + \tau_T\} \quad (31)$$

The derived value of Φ_S and Φ_{ions} are collected in Table 7. The value of Φ_{ions} may be related to the limiting quantum yield of $MV^{+\cdot}$ production (Φ_{lim}) determined in the presence of TEOA. It is noticeable that the estimated value of Φ_{ions} for EY^{2-}, 0.13, is as large as the value determined for tris(2,2'-bipyridine)-ruthenium (II) (Φ_{ions}=0.1 - 0.25).[29]

7. Comparison of the Quantum Yields for $MV^{+\cdot}$ Production Among the Sensitizers Employed

The limiting quantum yield for EY^{2-}-sensitized $MV^{+\cdot}$ production is equal to or higher than the quantum yield in the cases of ruthenium complexes as a sensitizer (Table 8). This result might be related to the difference of the redox potentials among sensitizers. With the use of EY^{2-} standard free energy change (ΔG_0) for the electron transfer to MV^{2+} is more negative than that employing ruthenium complexes; this nature will accelerate the forward electron transfer. Moreover, the geminate ion pair formed by the forward electron transfer is a triplet

radical ion pair, so that the back electron transfer can proceed after the spin inversion of the ion pairs. Previously, several workers[3,9,10] indicated that the negative value of $Z_A \cdot Z_B$ such as the EY^{2-}-MV^{2+} system is unfavorable to yield redox products for the substantial electrostatic attraction within the ion pair.[3,9,10] However, the formation of separated ion products (Φ_{ions} and Φ_{lim}) in the present system is favored despite the negative $Z_A \cdot Z_B$ value. This fact suggests that the negative charge on $EY^{-\cdot}$ is localized in the benzene moiety oriented perpendicular to the xanthene framework, so that the components of the produced geminate radical ion pair diffuse from each other.

Conclusion

The present work shows that EY^{2-} photosensitizes the reduction of MV^{2+} into $MV^{+\cdot}$ with high efficiency. The limiting quantum yield for the reduction of MV^{2+}, under the present conditions, reached ca. 0.3. This value is equal to or higher than the values observed in the systems employing ruthenium complexes as a sensitizer. The resulting $MV^{+\cdot}$ in the present system reduces water to hydrogen in the presence of colloidal platinum. Moreover, we have shown the detailed study of kinetics and mechanism for the reaction by nanosecond and microsecond laser flash photolysis techniques. In this system, the reaction is initiated by electron transfer from triplet excited EY^{2-} to MV^{2+} followed by electron transfer to the resulting $EY^{-\cdot}$ from TEOA. This is the first mechanistic investigation of electron transfer reaction from a donor to MV^{2+} sensitized by an organic dye.

Experimental

Materials. Eosin Y (2′,4′,5′,7′-tetrabromofluorescein disodium salt) (Chroma) was recrystallized three times from a 9:1 ethanol-water mixture. Methylene blue (Merck, extra), methyl viologen (N,N′-dimethyl-4,4′-bipyridinium dichloride) (Nakarai, GR), triethanolamine (Nakarai, GR), were used without further purification. Colloidal platinum was prepared according to the literature.[35] Ethanol and 2-propanol (Nakarai, SPR) were dried over Zeolite 3-A (Wako) for at least three days and distilled before use. Non-fluorescent water (Dojin) was used as received and adjusted to pH 5 with phthalate buffer (Clark-Lubs buffer solution).

Determination of absorption spectrum change on continuous light irradiation. Each sample (4 ml) was deaerated in a quartz cell with a long neck by bubbling with nitrogen or argon for at least 30 min before irradiation. Steady-state irradiation was performed by employing a 650 W tungsten-bromine lamp through a Toshiba Y-45 and an O-55 glass filter to isolate visible light of λ>450 nm and λ>550 nm, respectively. The visible and UV absorption spectra of the irradiated reaction mixtures were measured on a Hitachi 200-20 spectrophotometer.

Measurement of redox potentials. The redox potentials

were measured in acetonitrile and aqueous solutions with conventional three-electrodes, a platinum wire as the working electrode, a platinum gauze as the counter electrode, and an Ag/0.1 mol/dm^3 $AgNO_3$ or a saturated calomel electrode (SCE) as a reference electrode. In acetonitrile solutions tetraethylammonium perchlorate (0.1 mol/dm^3) was employed as a supporting electrolyte. In aqueous solutions, potassium phthalate and sodium hydroxide employed to adjust pH to 5 worked as supporting electrolytes.

Measurement of the equilibrium constant for complex formation. The equilibrium constant for complex formation was determined by two methods. One method employed absorption spectrum change of EY^{2-} on addtion of varying concentrations of MV^{2+}. The other method was carried out by quenching of EY^{2-} fluorescence intensity and lifetime by varying concentrations of MV^{2+}. Fluorescence spectra of EY^{2-} with and without MV^{2+} were measured on a Hitachi MPF-2A fluorescence spectrometer. The fluorescence lifetime of EY^{2-} was determined on a nanosecond single photon counting apparatus, Applied Photophysics Model SP-3X, and the data were analyzed by deconvolution techniques.

Measurement of quantum yields. All quantum yields were determined on illumination of sample solutions in a mixture (1:1 by volume, 4 ml) of ethanol and water adjusted to pH 5 with

phthalate buffer placed in a 1 x 1 x 4 cm quartz cell with a long neck. Illumination was done with 490 nm light obtained through a Baush and Lomb monochromator (slit width: 20 nm) from a 500 W Ushio UI-501C xenon lamp. The light intensity was determined with the use of a chemical actinometer, potassium tris(oxalato)-ferrate (III).[36] The sample solutions were deaerated by bubbling with argon for at least 30 min before irradiation.

The quantum yields for disappearance of EY^{2-} (8.6×10^{-5} mol /dm^3) in the presence of TEOA [$(3.0\text{-}12.0) \times 10^{-3}$ mol/dm^3] were determined by following the decrease of the absorption of EY^{2-} at 480 nm (molar absorption coefficient: 2.03×10^4 dm^3 mol^{-1} cm^{-1}).

The quantum yields for $MV^{+\cdot}$ production in the three-component system (EY^{2-}/MV^{2+}/TEOA) were determined by measuring the absorption of the resulting $MV^{+\cdot}$ as described below (Figure 24). The excitation light (λ=490 $\pm$ 10 nm) was obtained as above. A 100 W tungsten-halogen lamp was employed as a monitoring light source. The lamp was equipped with an R-60 (Toshiba) glass filter which allowed radiation of light with λ>600 nm. The monitoring light was passed through an Applied Photophysics M300 monochromator and was detected with an Applied Photophysics IP28 photomultiplier and a Kawasaki Electronica TM-1410 transient memory. The rising curves of $MV^{+\cdot}$ were read into the transient memory and put out on a Rikadenki R-21 recorder. The quantum yields for the $MV^{+\cdot}$ generation in the three-component system were

performed by irradiating EY^{2-} (8.6×10^{-5} mol/dm^3) either with varying concentrations of TEOA [$(3.0-12.0) \times 10^{-3}$ mol/dm^3] in the presence of a fixed concentration of MV^{2+} (1.0×10^{-3} mol/dm^3) or with varying concentrations of MV^{2+} (1.0×10^{-5} -1.0×10^{-3} mol/dm^3) in the presence of TEOA (1.0×10^{-2} mol/dm^3).

Determination of hydrogen evolution. Figure 25 shows the apparatus for measurement of the hydrogen evolution. The sample solution containing colloidal platinum was prepared by the following procedures. An appropriate amount of colloidal platinum in an ethanol-water solution (6.6×10^{-5} mol/dm^3 in 10 ml) was placed in a Shelenck flask and the solvent (ethanol-water) in the flask was evaporated completely. An aqueous ethanol solution (10 ml) of EY^{2-}(5.0×10^{-5} or 5.0×10^{-4} mol/dm^3) containing TEOA (1.0×10^{-2} mol/dm^3) and varied concentrations of MV^{2+} ($0-1.0 \times 10^{-3}$ mol/dm^3) was added to the colloidal platinum in the flask and the resulting mixture was stirred vigorously. The dissolved oxygen was removed by bubbling with argon for at least 30 min. The temperature of the mixture was controlled at 25°C by circulating water from a Haake circulator. The mixture was irradiated with light of λ>450 nm through a Toshiba Y-45 glass filter from a 500 W xenon lamp (Ushio UI-501C). The resulting hydrogen was analyzed at 60°C on a Hitachi 023 gas chromatograph with TCD with a Molecular Sieves 5A column.

Laser flash photolysis. Figure 26 shows a schematic diagram of the apparatus. The photolysis cell was a quartz cell of 0.5 x 0.5 cm and 5 cm in height. Each sample of the two-component system (EY^{2-}/MV^{2+}) in aqueous ethanol (1:1 by volume) was deaerated by repeated freeze-thaw cycles. The dissolved oxygen of the three-component system (EY^{2-}/MV^{2+}/ TEOA) in aqueous ethanol (1:1 by volume) was removed by bubbling with argon for at least 30 min.

The excitation was done by a nitrogen pulsed laser (Lambda Physik EMG101), capable of providing up to 8 mJ per pulse at 337.1 nm, having a pulse duration of 7 ns at half height width. The laser beam was collected by a lens positioned at the focal length from the sample. The energy of the incident laser pulse was controlled to be below 8 mJ per pulse by employing a variant semi-transparent mirror. The monitoring light was provided by a 150 W Osram DXO-150 or a Wacom KXL-151 xenon lamp. The monitoring light was oriented perpendicular to the laser beam at the part of the sample cell where photolysis takes place. On measurement of the transient absorption the monitoring xenon lamp was triggered by opening a shutter to the sample cell to give maximum intensity of light at the same time as the laser pulse excitation. The shutter was used for minimizing exposure of samples to the monitoring light. The monitoring light was passed through a Jasco CT-25C grating monochromator and was

detected with a Hamamatsu Photonix R-446 photomultiplier and a Tektronix 475A oscilloscope.

References

1) For example, D. G. Whitten, Acc. Chem. Res., 13, 83 (1980); M. Gratzel, ibid., 14, 376 (1981).

2) For example, N. Sutin, J. Photochem., 10, 19 (1979); N. Sutin and C. Creutz, Pure Appl. Chem., 52, 2717 (1980).

3) K. Kalyanasundaram and M. Gratzel, Helv. Chim. Acta, 63, 478 (1980).

4) G. McLendon and D. S. Miller, J. Chem. Soc., Chem. Commun., 1980, 533.

5) I. Okura, S. Aono, M. Takeuchi, and S. Kusunoki, Bull. Chem. Soc. Jpn., 55, 3637 (1982).

6) A. Harriman and M.-C. Richoux, J. Photochem., 15, 335 (1981).

7) N. Carnieri and A. Harriman, J. Photochem., 15, 341 (1981).

8) I. Tabushi and A. Yazaki, J. Org. Chem., 46, 1899 (1981).

9) A. Harriman, G. Porter, and M.-C. Richoux, J. Chem. Soc., Faraday Trans. 2, 77, 833 (1981).

10) M.-C. Richoux and A. Harriman, J. Chem. Soc., Faraday Trans. 1, 78, !873 (1982).

11) M. Rougee, T. Ebbesen, F. Ghetti, and V. Bensasson, J. Phys. Chem., 86, 4404 (1982).

12) J. A. Shelnutt, J. Am. Chem. Soc., 105, 7179 (1983).

13) For example, J. Darwent, J. Chem. Soc., Chem. Commun., 1980, 805; A. Harriman and M.-C. Richoux, J. Photochem.,

14, 253 (1980); A. Harriman and M.-C. Richoux, J. Chem. Soc., Faraday Trans. 2, 76, 1618 (1980); T. Tanno, D. Wohrle, M. Kaneko, and A. Yamada, Ber. Bunsenges. Phys. Chem., 84, 1032 (1980); A. Harriman, G. Porter, and M.-C. Richoux, J. Chem. Soc., Faraday Trans. 2, 77, 1175 (1981); T. Ohno, S. Kato, and N. N. Lichtin, Bull. Chem. Soc. Jpn., 55, 2753 (1982).

14) J. S. Bellin, R. Alexander, and R. D. Mahoney, Photochem. Photobiol., 17, 17 (1973).

15) K. Kalyanasundaram and M. Gratzel, J. Chem. Soc., Chem. Commun., 1979, 1137.

16) K. Kalyanasundaram and D. Dung, J. Phys. Chem., 84, 2551 (1980).

17) M. S. Chan and J. R. Bolton, Photochem. Photobiol., 34, 537 (1981).

18) A. Krasna, Photochem. Photobiol., 29, 267 (1979); ibid, 31, 75 (1980).

19) M. Koizumi, S. Kato, N. Matsuura, and Y. Usui, "Photosensitized Reactions," Kagaku Dojin, Kyoto (1978), pp. 168-190.

20) K. Kimura, T. Miwa, and M. Imamura, Bull. Chem. Soc. Jpn., 43, 1329 (1970).

21) R. Bonneau, P. Fornier de Violet, and J. Joussot-Dubien, Photochem. Photobiol., 19, 129 (1974); R. Bonneau, J. Joussot-Dubien, and J. Faure, ibid., 17, 313 (1973);

R. Bonneau and J. Pereyre, ibid., 21, 173 (1975); U. Steiner, G. Winter, and H. E. Kramer, J. Phys. Chem., 81, 1104 (1977).

22) H. Misawa, H. Sakuragi, Y. Usui, and K. Tokumaru, Chem. Lett., 1983, 1021.

23) Professor Y. Usui (Ibaraki University) private communication.

24) T. Ohno, S. Kato, and M. Koizumi, Bull. Chem. Soc. Jpn., 39, 232 (1966); M. Koizumi, Nihon Kagaku Zasshi, 90, 117, (1969).

25) The microsecond laser flash photolysis (dye laser excitation, excitation wavelength: 500 nm) was done at Ibaraki University (Professor Y. Usui).

26) E. M. Kosower and J. L. Cotter, J. Am. Chem. Soc., 86, 5524 (1964).

27) A. Harriman and G. Porter, J. Chem. Soc., Faraday Trans. 2, 78, 1937 (1982).

28) P. Debye, Trans. Electrochem. Soc., 82, 265 (1942).

29) K. Kalyanasundaram, J. Kiwi, and M. Gratzel, Helv. Chim. Acta, 61, 2720 (1978).

30) Y. Usui, Chem. Lett., 1973, 743.

31) T. Matsuura, "Sansosanka Hanno," Maruzen (1977), p. 224.

32) P. J. DeLaive, C. Giannotti, and D. G. Whitten, J. Am. Chem. Soc., 100, 7413 (1978).

33) R. J. Crutchley and A. B. P. Lever, J. Am. Chem. Soc., 102, 7129 (1980).

34) G. M. Brown, S. F. Chan, C. Creutz, H. A. Schwarz, and N. Sutin, J. Am. Chem. Soc., 101, 7638 (1979).

35) N. Toshima, M. Kuriyama, Y. Yamada, and H. Hirai, Chem. Lett., 1981, 793.

36) S. L. Murov, "Handbook of Photochemistry," Marcel Dekker, New York, 1973.

Table 1. Temperature Effect for Hydrogen Evolution

Temperature /°C	H_2 Yield a) /ml
25	0.61
50	0.82

a) $[EY^{2-}]=2.0 \times 10^{-5}$ mol/dm^3
$[MV^{2+}]=1.0 \times 10^{-4}$ mol/dm^3
[EDTA-2Na]$=1.0 \times 10^{-2}$ mol/dm^3
Solvent: EtOH-H_2O (pH 5)=(1/1)

Table 2. Solvent Effect for Hydrogen Evolution

Organic Solvent [a]	H_2 Yield [b] /ml
acetonitrile	0.18
ethanol	0.61
methanol	0.48

a) (organic solvent)-H_2O (pH 5)=(1/1)

b) $[EY^{2-}]=2.0 \times 10^{-5}$ mol/dm^3

$[MV^{2+}]=1.0 \times 10^{-4}$ mol/dm^3

[EDTA-2Na]$=1.0 \times 10^{-2}$ mol/dm^3

Table 3. Effect of Additives for Hydrogen Evolution

Additive	H_2 Yield[a] /ml
----	0.14
KCl (0.1 mol/dm^3)	0.23
Na_2SO_4 (0.1 mol/dm^3)	0.23

a) $[EY^{2-}]=2.0 \times 10^{-5}$ mol/dm^3
$[MV^{2+}]=5.0 \times 10^{-4}$ mol/dm^3
[EDTA-2Na]$=1.0 \times 10^{-2}$ mol/dm^3
Solvent: EtOH-H_2O (pH 5)=(1/1)

Table 4. Redox potentials of ground and excited state of sensitizers

Dye	solvent	Dye^{+}/Dye	Dye/Dye^{-}	$Dye^{+}/{}^{3}Dye^{*}$	${}^{3}Dye^{*}/Dye^{-}$
		V			
EY^{2-}	MeCN [a]	+0.38	-1.56	-1.52 [c]	+0.34 [c]
	H_2O [b]	+0.80	<-1.0	-1.10 [c]	<+0.9 [c]
MB^{+}	MeCN [a]	+0.76	-0.73	-0.74 [d]	+0.77 [d]
	H_2O [b]	+1.17	-0.15	-0.33 [d]	+1.35 [d]

a) vs. Ag/0.1 mol/dm^3 $AgNO_3$ with Et_4NClO_4. b) vs. SCE, water adjusted at pH 5. c) E_T=1.9 eV [31]. d) E_T=1.5 eV [31]

Table 5. Free energy change of the electron transfer processes.

Dye	Eq 11 [b]	Eq 12 [c]	Eq 13 [d]
	kcal/mol		
EY^{2-}	-1.66	-2.8	-17.7
MB^{+}	+1.4	-12.7	+1.6

a) The values are calculated by the redox potentials in MeCN in Table 4. b) $MV^{2+}/MV^{+\cdot}$=0.80 V vs. Ag/ 0.1 mol/dm^3 $AgNO_3$ in MeCN with Et_4NClO_4. c) $TEOA^{+\cdot}$/TEOA=+0.22 V vs. Ag/ 0.1 mol/dm^3 $AgNO_3$ in MeCN with Et_4NClO_4

Table 6. Rate constants of the forward electron transfer processes for EY^{2-}-MV^{2+} system

$k(MV^{2+})$	$k(MV^{2+})^0$	k_{DIFF}	k_{DISS}	k_A	P
	$dm^3\ mol^{-1}\ s^{-1}$		s^{-1}		/%
3.0×10^9	1.8×10^{10}	3.3×10^{10}	4.2×10^8	5.0×10^8	55

Table 7. Rate constants of the back electron transfer processes and efficiency of charge separation for EY^{2-}-MV^{2+} system

k_C	k_B	k_{-C}	Φ_{ions}	Φ_S	Φ_T [a]	Φ_Q [b]	Φ_{lim} [c]
s^{-1}		$/dm^3\ mol^{-1}\ s^{-1}$					
1.1×10^{10}	4.0×10^{10}	1.2×10^{10}	0.13	0.22	0.64	0.92	0.29

a) Reference 30). b) $[MV^{2+}]=7.03 \times 10^{-4}$ mol/dm^3. c) Limiting quantum yield of $MV^{+\cdot}$ production in EY^{2-}-MV^{2+}-TEOA system.

Table 8. Quantum yields for $MV^{+\cdot}$ production in several systems.

System	$\Phi_{MV^{+\cdot}}$
$Ru(bpy)_3^{2+}$ [a] /MV^{2+}/2,6-lutidine	0.02 [32]
$Ru(bpy)_3^{2+}$ [a] /MV^{2+}/TEA [b]	0.17 [32]
$Ru(bpy)_3^{2+}$ [a] /MV^{2+}/TEOA	0.19 [33]
$Ru(bpy)_3^{2+}$ [a] /$Rh(bpy)_3^{2+}$ [c] /MV^{2+}/TEOA	0.33 [34]
$Ru(bpy)_3^{2+}$ [a] /MV^{2+}	0.1~0.25 [29]
$Ru(bpz)_3^{2+}$ [d] /MV^{2+}/TEOA	0.77 [33]
RuL_3^{2+} [e] /MV^{2+}/2,6-lutidine	0.07 [32]
RuL_3^{2+} [e] /MV^{2+}/TEA [b]	0.4 [32]
Proflavine/MV^{2+}/EDTA	0.72 [14]

a) $Ru(bpy)_3^{2+}$, where bpy = 2,2'-bipyridine. b) TEA = triethylamine. c) $Rh(bpy)_3^{2+}$, where bpy = 2,2-bipyridine. d) $Ru(bpz)_3^{2+}$, where bpz = bipyrazyl. e) RuL_3^{2+}, where L = 4,4'-dicarboxy-2,2'-bipyridine diisopropyl ester.

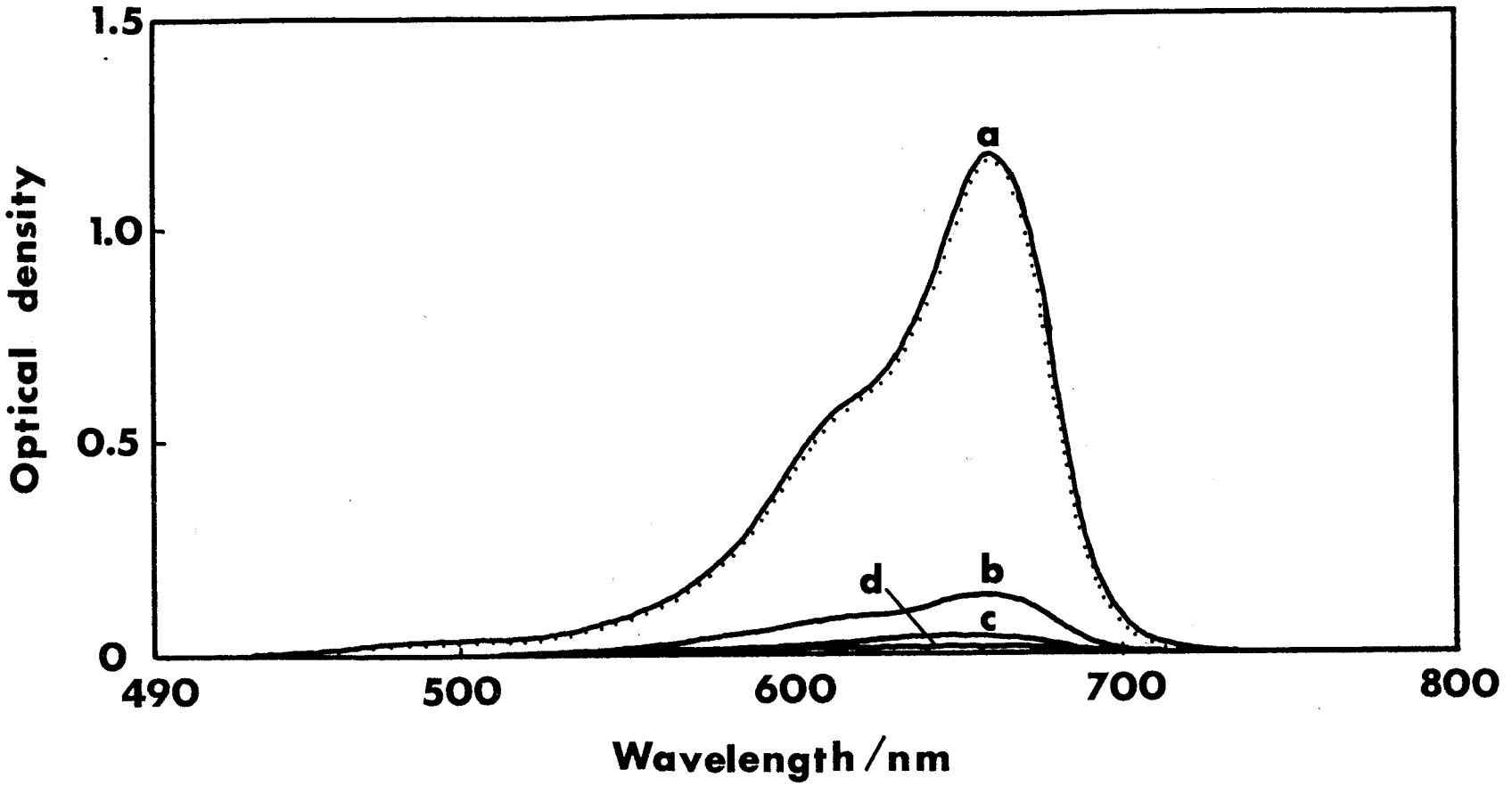

Figure 1. Spectral change of an aqueous ethanol solution of MB^+/TEOA on irradiation under N_2 (———) and on introduction of air after photolysis (·····); irradiation periods as follows: a) 0, b) 5, c) 25, d) 50 s.

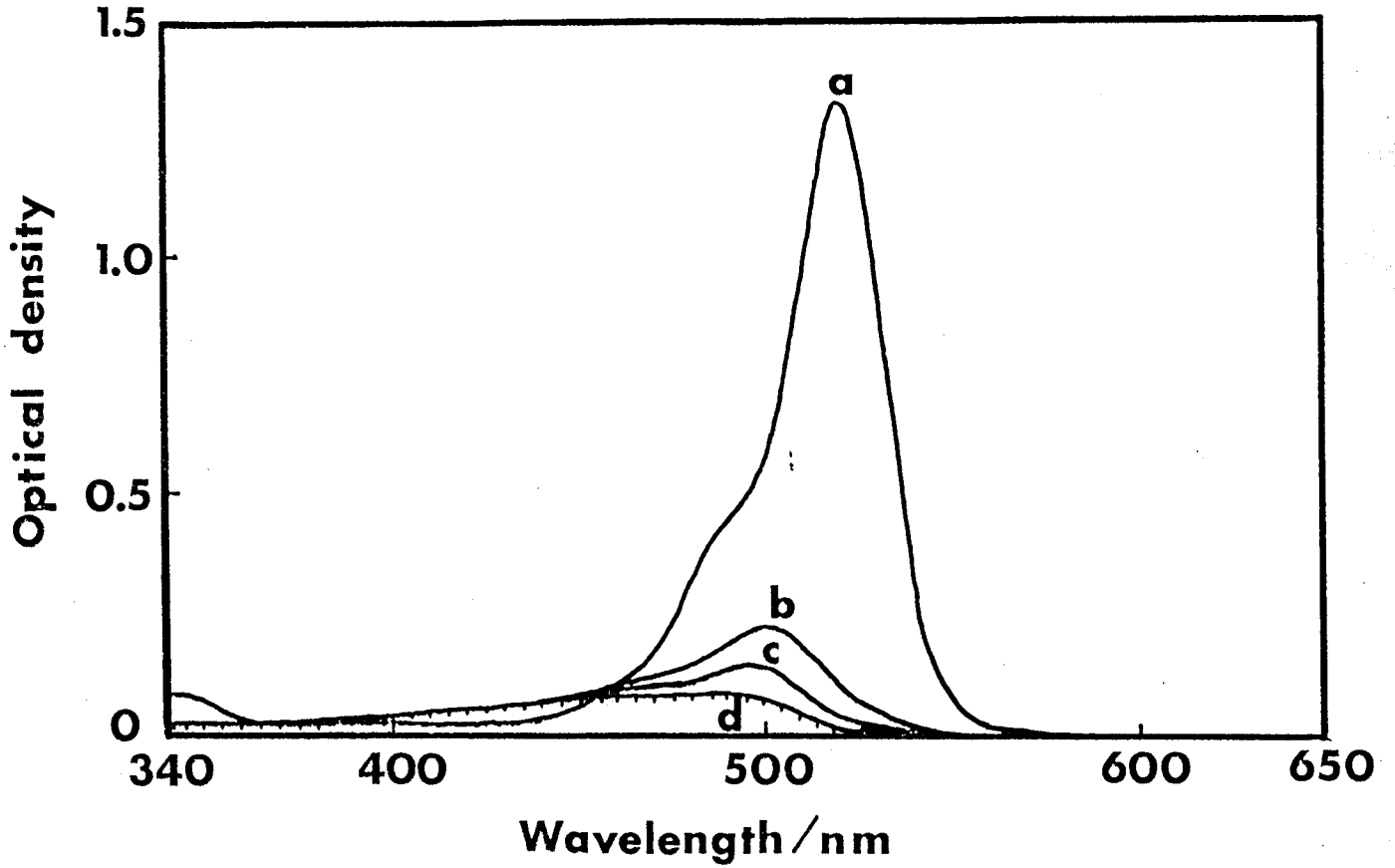

Figure 2. Spectral change of an aqueous ethanol solution of EY^{2-}/TEOA on irradiation under N_2 (———) and on introduction of air after photolysis (·····); irradiation periods as follows: a) 0, b) 10, c) 30, d) 60 s.

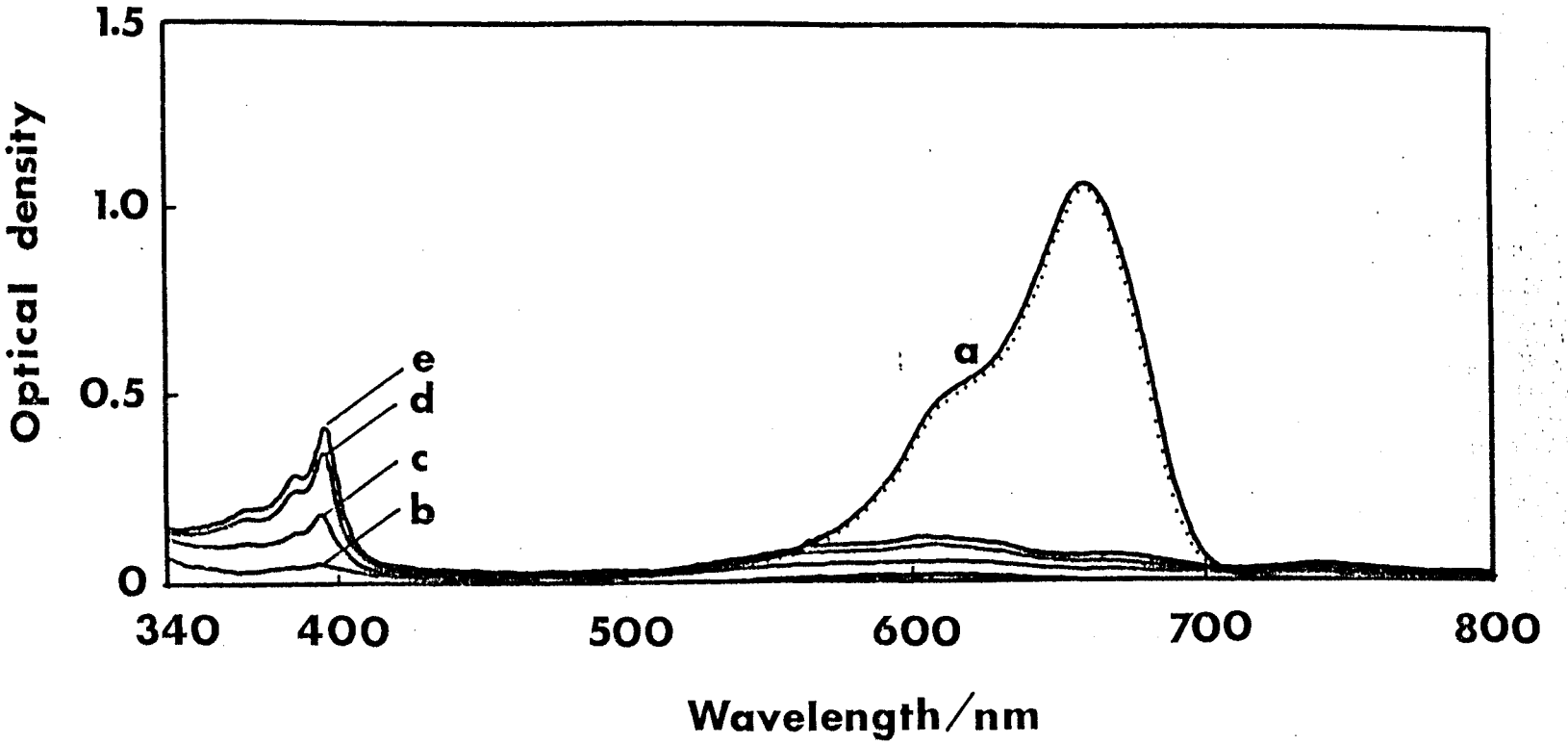

Figure 3. Spectral change of an aqueous ethanol solution of MB^{+}/MV^{2+}/TEOA on irradiation under N_2 (———) and on introduction of air after photolysis (·····); irradiation periods as follows: a) 0, b) 2, c) 4, d) 6, e) 8 min.

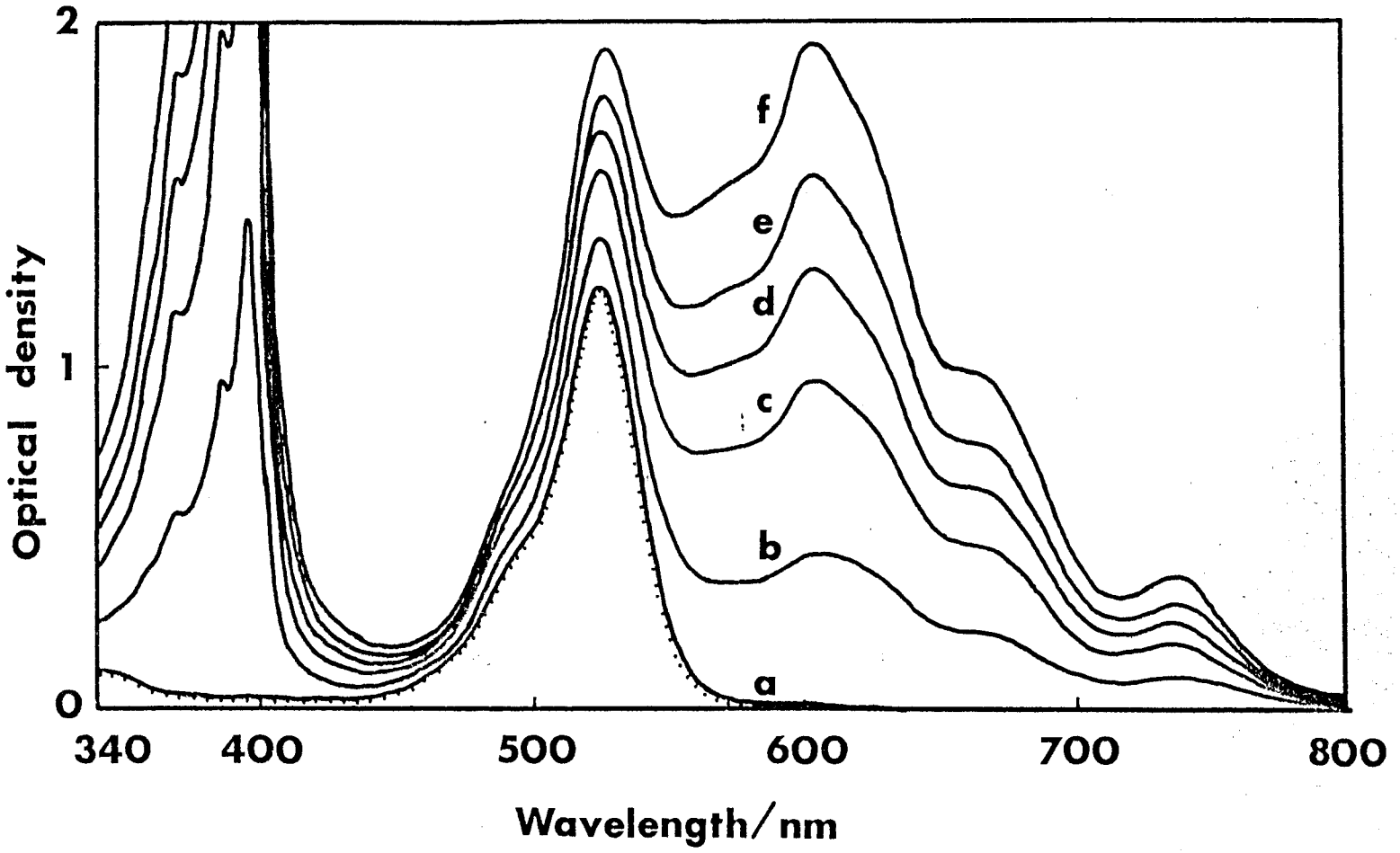

Figure 4. Spectral change of an aqueous ethanol solution of EY^{2-}/MV^{2+}/TEOA on irradiation under N_2 (———) and on introduction of air after photolysis (·····); irradiation periods as follows: a) 0, b) 15, c) 30, d) 45, e) 60, f) 90s.

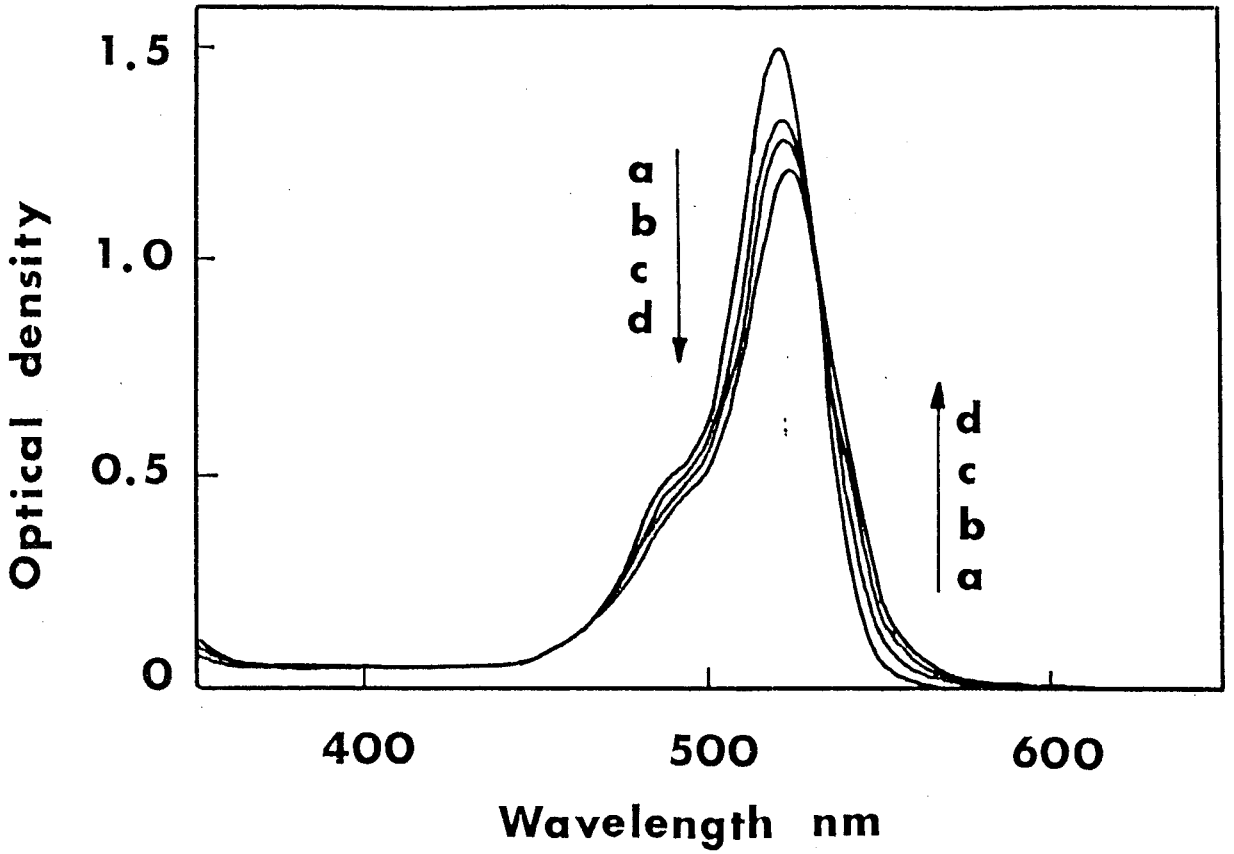

Figure 5. Spectral change of EY^{2-} in aqueous ethanol on addition of MV^{2+}; MV^{2+} concentrations as follows: a) 0, b) 1.51×10^{-4}, c) 5.02×10^{-4}, d) 5.02×10^{-3} mol/dm^3.

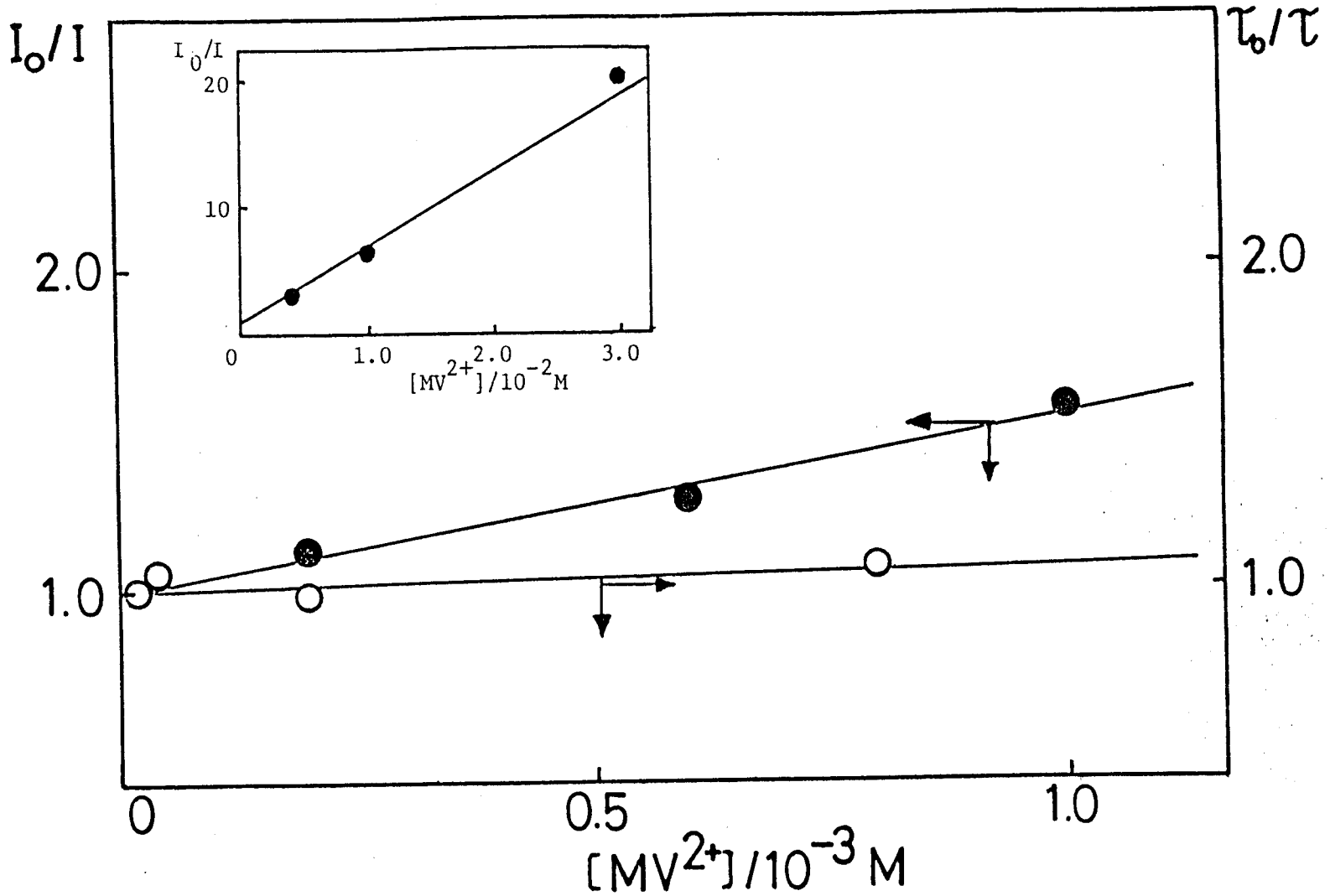

Figure 6. EY^{2-} fluorescence quenching by MV^{2+}; (●): fluorescence intensity, (O): fluorescence lifetime.

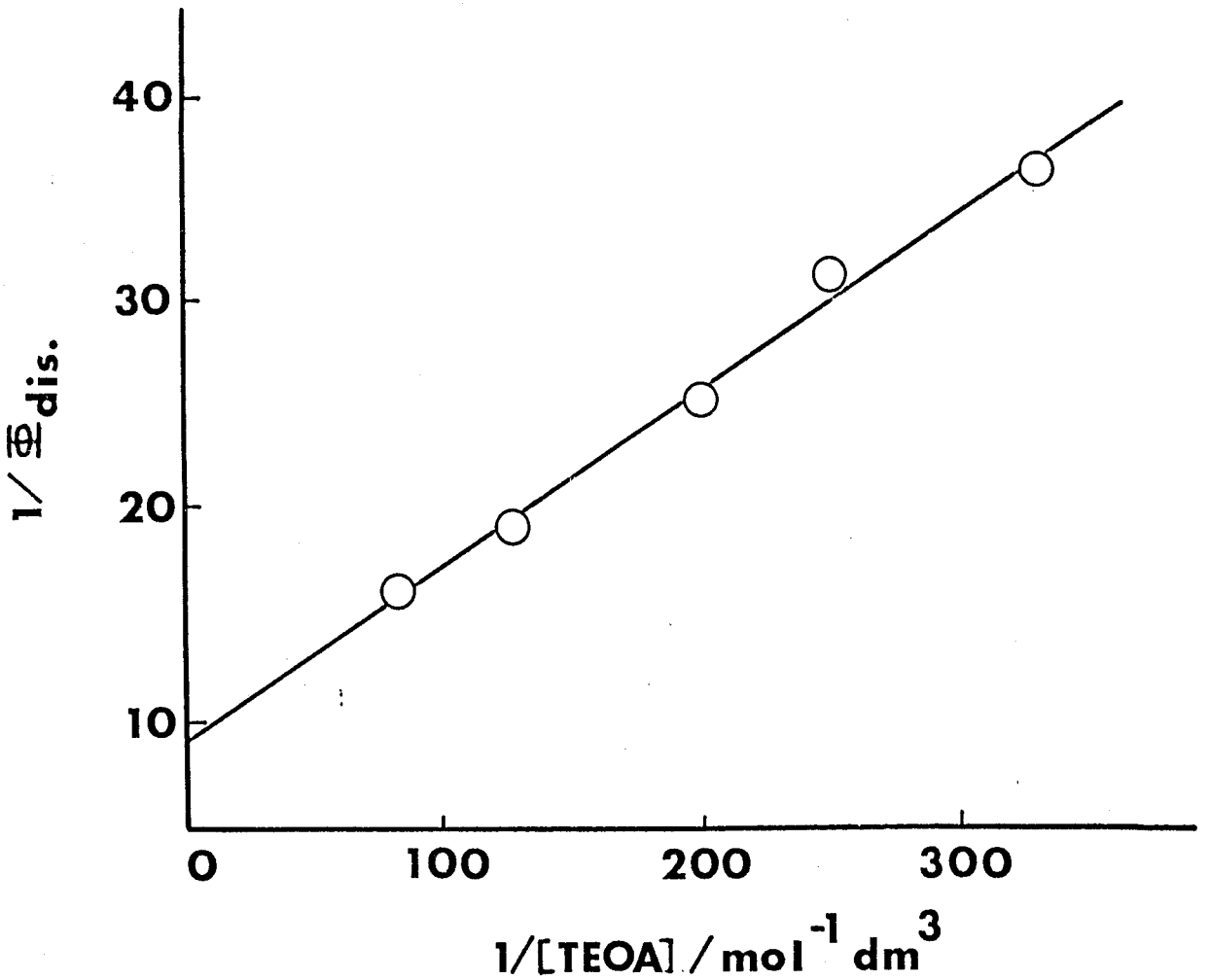

Figure 7. Stern-Volmer plot for disappearance of EY^{2-} on irradiation of EY^{2-}/TEOA in aqueous ethanol.

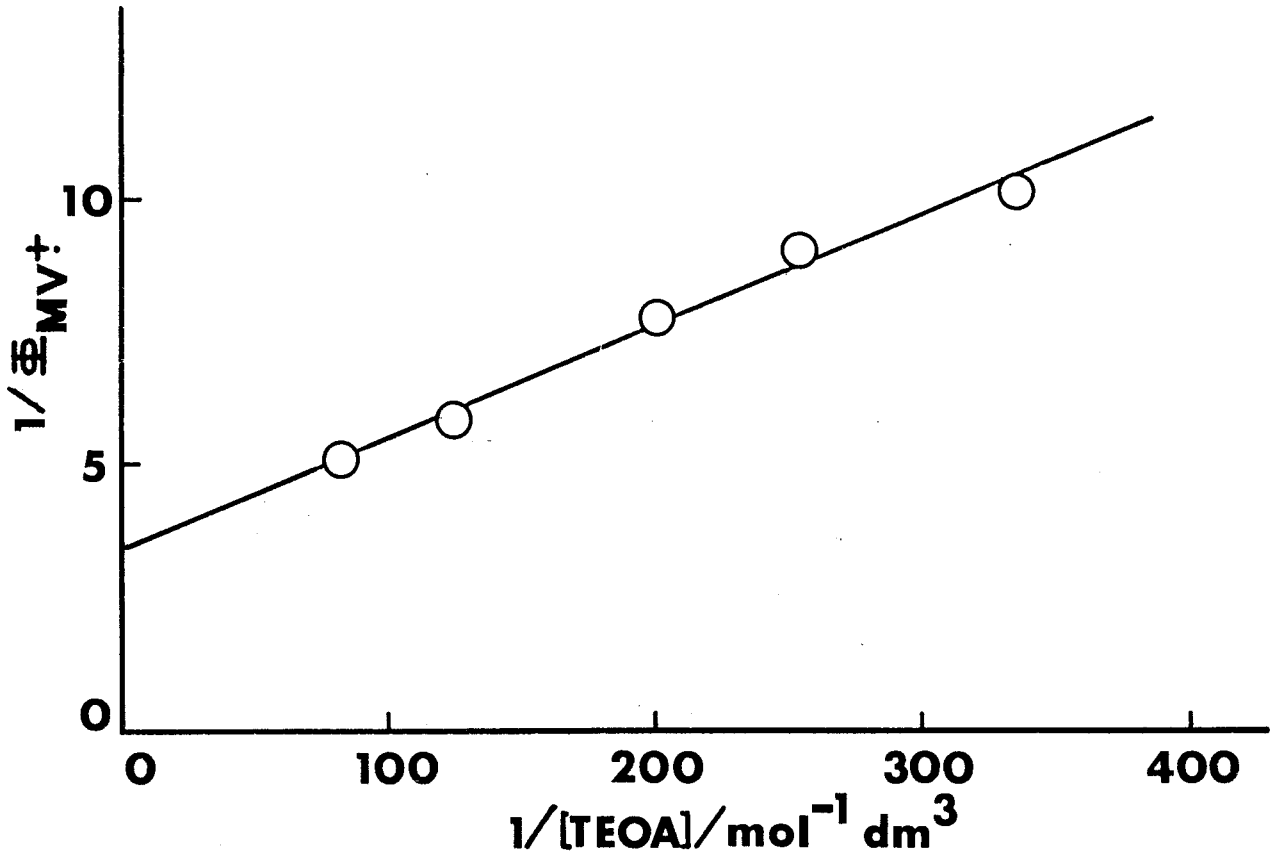

Figure 8. Stern-Volmer plot for $MV^{+\cdot}$ formation on irradiation of EY^{2-}/MV^{2+}/TEOA in aqueous ethanol.

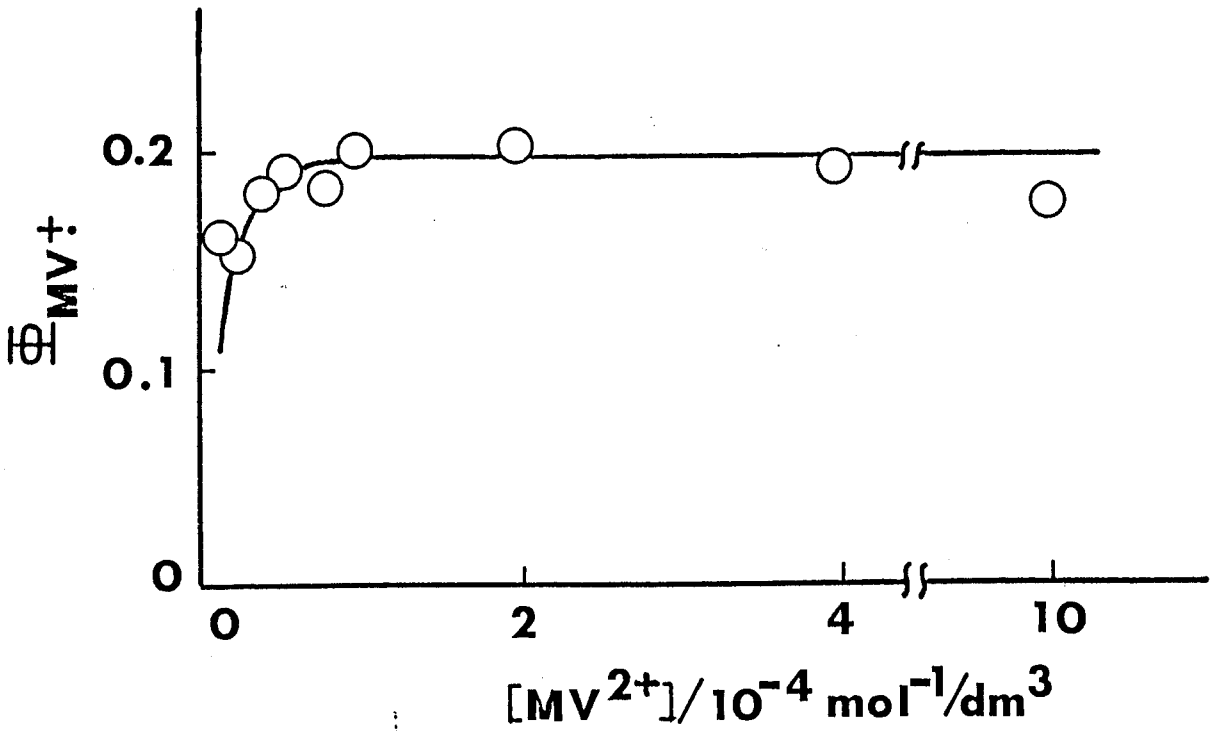

Figure 9. Quantum yields for $MV^{+\cdot}$ formation as a function of MV^{2+} concentration on irradiation of EY^{2-}/MV^{2+}/TEOA in aqueous ethanol.

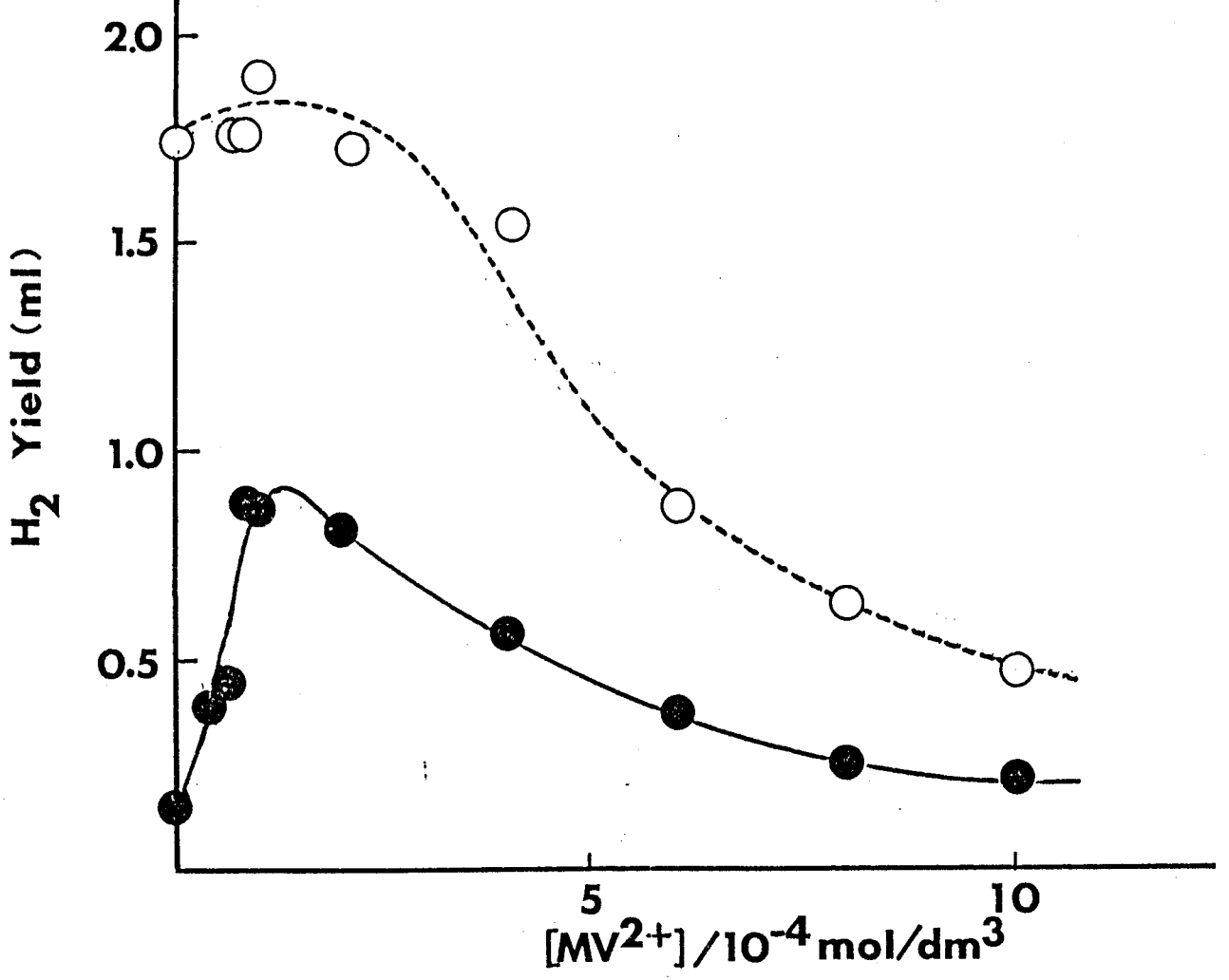

Figure 10. Variation of hydrogen yield with MV^{2+} concentration from EY^{2-}/MV^{2+}/TEOA/colloidal Pt in EtOH-H_2O (pH 5) =(1:1). (○): $[EY^{2-}]=5.0 \times 10^{-4}$ mol/dm^3, (●): $[EY^{2-}]=5.0 \times 10^{-5}$ mol/dm^3, [TEOA]=0.01 mol/dm^3, [colloidal Pt]=6.6×10^{-5} mol/dm^3, solvent:10 ml, irradiation time:5 h.

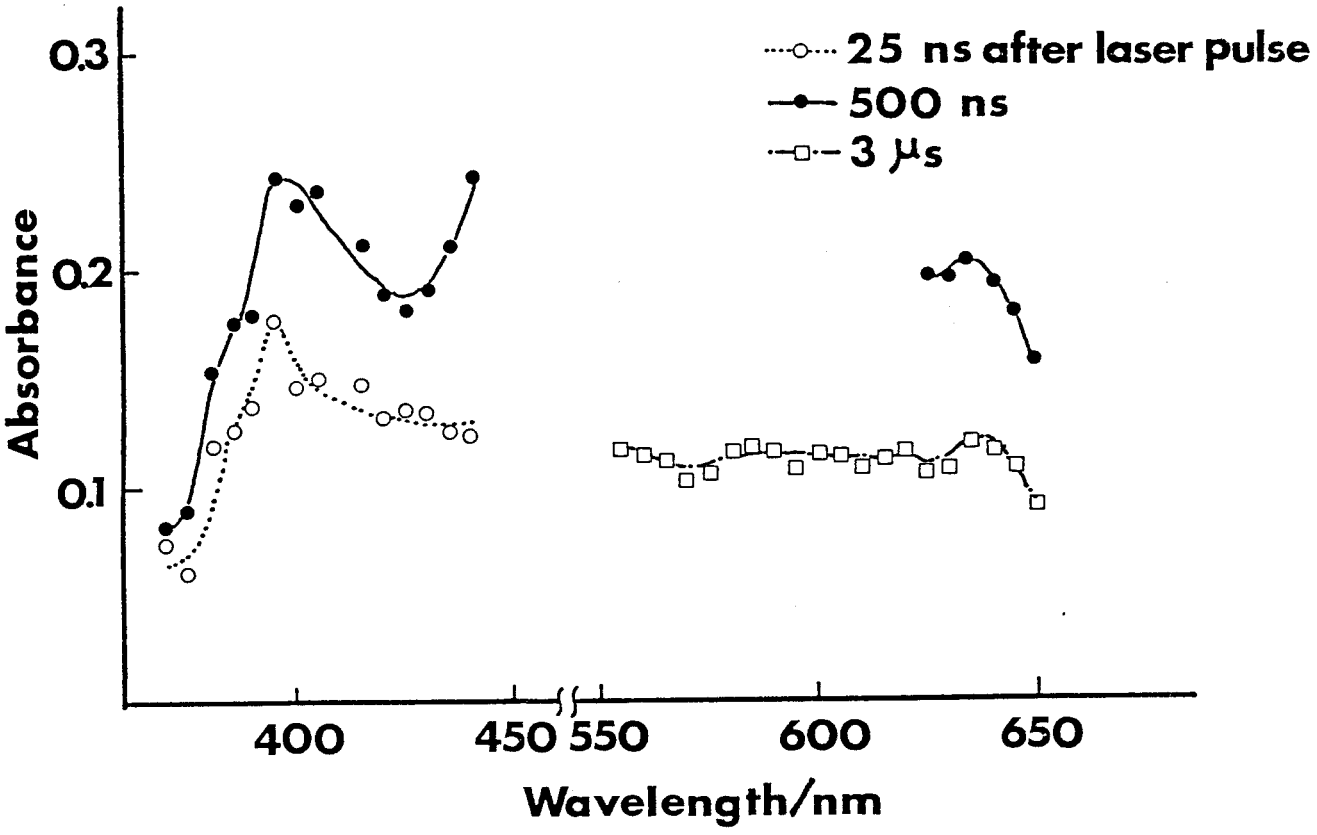

Figure 11. Transient absorption spectra in the laser flash photolysis of EY^{2-} in aqueous ethanol under argon.

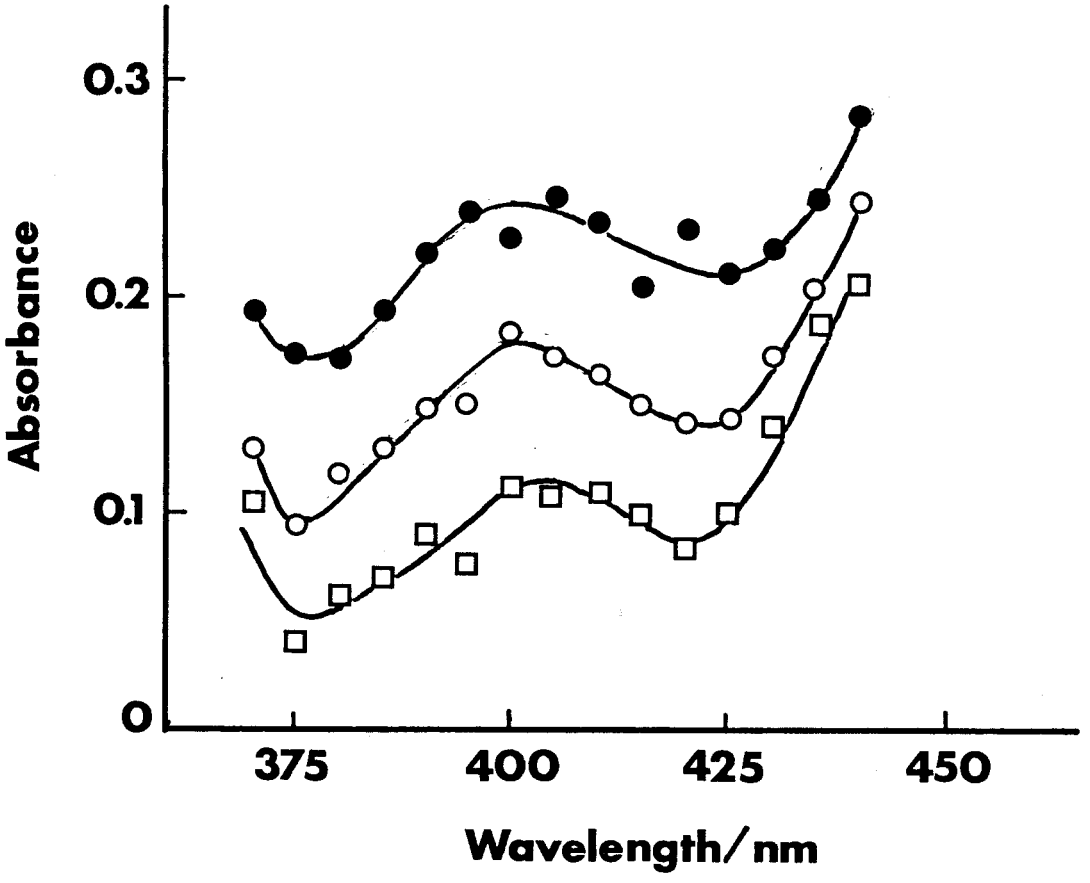

Figure 12. Transient absorption spectra in the laser flash photolysis of EY^{2-} in aqueous ethanol under oxygen. (●): 50 ns after laser pulse, (○): 200 ns after laser pulse, (□): 400 ns after laser pulse.

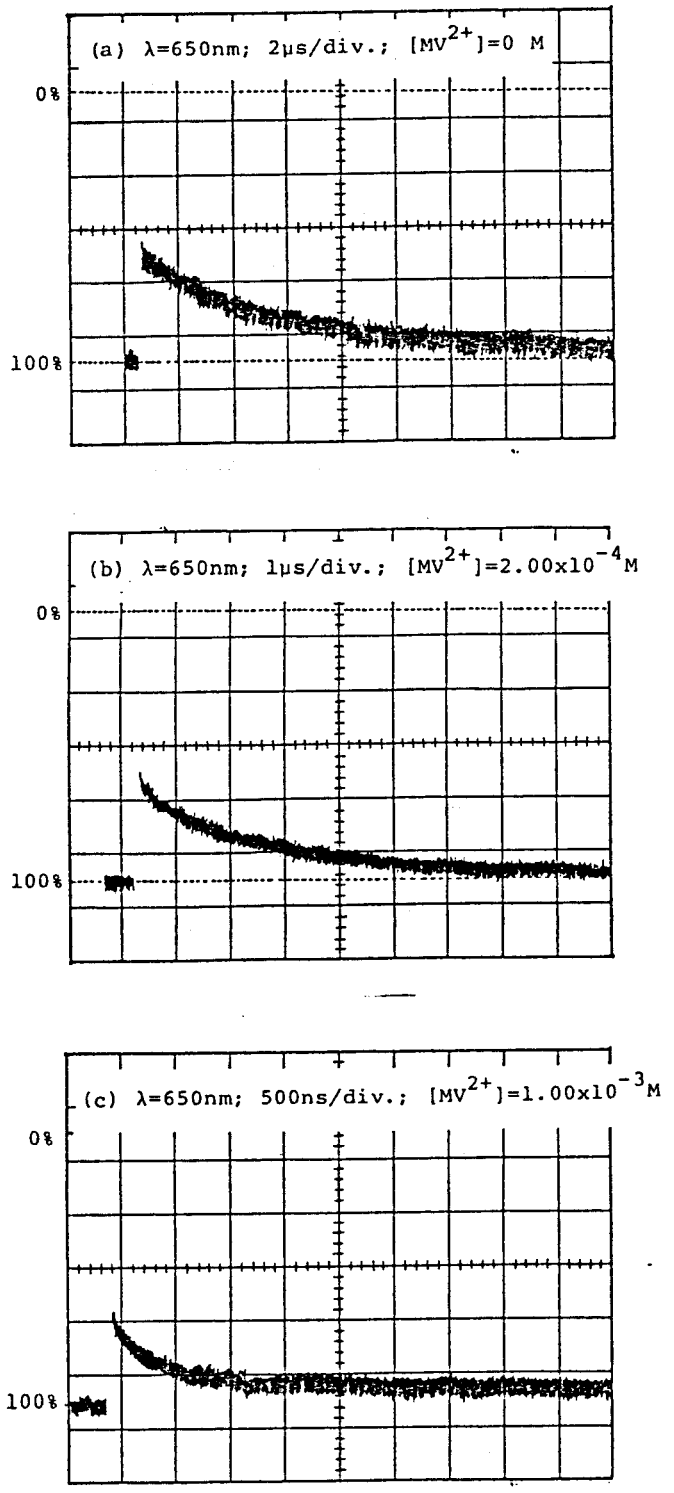

Figure 13. Oscilloscope traces monitored at λ=650 nm in the flash photolysis of EY^{2-} with MV^{2+}.

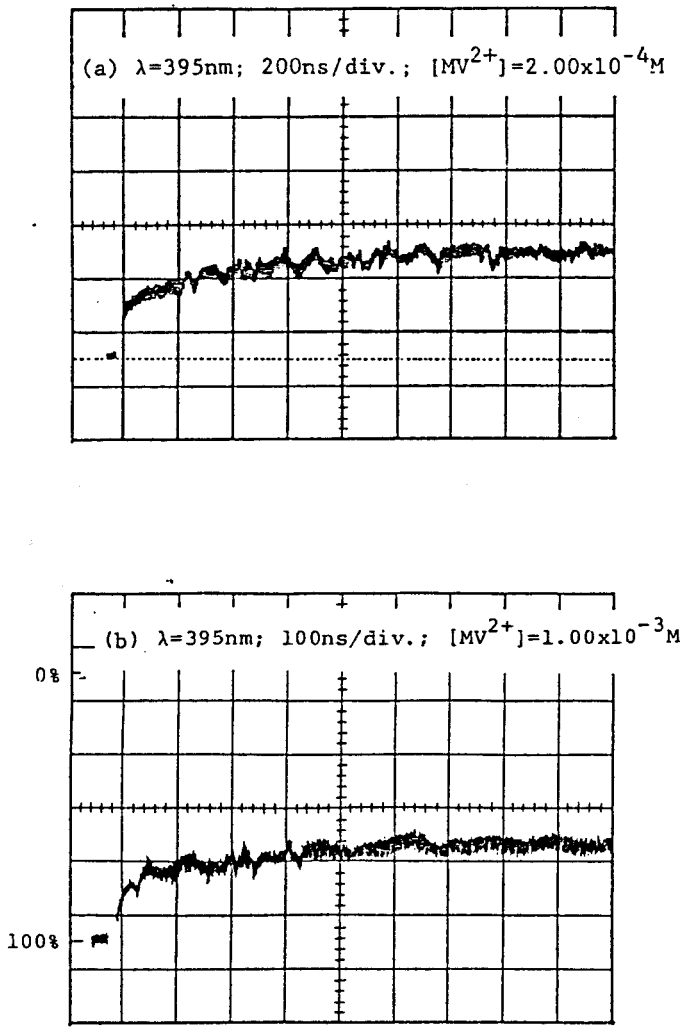

Figure 14. Oscilloscope traces monitored at λ=395 nm in the flash photolysis of EY^{2-} with MV^{2+}.

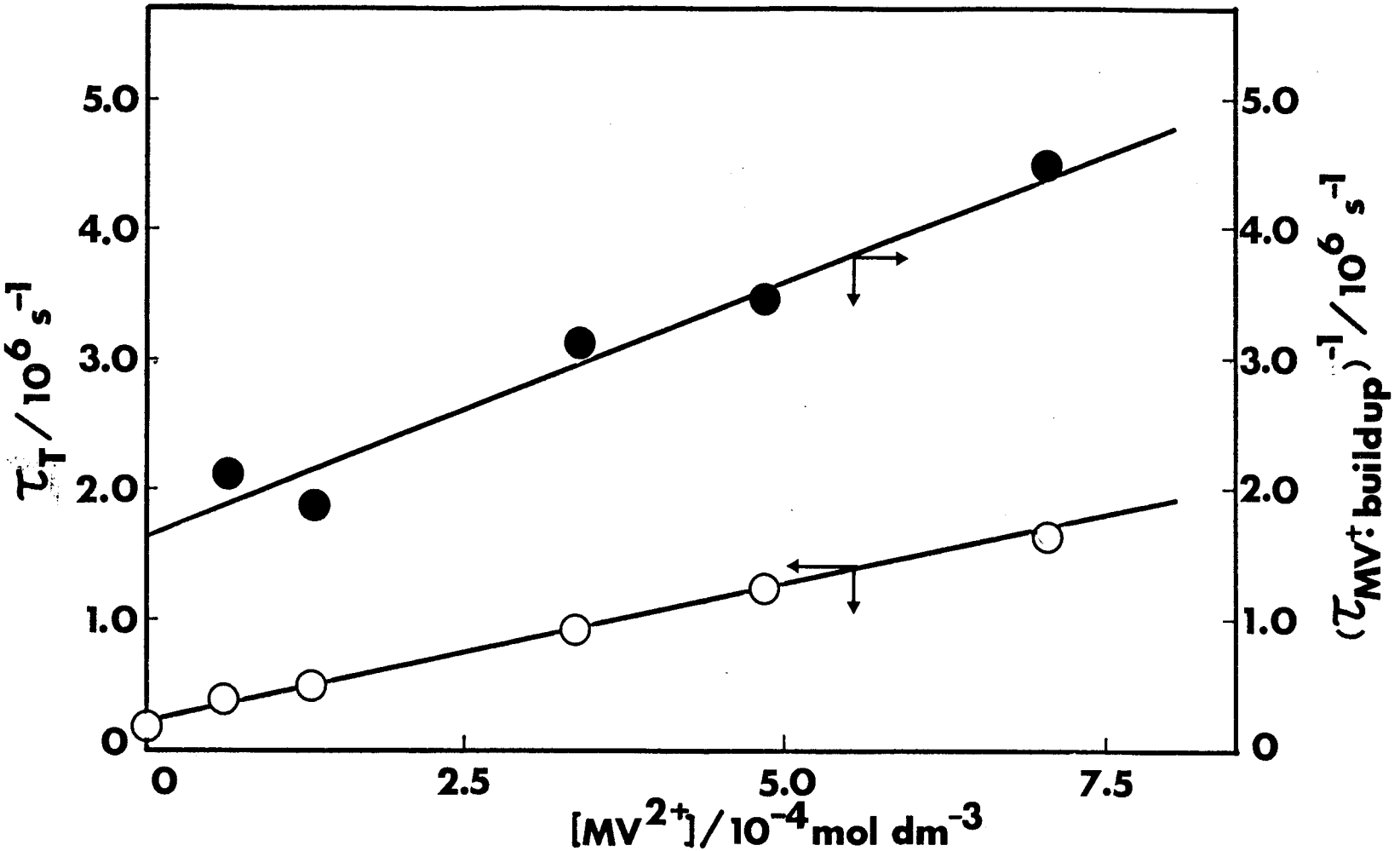

Figure 15. Quenching of triplet EY^{2-} by MV^{2+} (○) and buildup of MV^{+} (●) in aqueous ethanol under degassing.

(a) : $[EY^{2-}]=9.7\times10^{-5}M,[MV^{2+}]=1.0\times10^{-4}M/EtOH-H_2O$

(pH5)(1/1) Excitation: Dye Laser

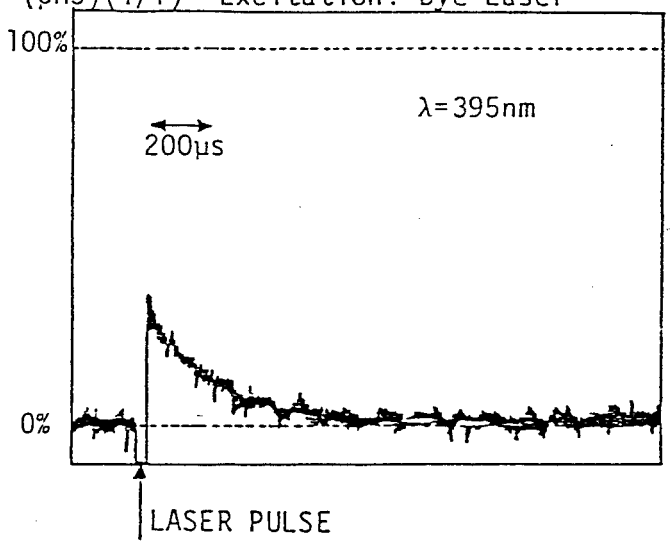

(b) : $[EY^{2-}]=9.7\times10^{-5}M,[MV^{2+}]=1.0\times10^{-4}M/EtOH-H_2O$

(pH5)(1/1) Excitation: Dye Laser

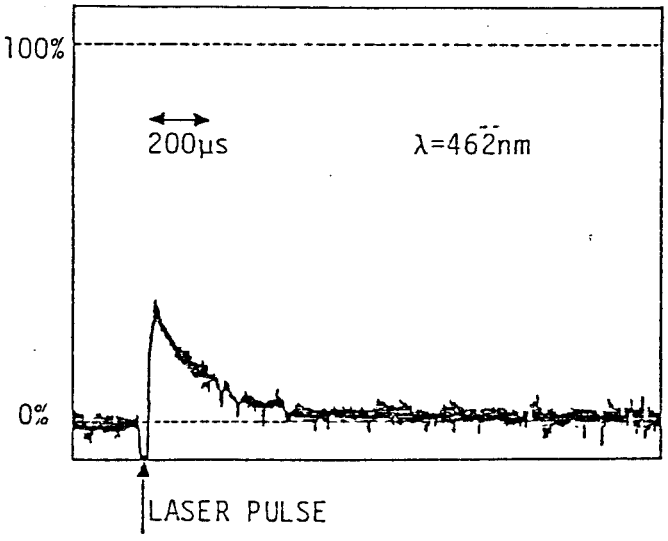

Figure 16. Oscilloscope traces monitored at λ=395 nm (a) and λ=462 nm (b) in the flash photolysis of EY^{2-} with MV^{2+}.

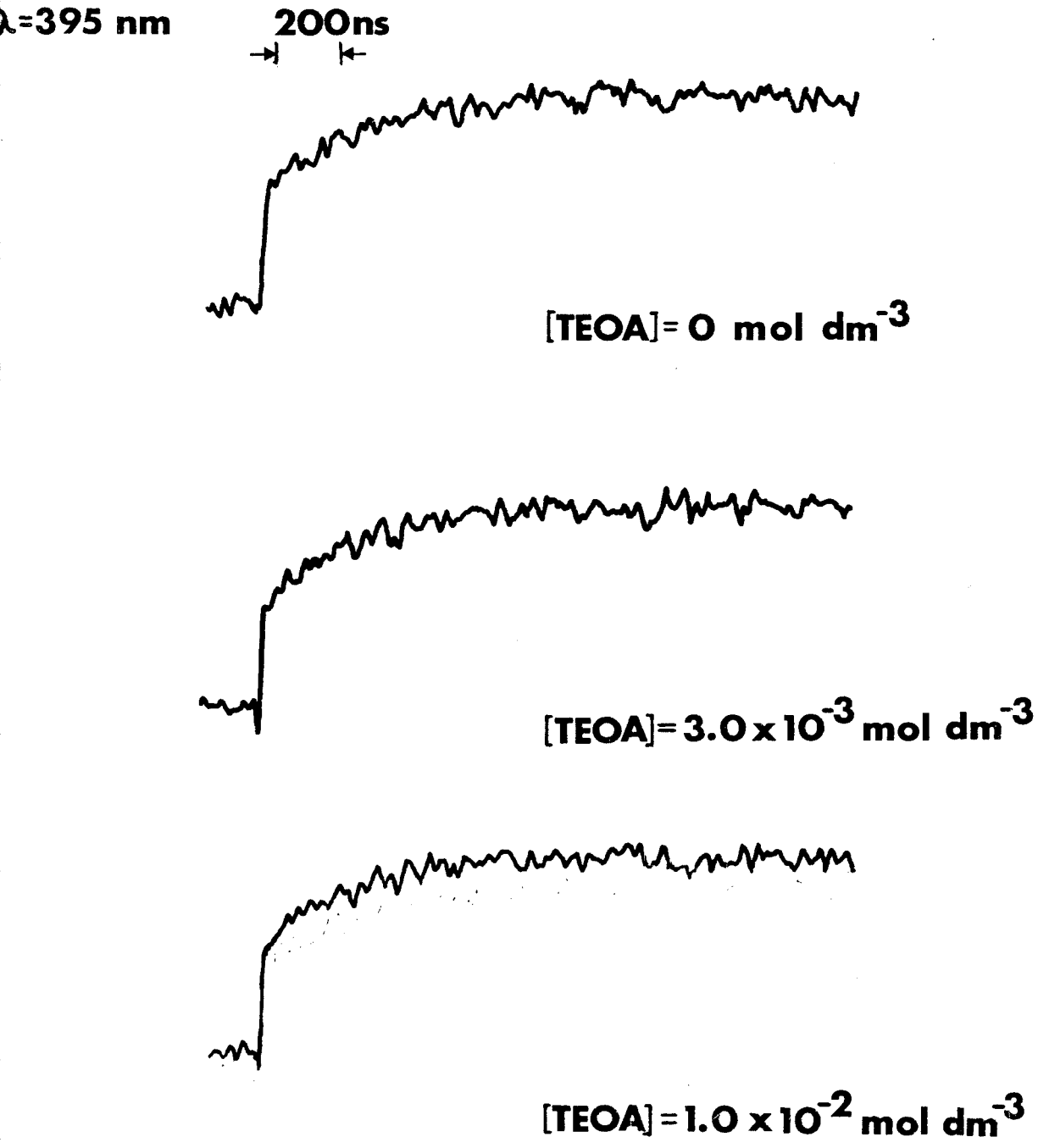

Figure 17. Oscilloscope traces monitored at λ=395 nm in the flash photolysis of the three component system, EY^{2-}/MV^{2+}/TEOA.

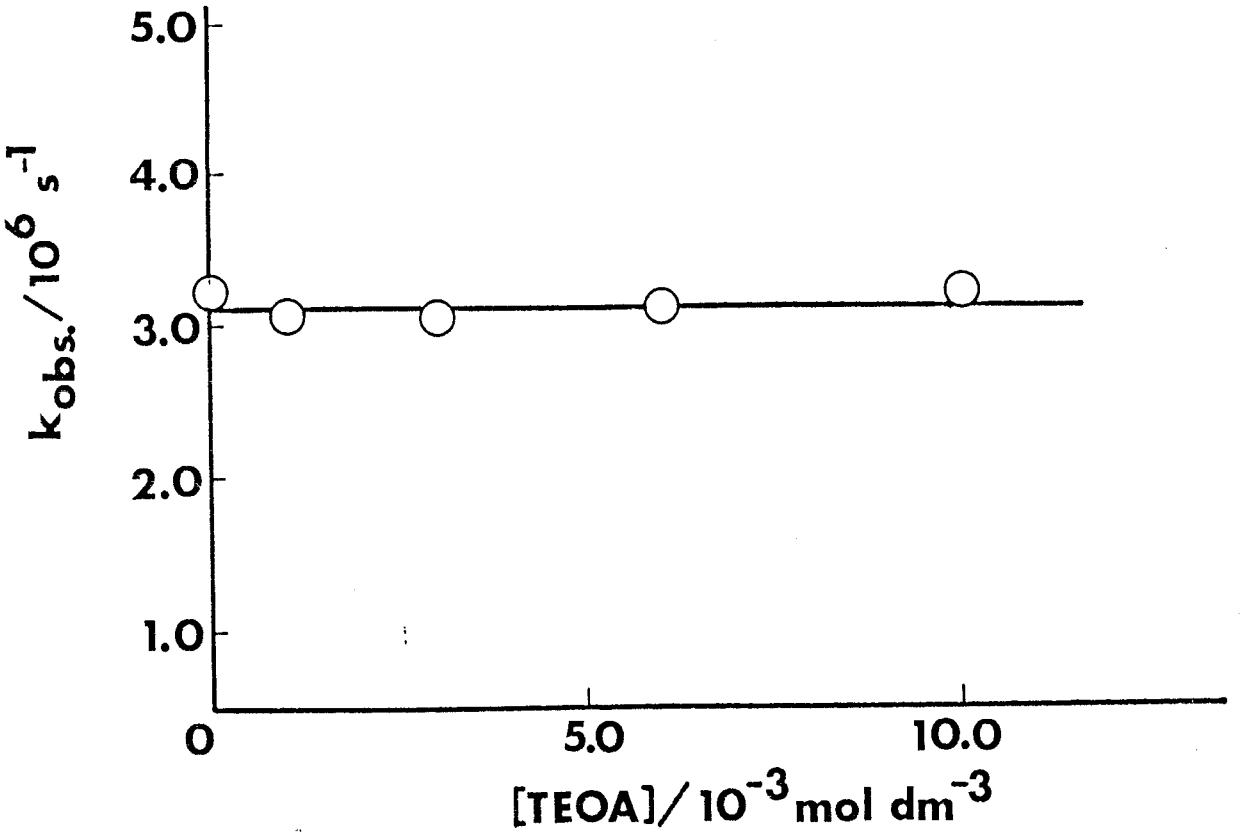

Figure 18. Rate constants for $MV^{+\cdot}$ formation against TEOA concentration (EY^{2-}/MV^{2+}/TEOA).

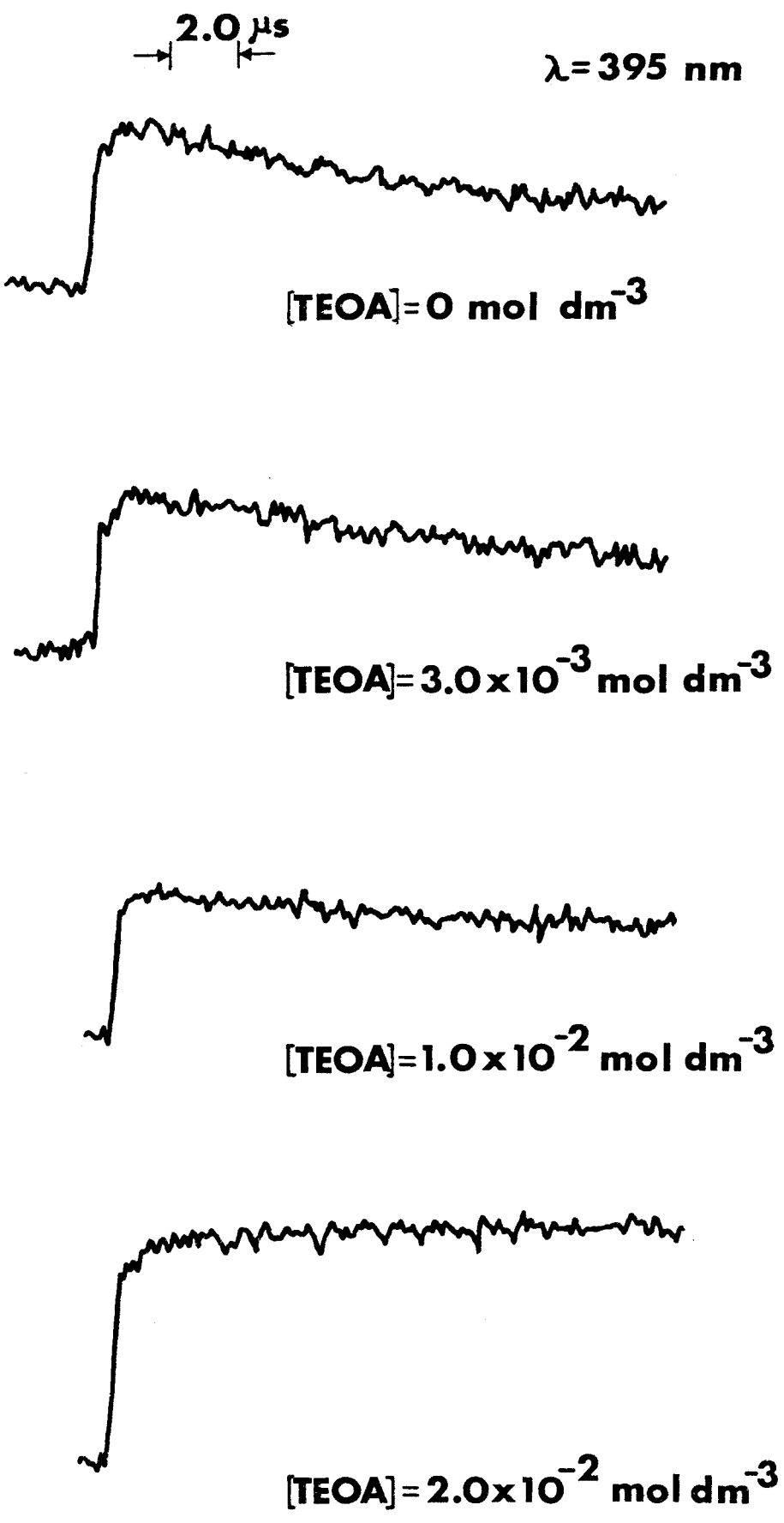

Figure 19. Oscilloscope traces monitored at λ=395 nm in the flash photolysis of the three component system, EY^{2-}/MV^{2+}/TEOA.

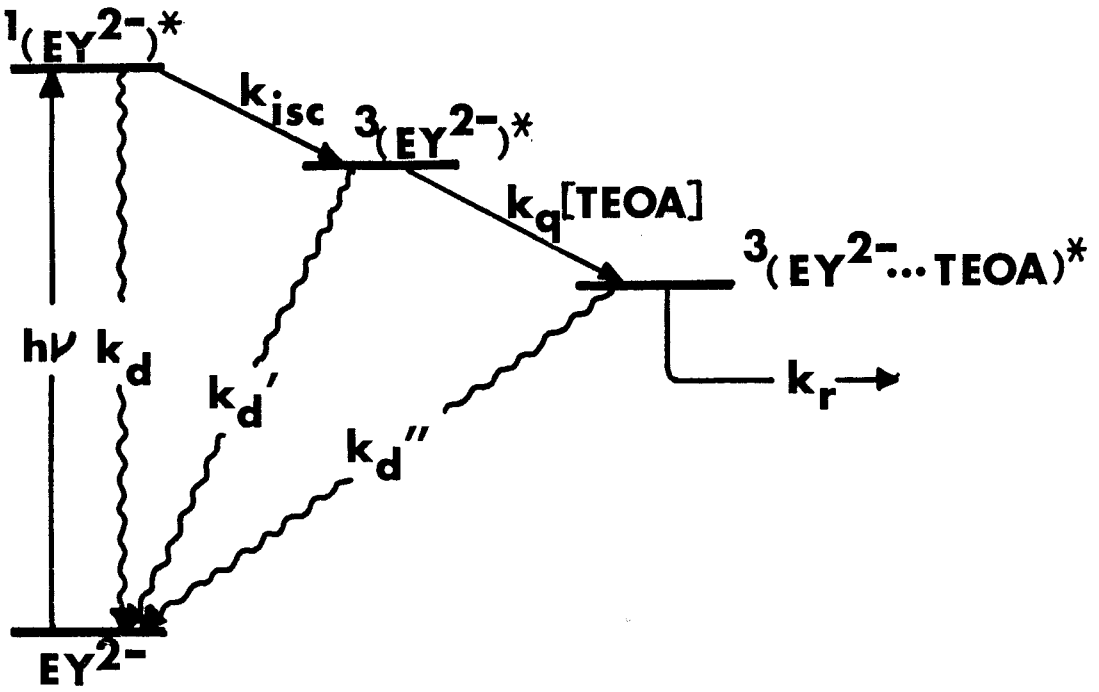

Figure 20. Reaction scheme of the photoreduction of EY^{2-} by electron transfer from TEOA.

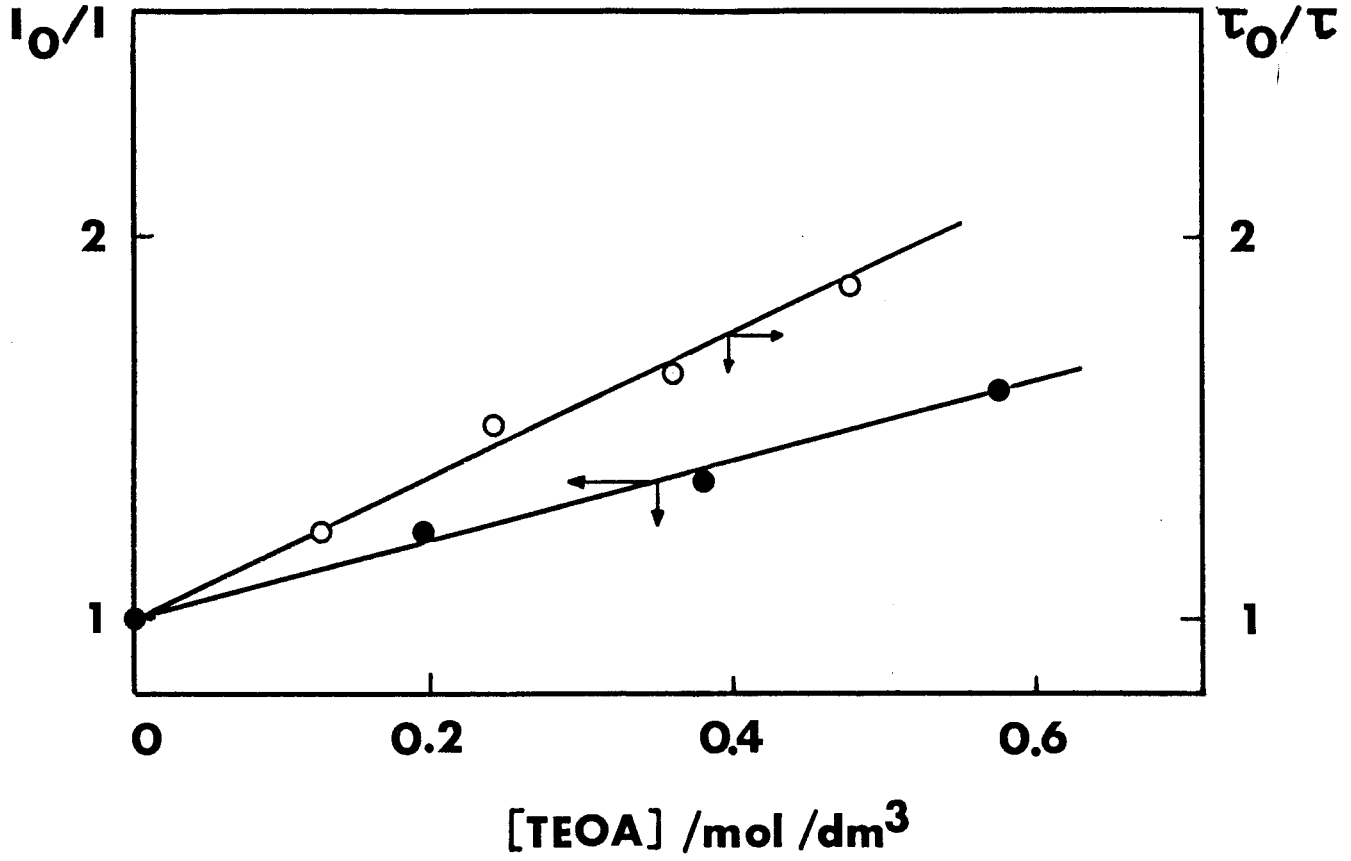

Figure 21. Stern-Volmer plots for EY^{2-} fluorescence quenching by TEOA; (●): fluorescence intensity, (O): fluorescence lifetime.

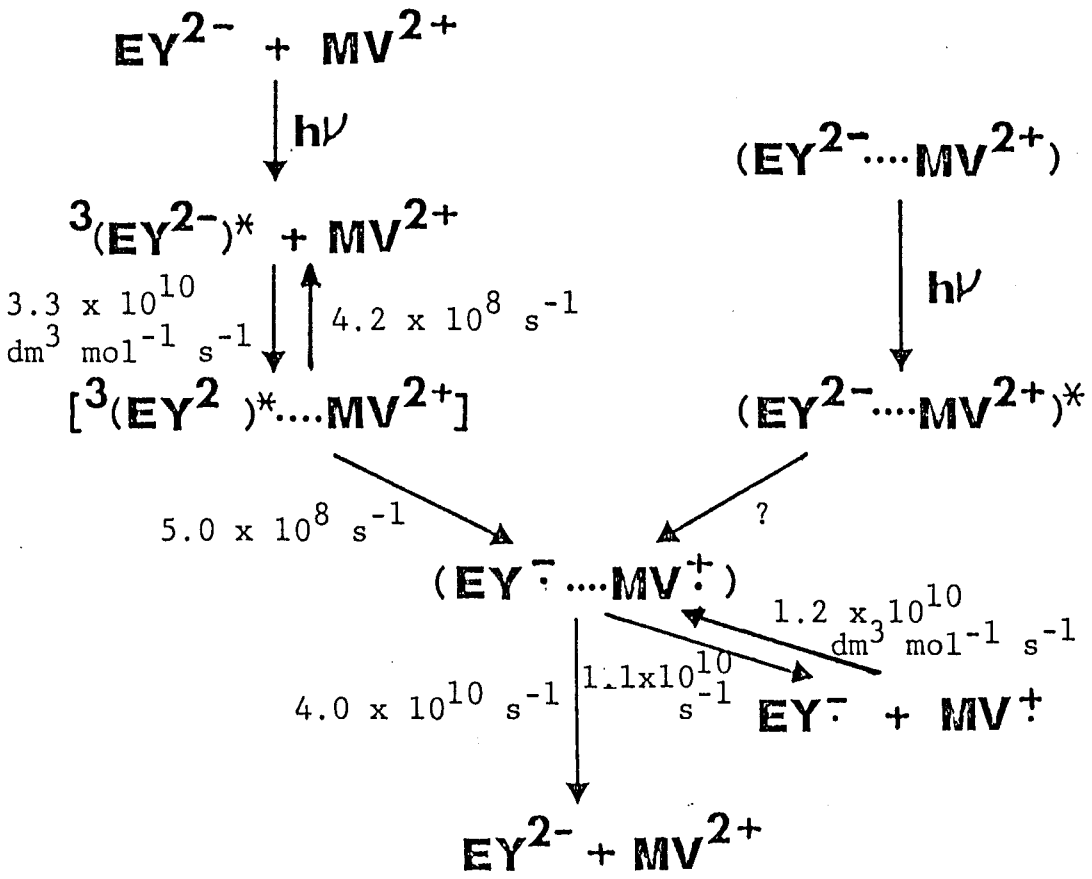

Figure 22. Summary of the rate constants for EY^{2-}-MV^{2+} system.

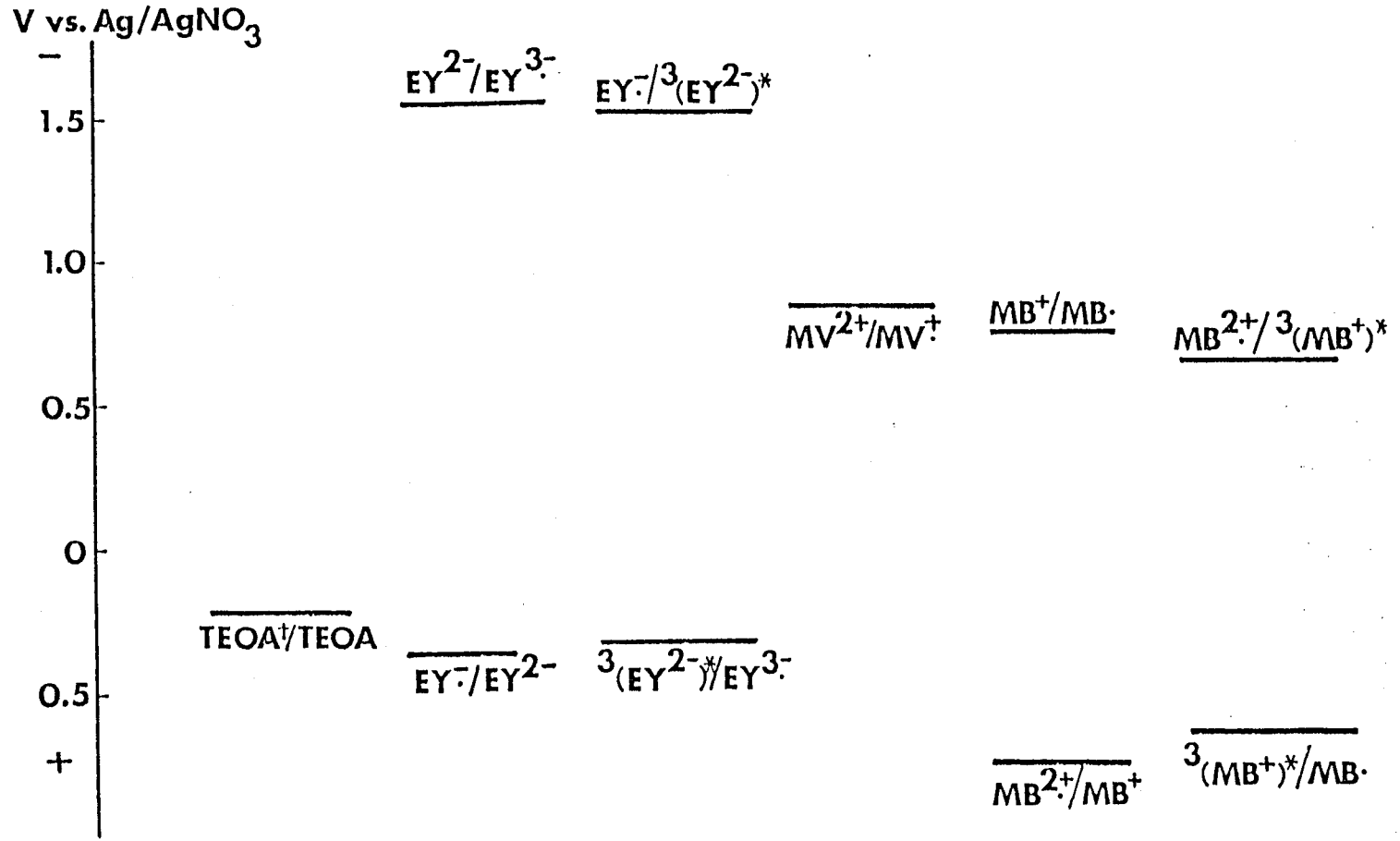

Figure 23. Ground and excited state redox potentials vs. Ag/0.1 mol/dm^3 $AgNO_3$ in MeCN with Et_4NClO_4.

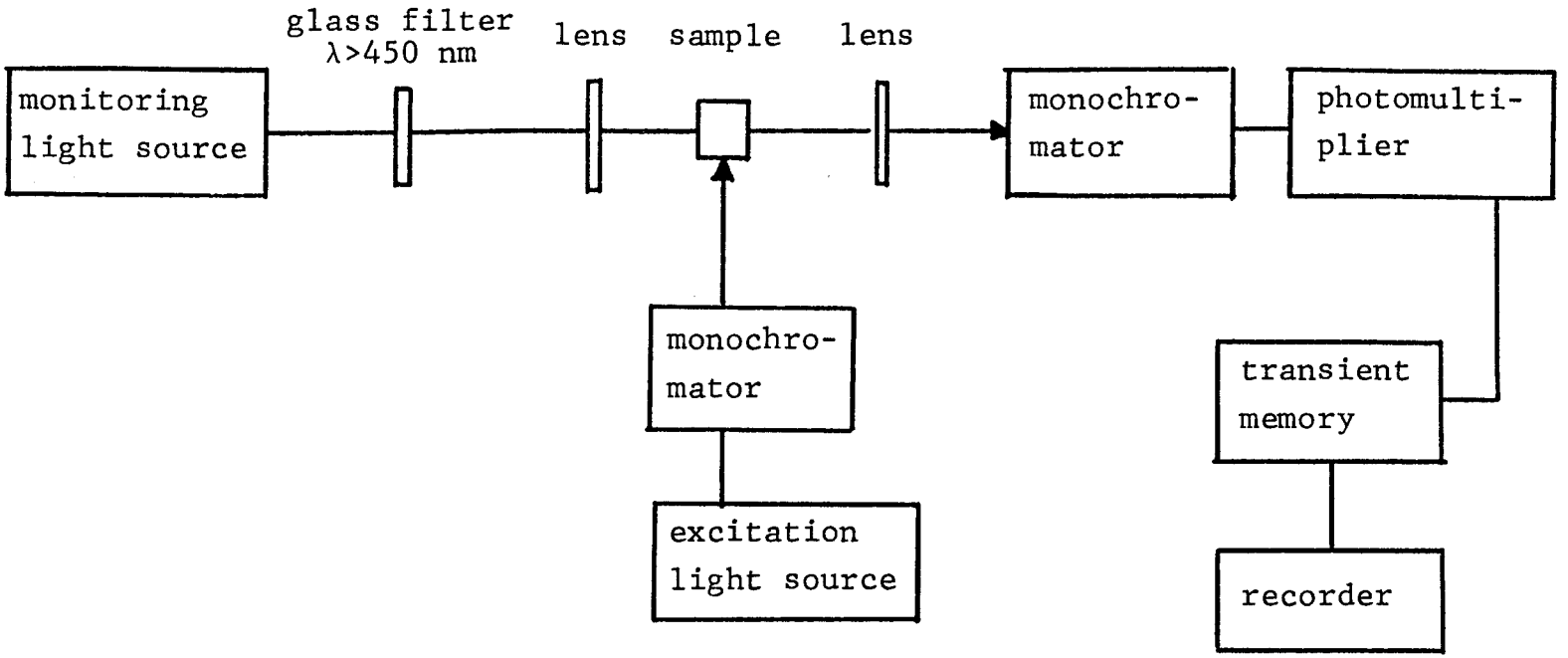

Figure 24. Apparatus for the measurement of quantum yields for $MV^{+\cdot}$ production

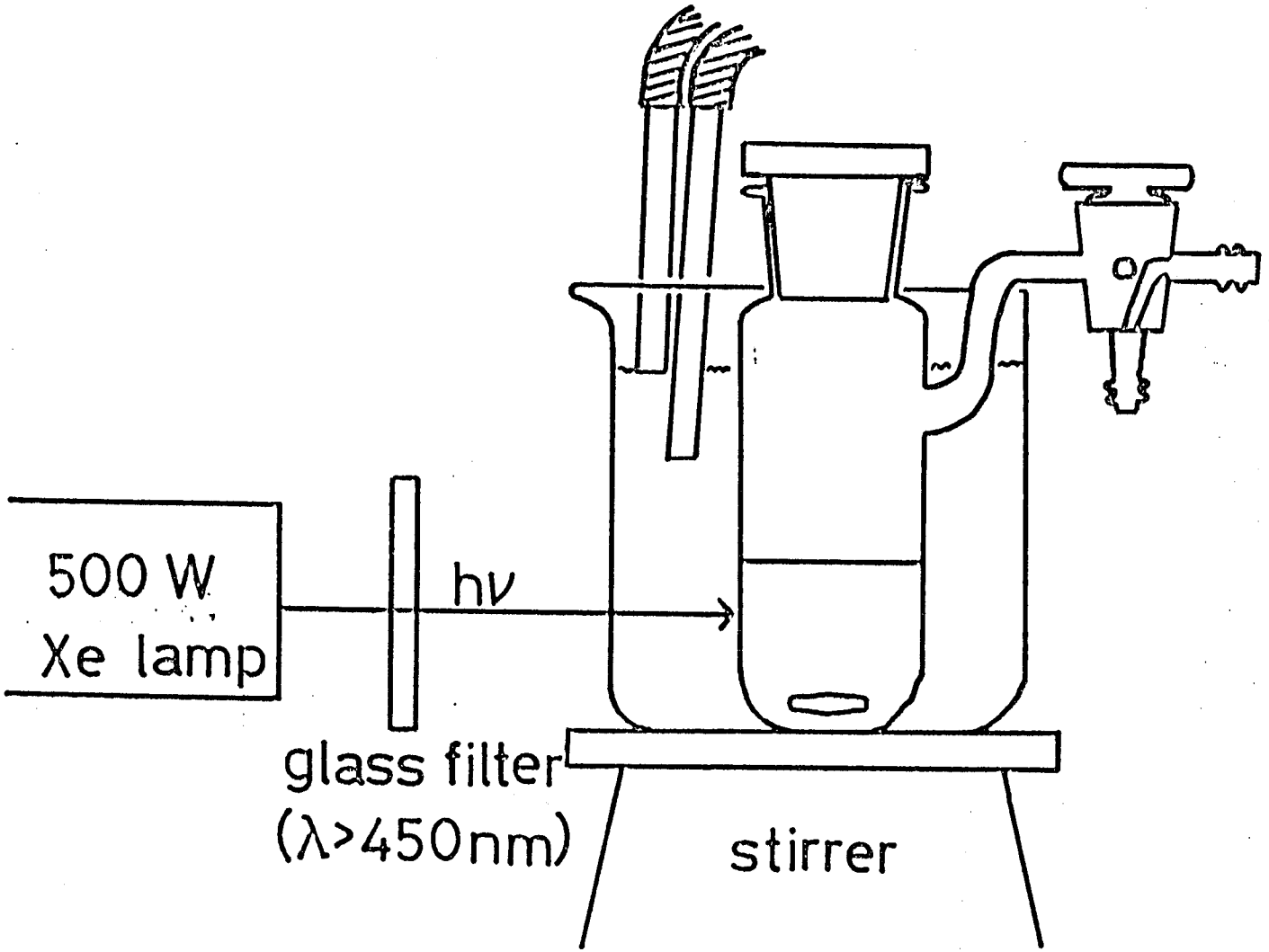

Figure 25. Apparatus for the measurement of hydrogen evolution.

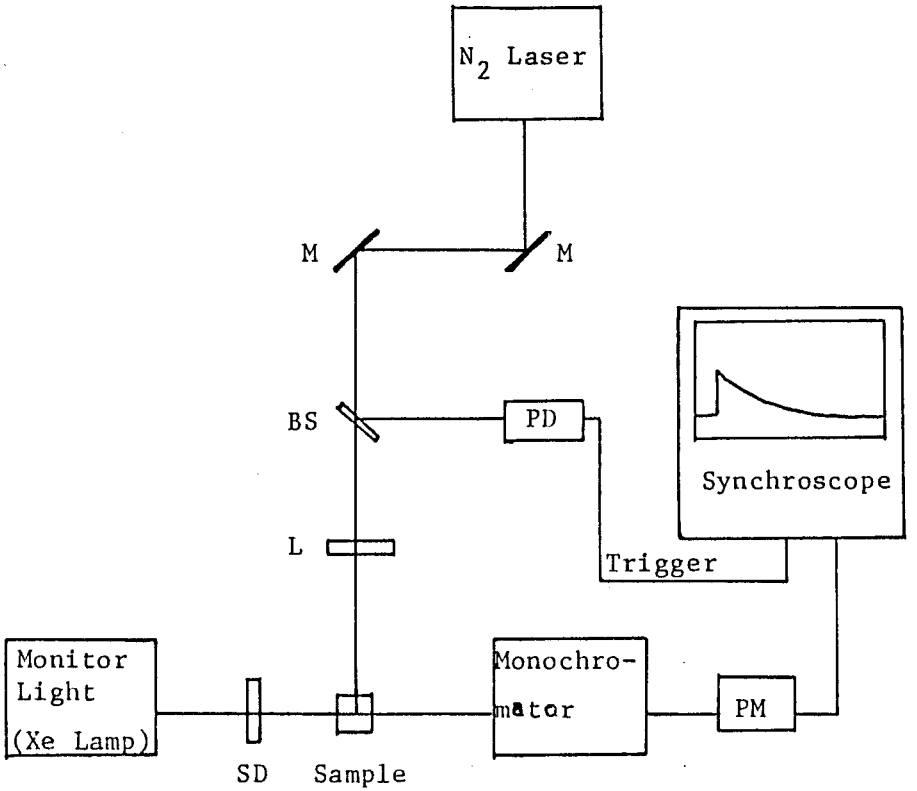

Figure 26. Schematic diagram of the nanosecond laser flash photolysis apparatus. M: Mirror, BS: beam splitter, PD: photodiode, L: lens, SD: shutter driver, PM: photomultiplier.

Appendix 1

PHOTOREDUCTION OF SODIUM ANTHRAQUINONE-2-SULFONATE SENSITIZED BY EOSIN Y

Summary

The photosensitized reaction of Eosin Y (EY^{2-}) with sodium anthraquinone-2-sulfonate (AQS) has been investigated by continuous light irradiation. The production of $AQS^{-\cdot}$ was observed by absorption spectroscopy.

Introduction

Recently, it has been indicated that quinones play an important part in the primary electron transport in the photosynthesis of green plants, and a plastoquinone is considered to be a part of the link between photosystems I and II.[1] Previously Dawent and Kalayanasundarum reported a study of the quenching of excited tris(2,2′-bipyridine)-ruthenium(II) by quinones and hydroquinones.[2]

This part attempts to examine the photoreduction of sodium anthraquinone-2-sulfonate (AQS) with Eosin Y (EY^{2-}) as a sensitizer. The free energy change of the electron transfer reaction from 2-propanol to AQS is larger than that from triethanolamine (TEOA) to MV^{2+} in the system of Eosin Y-MV^{2+}-TEOA.

Results and Discussion

Irradiation of EY^{2-} (1.5×10^{-5} mol/dm^3) and AQS (1.0×10^{-3} mol/dm^3) in a 4:1 2-propanol-water mixture containing sodium hydroxide (2×10^{-2} mol /dm^3) with visible light of λ>500 nm from a 500 W xenon lamp under argon atmosphere caused growth of absorption bands around 400 and 505 nm due to production of the radical anion of AQS. On introduction of air into the irradiated mixture, the resulting absorption disappeared completely and the absorption band of EY^{2-} was recovered quantitatively (Figure 1). The radical anion was not generated without EY^{2-} under otherwise the same conditions as above. These results indicate that EY^{2-} works as an efficient sensitizer for reduction of AQS into $AQS^{-}\cdot$ in alkaline aqueous 2-propanol without TEOA. It is surprising that EY^{2-} can reduce AQS, of which reduction potential (-0.92 V vs. SCE in acetonitrile; supporting electrolyte: tetraethylammonium perchlorate) is more negative than that of MV^{2+}, with 2-propanol as an electron donor under visible light irradiation. Since the triplet energy of AQS(E_T=~68 kcal/mol)[3] is greater than that of EY^{2-} (E_T=43~46 kcal/mol)[4], energy transfer from $^3(EY^{2-})^*$ to AQS followed by reactions (1)~(3) mentioned below cannot occur, and $AQS^{-}\cdot$ production will result from electron transfer between EY^{2-} and AQS (eq. 4, 5, 6, or 7).

$$^3(EY^{2-})^* + AQS \longrightarrow EY^{2-} + {}^3AQS^* \quad (1)$$

$$^3AQS^* + Me_2CHOH \longrightarrow AQSH^{\cdot} + {}^{\cdot}CMe_2OH \quad (2)$$

$$AQSH^{\cdot} \rightleftharpoons AQS^{-\cdot} + H^+ \quad (3)$$

$$^3(EY^{2-})^* + AQS \longrightarrow EY^{-\cdot} + AQS^{-\cdot} \quad (4)$$

$$EY^{-\cdot} + Me_2CHOH \longrightarrow EY^{2-} + [Me_2COH]^{+\cdot} \quad (5)$$

$$^3(EY^{2-})^* + Me_2CHOH \longrightarrow EY^{3-\cdot} + [Me_2COH]^{+\cdot} \quad (6)$$

$$EY^{3-\cdot} + AQS \longrightarrow EY^{2-} + AQS^{-\cdot} \quad (7)$$

Previously, Inoue and Hida reported that $AQS^{-\cdot}$, which was produced on irradiation of UV light (λ>365 nm) could reduce much anodic substrates such as benzonitrile in a reversed micellar system under visible light (λ>450 nm) illumination.[5] On the other hand, Eriksen and coworkers investigated that the fluorescence of the radical anion of anthraquinone ($AQ^{-\cdot}$) was quenched by organic acceptor molecules such as bromobenzene.[6] If an effective irreversible electron transfer from the excited $AQS^{-\cdot}$ to an appropriate electron acceptor is carried out satisfactorily, the EY^{2-}-AQS system in alkaline aqueous 2-propanol should be expected to cover a wide range of redox potential which can reduce carbon dioxide by the stepwise two photon excitation with a visible light after photosynthesis of green plants.

Experimental

Materials. Sodium anthraquinone-2-sulfonate (Nakarai, SPR) was three times salted out from aqueous concentrated sodium chloride and repeatedly recrystallized from water until the extinction coefficient at λ_{max} in the UV spectrum became constant.[5] 2-Propanol (Nakarai, SPR) was dried over Zeolite 3-A (Wako) for at least three days and distilled before use.

Procedures. A sample of EY^{2-} (1.5×10^{-5} mol/dm^3) and AQS (1.0×10^{-3} mol/dm^3) in a 4:1 2-propanol-water mixture (4 ml) was deaerated in a quartz cell with a long neck by bubbling with argon for at least 30 min. Continuous light irradiation was performed by employing a 500 W Ushio UI-501C xenon lamp through a Toshiba Y-50 glass filter for irradiation with visible light of λ>500 nm. The visible and UV absorption spectra of irradiation mixtures were measured on a Hitachi 200-20 spectrophotometer.

References

1) J. Amesz, Biochim. Biophys. Acta, 1973, 301.

2) J. R. Darwent and K. Kalyanasundaram, J. Chem. Soc., Faraday Trans. 2, 77, 373 (1981).

3) H. Inoue and M. Hida, Yuki Gosei Kagaku Kyokai Shi, 32, 348 (1974).

4) T. Matsuura, "Sansosanka Hanno," Maruzen, (1977), p. 224.

5) H. Inoue and M. Hida, Bull. Chem. Soc. Jpn., 55, 1880 (1982).

6) J. Eriksen, H. Lund, and A. I. Nyvad, Acta. Chem. Scand., B37, 459 (1983).

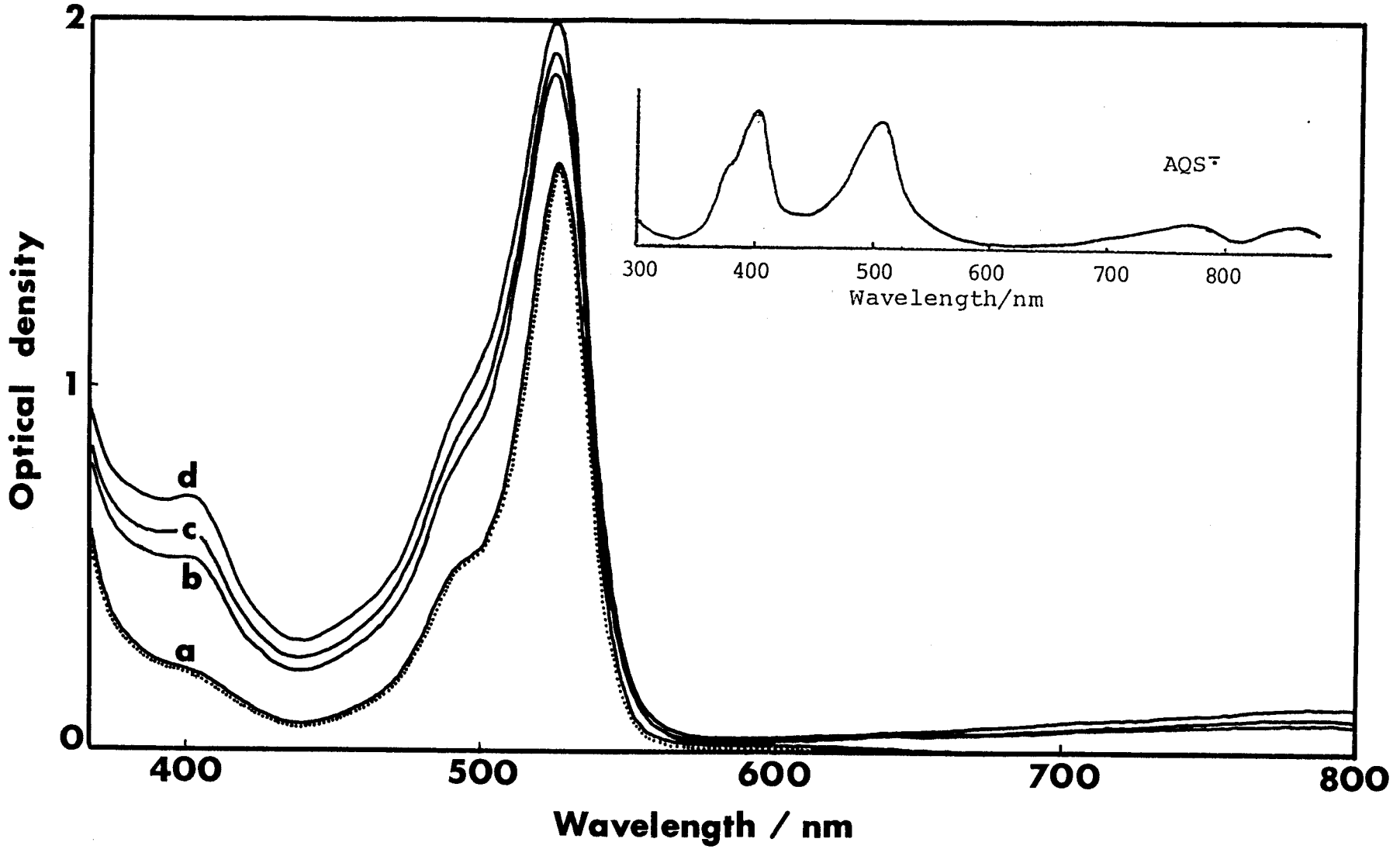

Figure 1. Spectral change of aqueous 2-propanol solution of Eosin Y/AQS containing 0.02 mol/dm^3 NaOH on irradiation under Ar (——) and on introduction of air after photolysis (····); irradiation periods as follows: a) 0, b) 3, c) 5, d) 8 min.

Appendix 2

CONSTRUCTION OF A PHOTOGALVANIC CELL USING THE EOSIN Y-METHYL VIOLOGEN-TRIETHANOLAMINE SYSTEM

A photogalvanic cell is a battery in which the cell solution absorbs light energy directly to generate species which, upon back reaction through an external circuit with the aid of suitable electrodes, produce electric power, and hence photoactivation of the electrodes is not involved. Most of the previous work of the photogalvanic effect has been done on thionine-ferrous ion (Fe^{2+}) systems.[1-4] Kamiya and Okawara reported that especially high photovoltages and photocurrents were obtained from photogalvanic cells with organic dyes and aliphatic amines as reducing agents,[5] and moreover that the effect in the proflavin-triethanolamine(TEOA)-system is considerably enhanced by addition of methyl viologen (MV^{2+}).[6] On the other hand, recently, Tsubomura and coworkers described the effect of aliphatic reducing agents and MV^{2+} in photogalvanic cells, containing a dye (thionine, reboflavin, or proflavin).[7]

In this part, the photogalvanic processes are examined employing the EY^{2-}-TEOA (two component) system and the EY^{2-}-MV^{2+}-TEOA (three component) system. Figure 1 shows the apparatus for the measurement of photovoltages and photocurrents. Platinum plates were employed as light and dark electrodes. The light electrode potentials with respect to an SCE and the photocurrents between the light and dark electrodes were measured by use of a Hokuto HA-201 potentiostat. Light irradiation was performed employing a 1 kW xenon lamp (Ushio) through a Toshiba Y-45 glass filter for irradiation by visible light of λ>450 nm. The

resulting photocurrents (I_p) and photovoltages (V_p) are depicted in Figure 2, 3, and listed in Table 1.

References

1) E. Rabinowitch, J. Chem. Phys., 8, 551, 560 (1940).

2) K. Shigehara and E. Tsuchida, J. Phys. Chem., 81, 1883 (1977).

3) P. D. Wildes and N. N. Lichtin, J. Phys. Chem., 82, 981 (1978).

4) P. D. Wildes, N. N. Lichtin, M. Z. Hoffman, L. Andrews, and H. Linschitz, Photochem. Photobiol., 25, 21 (1977).

5) N. Kamiya and M. Okawara, Denki Kagaku, 36, 506 (1968); Idem, ibid, 38, 273 (1970).

6) N. Kamiya and M. Okawara, Kogyo Kagaku Zasshi, 72, 96 (1969).

7) H. Tsubomura, Y. Shimoura, and S. Fujiwara, J. Phys. Chem., 83, 2103 (1979).

Table 1. Photocurrents (i_p) and Photovoltages (V_p) in Various Photogalvanic Cells[a]

$[MV^{2+}]$ / mol/dm^3	solvent	i_p / A/cm^2	V_p / mV
5.0×10^{-3}	EtOH-H_2O (pH 9)=(1/1)	43	-170
5.0×10^{-3}	H_2O (pH 9)	40	-440
0	H_2O (pH 9)	6.4	-320

[a]The concentration are 1.75×10^{-5} mol/dm^3 for EY^{2-}, 1.0×10^{-2} mol/dm^3 for TEOA.

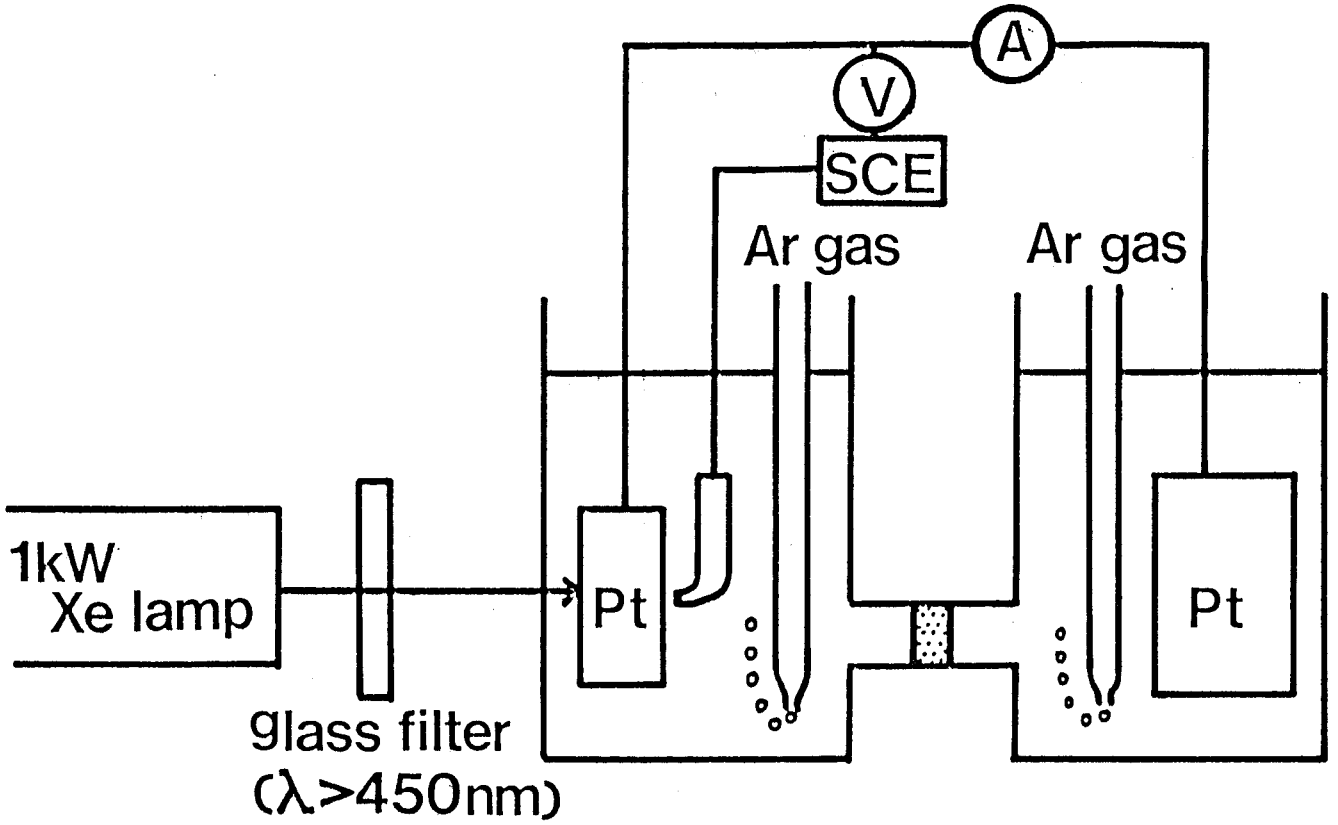

Figure 1. Apparatus for the measurement of photocurrents and photovoltages in a photogalvanic cell

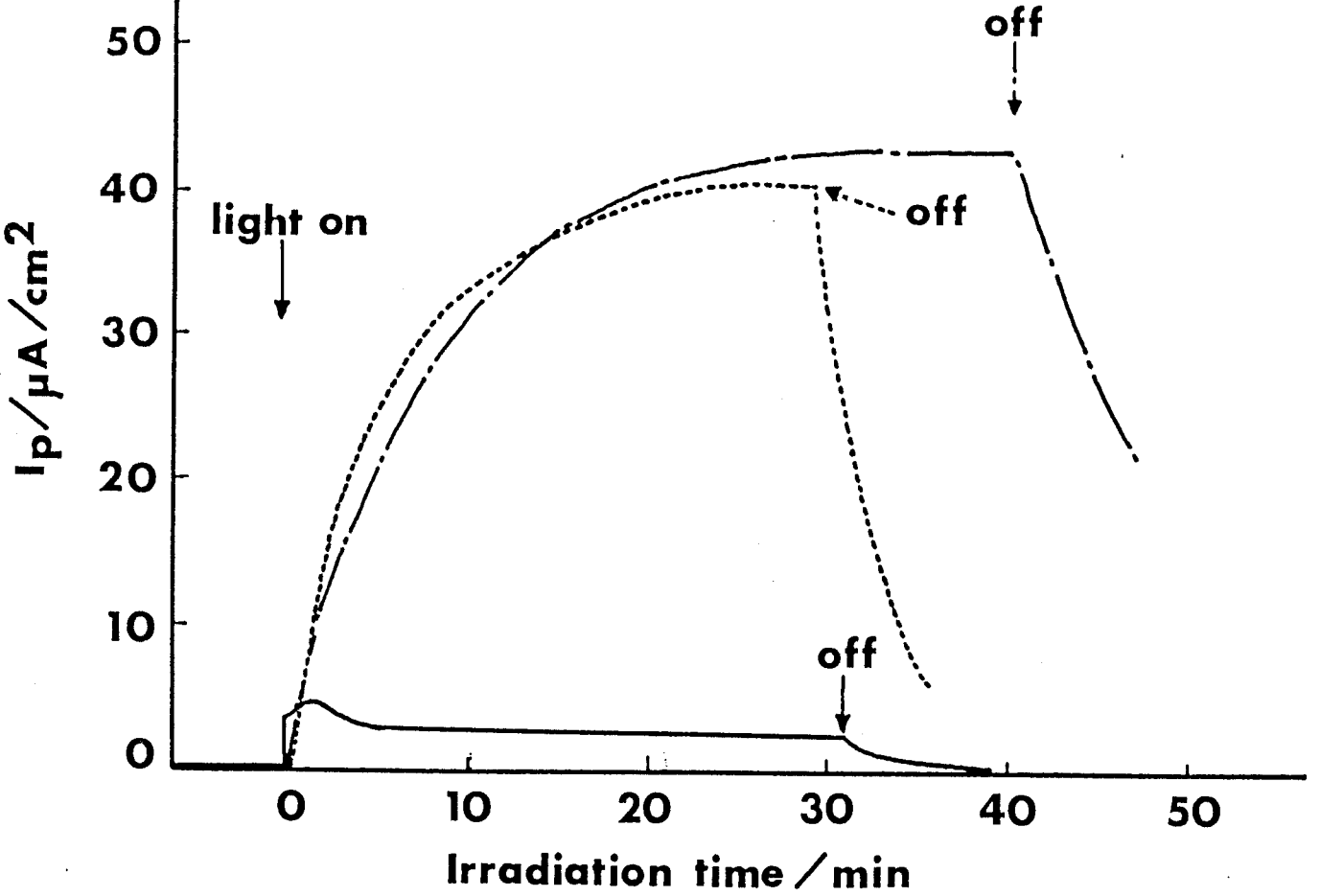

Figure 2. The change of photocurrents (i_p) with irradiation.
$[EY^{2-}]=1.75 \times 10^{-5}$ mol/dm^3, $[TEOA]=1.0 \times 10^{-2}$ mol/dm^3,
(———): $[MV^{2+}]=0$ mol/dm^3; solvent=H_2O (pH 9),
(·····): $[MV^{2+}]=5.0 \times 10^{-3}$ mol/dm^3; solvent=H_2O (pH 9),
(—·—): $[MV^{2+}]=5.0 \times 10^{-3}$ mol/dm^3; solvent=EtOH-H_2O (pH 9).

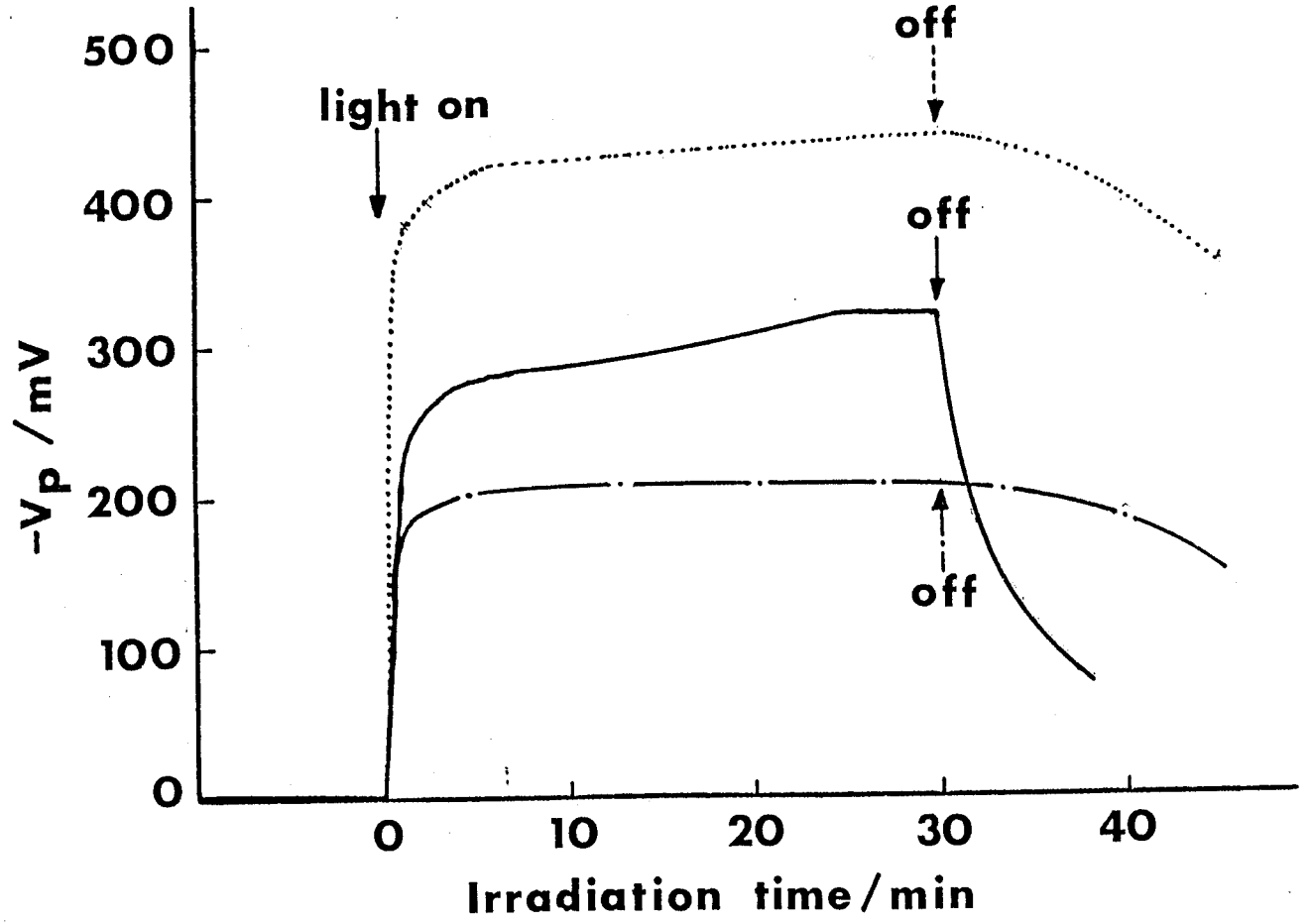

Figure 3. The change of photovoltages (V_p) with irradiation.
$[MV^{2+}]=1.75 \times 10^{-5}$ mol/dm^3, $[TEOA]=1.0 \times 10^{-2}$ mol/dm^3,
(———): $[MV^{2+}]=0$ mol/dm^3; solvent=H_2O (pH 9),
(·····): $[MV^{2+}]=5.0 \times 10^{-3}$ mol/dm^3; solvent=H_2O (pH 9),
(—·—): $[MV^{2+}]=5.0 \times 10^{-3}$ mol/dm^3; solvent=EtOH-H_2O (pH 9).